TURBULENCE STRUCTURE AND RIFFLE-POOL MORPHOLOGY IN COARSE-GRAINED CHANNELS: A FIELD STUDY OF THE ROUGE RIVER, TORONTO, ONTARIO, CANADA

JOSH ARNETT

A THESIS SUBMITTED TO THE FACULTY OF GRADUATE STUDIES IN PARTIAL FULFILLMENT OF THE REQUIREMENTS FOR THE DEGREE OF MASTER OF SCIENCE

GRADUATE PROGRAM IN GEOGRAPHY

YORK UNIVERSITY

TORONTO, ONTARIO

OCTOBER 2013

ABSTRACT

TURBULENCE STRUCTURE AND RIFFLE-POOL MORPHOLOGY IN COARSE-GRAINED CHANNELS: A FIELD STUDY OF THE ROUGE RIVER, TORONTO, ONTARIO, CANADA

Riffle-pool sequences play a crucial role in the fluid-sediment interactions that control bed scour, sediment transfer and deposition in rivers. Areas in rivers that experience changes in depth or width cause areas of differing flow acceleration and deceleration. Differing flow regimes strongly impact the turbulence structure and associated sediment transport processes. Past research has focused largely on the maintenance of riffle-pool sequences, specifically in the context of stage dependant velocity reversal hypotheses. However, little research has been completed on the three dimensional flow structures of these sequences and how this affects the depth of scour in pools and deposition height in riffles. Critical knowledge is lacking with respect to how these properties change or differ in straight versus meandering channels. Turbulence structure and sediment transport processes experience higher complexity in meandering reaches than straight reaches. Secondary circulations around meander bends create an asymmetrical profile that influences lateral sediment transport, thus leading to the occurrence of deep scour in pools.

The primary objective of this study was to assess the turbulence structure and scour in riffle-pool sequences in both straight and meandering channel sections of the Rouge River, Toronto, Ontario, Canada. The purpose was to assess the controlling factors that influence riffle height and depth of scour in pools and also how these factors differ in straight versus meandering reaches. The spatial and temporal variability of the turbulence structure and sediment transport will also be observed by comparing the responses to varying flow stages.

This study was comprised of a field-based project using an Acoustic Doppler Velocimeter (ADV). Sediment sorting and transport patterns were observed by using a combination of painted tracer particles, permanent bedload traps and handheld bedload samplers.

Results indicated that turbulent kinetic energy (TKE) and momentum exchange was typically observed 5 – 10 cm above the bed. Time series data indicated that the degree of curvature likely influenced secondary circulation and hence sediment transport and channel form. It was evident that riffle height and depth of scour in pools was strongly linked to channel morphology as well as micro scale bed variably.

ACKNOWLEDGEMENTS

First and foremost I would like to extend my greatest appreciation to Dr. André Robert for the opportunity to partake in my Masters of Science and to be given the opportunity to embark on a first time study using an ADV within a natural river setting at the Rouge River, Toronto, Ontario. As well, I would like to thank Dr. André Robert for his continuous guidance, advice, support and patience during this study and during the write up of this thesis. Additionally, I would like to thank York University, specifically the Geography department as well as NSERC (Natural Sciences and Engineering Research Council) and OGS (Ontario Graduate Scholarship), for providing funding and the opportunity to complete my own research. I would also like to thank Dr. Tarmo Remmel for his continuous guidance and support and for being a second reader for my thesis.

Appreciation is also extended to the TRCA (Toronto and Region Conservation Authority), in particular Derek Smith for providing valuable river data and insight, both of which were crucial for data analysis.

As well, I would like to thank Patrick Mojdehi and Mitchell Kingsland for their assistance during site set-up and data collection.

Finally, I would like to thank my family for their patience and continuous support throughout my Master's degree at York University. Last but not least, I would like to give a special thanks to all my friends who encouraged me and keep me motivated to finish my thesis, especially when times were tough.

TABLE OF CONTENTS

LIST OF FIGURES

LIST OF TABLES

SECTION ONE: INTRODUCTION

1.1 Introduction

Rivers are complex in nature and are characterized by a variety of morphologic structures at a variety of scales. For example, pools and riffles and mid-channel and lateral bars and meander bends are all characterized by differential morphologic structures at varying scales. In order to completely understand fluvial form and process, an assessment of morphologic complexity (at varying scales) must be completed (Rayburg and Neave, 2008).

Since the 1950's, process based fluvial geomorphic research has gained considerable momentum within the realm of Geomorphology. Ashmore et al. (2000) stated that although there has been a recent emphasis on applied interdisciplinary research, there still remains a demand to continually understand fundamental process-based fluvial science. Similarly, Rayburg and Neave (2008) stated that to adequately describe the full spectrum of morphologic diversity and complexity in fluvial systems, it is important to have a study by which multi-scale morphologic structures and their internal variability can be assessed.

Similarly, Robert (1993) observed that a considerable amount of research in the last couple of decades has been centralized around recent interest in the characterization of turbulent structures in river channels and their links with sediment transport processes. Robert (1993) also stated that flow competence and the threshold of motion are important

components of recent research with respect to interests in bedload transport processes as determined from the movement of individual clasts.

Riffle-pool sequences are common morphologic structures found in many river systems around the world. Riffle-pool sequences are commonly used as sites for ecological assessments and river health or condition (Thomson et al. 2001), as many invertebrate and fish species live and reproduce in these areas. Riffle-pool sequences are commonly observed features in coarse grained river channels and are an integral part of the mechanics of meander development and channel processes (Gregory et al. 1994). Alluvial riffle-pool units are the characteristic bedform within gravel bed rivers and generally have a slope of <1.5% (Grant el al., 1990; Montgomery and Buffington, 1997; MacVicar and Roy, 2011). Non-alluvial riffle-pool units generally contain elements such as boulders, bedrock outcrops and large woody debris. Riffle-pool sequences that contain non-alluvial elements can create “forced” riffle-pool units from a variety of plunging flow, backwater and lateral scour effects and generally have a river slope of up to 3% (Beschta and Platts, 1986; Bisson et al. 1987; Montgomery and Buffington, 1997). The mechanisms by which riffles and pools are formed and maintained are fundamental aspects of channel form and process. Over the past thirty years, the study of riffle-pool sequences has dominated geomorphic research and much progress has been made in terms of formation, maintenance and patterns of sediment transport (Keller, 1971; Clifford and Richards, 1992; Sear, 1996).

As previously stated, riffle-pool sequences are increasingly being studied by geomorphologists. In riffle-pool sequences, varying scales of the turbulent flow structure

are associated with varying bedforms and bed roughness so that average conditions are difficult to implement (Milan et al. 2001; Dollar, 2002). Riffle-pool sequences play a crucial role in the fluid-sediment interactions that control bed scour, sediment transfer and deposition in rivers (Booker et al. 2001). Understanding the flow regime in riffle-pool sequences is critical for the development of river engineering schemes, environmental policies and river restoration (Heritage and Milan, 2004). However, in order to implement successful river restoration projects, the function of riffle-pool sequences in terms of form and process must be completely understood.

Areas in rivers that experience changes in depth or width can cause areas of differing flow acceleration and deceleration. These differing flow regimes strongly impact turbulence generation and therefore, the associated sediment transport processes (Thompson and Wohl, 2009). Past research has focused largely on the maintenance of riffle-pool sequences, specifically in the context of stage dependant velocity reversal hypotheses ("VRH") (Keller, 1971). Numerous mechanisms have been proposed to explain riffle and pool formation and maintenance. However, little research has been completed on the three dimensional flow structures of these sequences and how this affects the depth of scour in pools and deposition height in riffles. More specifically, bed shear stresses are considered a fundamental variable in river studies with respect to calculating and analyzing sediment transport, scour and deposition along river reaches (Biron et al. 2004). However, little research exists with respect to the three-dimensional complexity of bed shear stresses (both laterally and longitudinally) due to the difficulty of estimating variables accurately in complex flow fields. Furthermore, the significance of

the turbulent structure in bed load transport has been well documented in the literature but poorly understood (Dollar, 2002). Additionally, the effect that spatial variations in mean and turbulent flow have on sediment mobility and maintenance of riffle-pool sequences is not well understood. Despite increasing understanding of the turbulent boundary layer, additional research is still needed in terms of understanding particle interactions and their implications for the mechanics of bed load transport and bedform development and maintenance (Dollar, 2002; Mazumder, 2000). In terms of riffle-pool sequences, the physical processes of sediment scour, transfer and deposition remain relatively unknown. Wohl and Thompson (2000) stated that an understanding of the variability along riffle-pool sequences is needed to completely understand bedload transport and bedform maintenance because of feedbacks between turbulence and the channel bed. For example, Clifford (1993), stated that differences in the near bed turbulence structure are caused by bed topography create differences in the entrainment of bed sediments, which then act to change bed topography.

Riffles and pools not only have a longitudinal segregation of bed sediments but also lateral sorting (Milne, 1982). Critical knowledge is lacking with respect to how these properties change or differ in straight versus sinuous channels. Rhoads and Welford (1991) indicated the need to embark on research that includes flow structure, sediment transport, bed morphology and bank erosion in both straight and sinuous streams. Welford's reasoning behind this had to do with the fact that the turbulence structure and sediment transport processes experience higher complexity in meandering reaches than straight reaches. The mechanisms of lateral bed material transport are related to

secondary circulations which form around meander bends. Milne (1982) stated that low sinuosity channels may reduce the incidence of very deep pools (scour holes). Secondary circulations around meander bends create an asymmetrical profile that influences lateral sediment transport, thus leading to the occurrence of deep scour in pools.

Milan et al. (2001) highlighted that additional research is needed on the turbulence structure, sediment transport and areal sorting mechanisms in riffle-pool sequences and in particular, a study that includes: 1) data from both straight versus curved reaches, 2) data that contains high-intensity turbulence measurements by providing point rather than cross-section averaged measurements and 3) data that observes a wide range of flow stages.

Figure 1.1 displays study site 1 and study site 2, as well as the surrounding area. The study sites are located along the Rouge River in Toronto, Ontario, Canada. More specifically, the study sites are located within the suburb of Scarborough within the City of Toronto (Latitude: 43.810455, Longitude: -79.141229).

The primary goal of this study is to assess the turbulence structure and potential scour in riffle-pool sequences in both straight and meandering channel sections of the Rouge River, Toronto, Ontario, Canada. More specifically this study will attempt to 1) assess the complex turbulent flow structure in riffle-pool sequences in the Rouge River at the study sites (Figure 1.1); 2) determine the role that the turbulence structure above riffles and pools plays in depth of scour in pools and deposition height on riffles (at varying flow stages), 3) assess how the controlling factors influencing riffle height and

scour depth differ in straight versus meandering reaches and 4) to characterize bed and sediment transport (at each site).

This thesis is organized into six sections. Section 1 discusses a brief introduction to the field study and related background information. Section 2 is a literature review that discusses relevant studies and field work already completed within the realm of riffles and pools. Section 3 and Section 4 are the methods and results section. Finally, Sections 5 and 6 present a brief discussion and overall conclusions for this study.

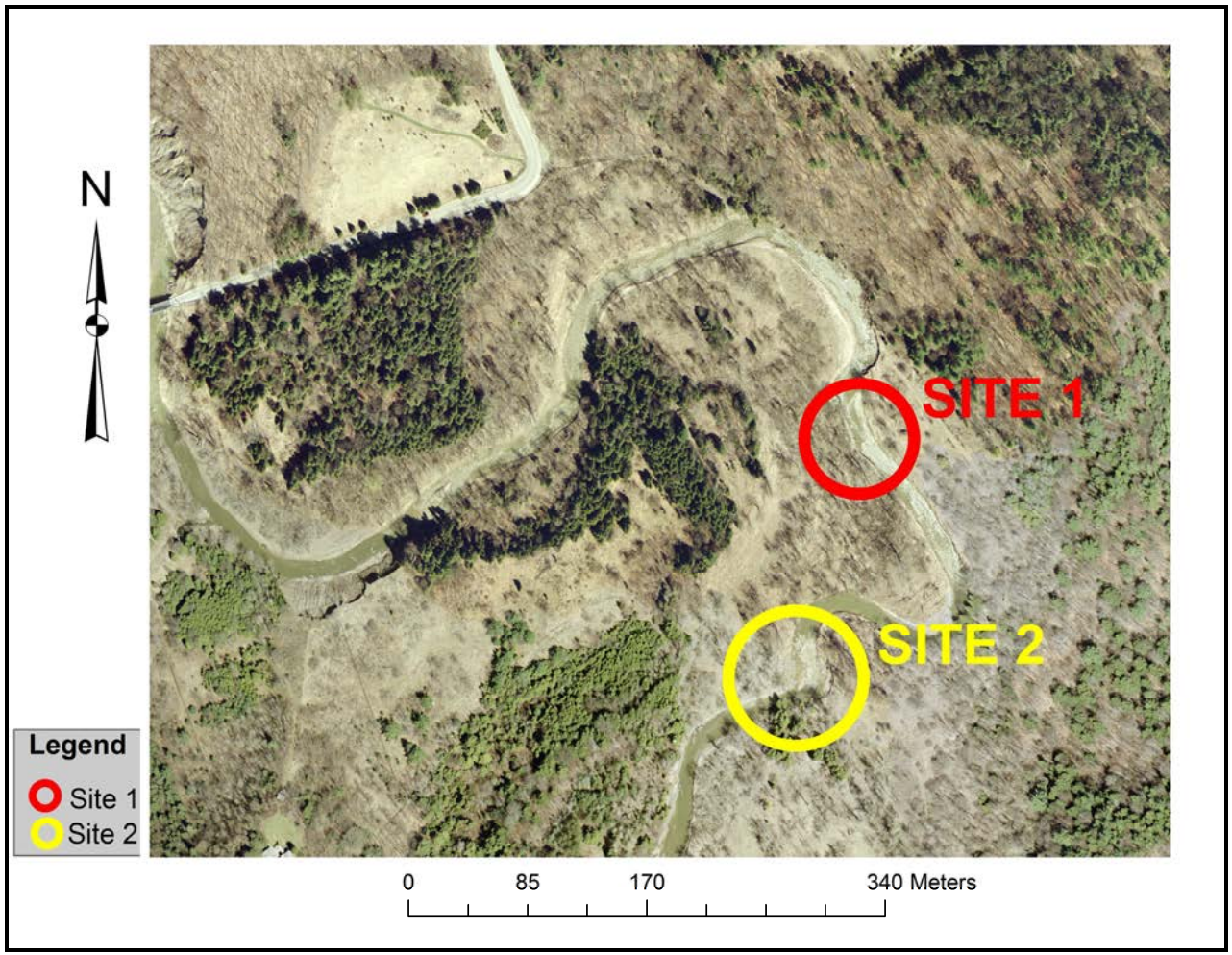

Figure 1.1: Orthorectified Imagery 2007 - Sites 1 and 2 (Latitude: 43.810455, Longitude: -79.141229) - Rouge River, Toronto, Ontario, Canada. Colour Air Photo (15 cm resolution) #649048520; Access granted by York University Map Library (First Base Solutions Inc. 2007)

SECTION TWO: LITERATURE REVIEW

2.1 Boundary Layer Theory

As water flows over the river bed, the interaction of water and the bed creates friction. The friction created is restricted to a layer (zone) adjacent to the river bed called the boundary layer (Allen, 1994; Robert, 2003). The velocities in the boundary layer range tremendously from approximately zero near the boundary river bed interface to the free-stream velocity at the outer edge of the boundary layer (Chanson, 1999; Robert, 2003). In natural setting most rivers are relatively shallow and characterized by relatively low roughness (i.e., small flow depth *d* to particle diameter D ratio), the boundary layer generally extends all the way to the surface (entire water column) (Robert, 2003).

The average bed shear stresses at a reach within the turbulent velocity profile can be defined as:

$$\tau = \rho g S d \tag{2.1}$$

where ρ is water density, g is acceleration due to gravity, S is slope and *d* is flow depth. The shear stress at any point within a turbulent flow, is defined by the relationship between the shearing force and the velocity gradient and is defined by:

$$\tau = (\mu + \varepsilon)\frac{du}{dy} \tag{2.2}$$

where ε is called the coefficient of eddy viscosity. Eddy viscosity is the friction within the flow that results from the vertical circulation of turbulent eddies (Robert, 2003). Since

dynamic viscosity μ is insignificant relative to the eddy viscosity, Richards (1982) and Robert (2003) simplified the equation and defined it as:

$$\tau = \varepsilon\rho \frac{du}{dy} \tag{2.3}$$

where eddy viscosity is not a constant value, rather, it varies with position above the bed and can be defined as:

$$\varepsilon = \iota^2 \frac{du}{dy} \tag{2.4}$$

where ι is the mixing length (Chanson, 1999; Robert 2003). The mixing length measures the degree of penetration of vortices within the flow. The degree of momentum exchange is dependent on the mixing length and the mixing length depends on the distance from the boundary and can generally be assumed to be equal to:

$$\iota = Ky \tag{2.5}$$

where K is known as the 'von Karman's constant' and is assumed to be 0.41 (Knighton, 1998). K is a dimensionless constant describing the logarithmic velocity profile of turbulent flows near the boundary. A turbulent velocity profile consists of three layers. Very close to the bed, a thin layer of laminar flows occurs and the thickness of the laminar sublayer can be defined by:

$$\delta = 11.6 \frac{v}{U*} \tag{2.6}$$

where U* is the shear velocity and shear velocity has the dimensions of velocity and can be determined from shear stress (Robert, 2003):

$$U* = \sqrt{\left(\frac{\tau_0}{\rho}\right)} \tag{2.7}$$

where τ_o is the bed shear stress. The thickness of the laminar sublayer decreases as the shear stress increases. Richards (1982) stated that this phenomenon is associated with the turbulence penetration close to the bed. This area of the bed is extremely important on the river bed as the fine bed materials become protected from the effects of turbulence generation (Richards, 1982). In most rivers, the flow is said to be 'hydrodynamically rough' (Robert, 2003). Under these flow conditions, the laminar sublayer may become disrupted by the formation of vortices from above the roughness elements and from the near bed individual particles (Robert, 2003). Therefore, in fully turbulent flow the velocity generally increases with height above the bed surface, in relation to:

$$U_y = b \ln\left(\frac{y}{y_0}\right) \tag{2.8}$$

where U_y is the average velocity at any point above the bed y and b is the velocity gradient that is present in the flow and y_o is the height above the bed where the velocity is found to be equal to zero. Richards (1982) and Robert (2003), stated that under uniform conditions, y_o is approximately D / 30.1 (where D is particle size). Finally, the value of b is used to estimate the shear stress exerted by the flow on the bed and can be defined as:

$$b = 2.5\, U* \tag{2.9}$$

And equation 2.8 can be rewritten as:

$$U_y = 2.5\, U* \ln\left(\frac{y}{y_0}\right) \tag{2.10}$$

where equation 2.10 is commonly referred to as the 'law of the wall' for the variation of velocity with height above the bed surface and is generally applicable to only the bottom 20% of the flow column. The law of the wall has mainly been used in empirical studies to

derive shear stress and roughness length (the point at which flow is still affected by interaction from the river bed) from measured velocity profiles and can be rewritten defined as:

$$U_y = b \ln y - b \ln y_o \tag{2.11}$$

When plotting U_y against *y* (elevation) above the bed, the relationship is expected to be linear between the two variables and can be expressed as (Robert, 2003):

$$U_y = a + b \ln y \tag{2.12}$$

where *a* and *b* are the intercept and the slope from the linear regression equations (i.e., velocity gradient) respectively. Robert (2003), showed that substituting equation 2.11 and 2.12, the following can be defined:

$$a = -b \ln y_o \tag{2.13}$$

and

$$-\frac{a}{b} = b \ln y_o \tag{2.14}$$

and

$$y_o = e^{\frac{-a}{b}} \tag{2.15}$$

Roughness length and bed shear stress estimates are determined from empirical measurements at a given vertical (i.e., position in the flow) and are therefore highly variable (Robert, 2003). The variability of the measurements is due to the local bed material conditions and/or the presence of bedforms (i.e riffle and pool units). A high density of measurements is needed in the near bed region (i.e., bottom 20% of the flow), in order to obtain an accurate and reliable estimate of bed shear stress and roughness

length (Biron et al. 1998; Robert, 2003). Lawless and Robert (2001) found that at greater distances above the bed, velocity profiles and therefore velocity gradients generally reflect the roughness exerted by the bed at larger spatial scales. Finally, in practice, Law of the Wall is generally used to describe the velocity distribution over the entire flow column for open channel flows.

2.2 Turbulence Structure in Fluvial Systems

In field studies, direct measurements with the use of a mobile ADV have hardly ever been attempted. Therefore, different indirect methods have been used (Dietrich and Whiting, 1989). Velocities are generally measured at a fixed point and are referred to as *Eulerian velocities.* Velocities at any point in the flow can be measured in three perpendicular directions as expressed in Table 2.1:

Table 2.1: ADV Measurement Chart

Velocity Component	**Coordinate Direction**	**Velocity Notation**
Downstream	*X*	*u*
Vertical	*Z*	*v*
Lateral	*Y*	*w*

The first direction is the downstream flow (*u*), the second is the vertical flow (*v*) and the third is the lateral flow (*w*). However, because the flow is turbulent, the velocity (in any which direction) is not constant, but rather it is variable through time (Robert, 2003).

Velocity fluctuations are defined by:

$$u' = u - U \tag{2.16}$$

Where u' is the deviation from the mean velocity U and *u* is the instantaneous velocity reading (downstream flow). Similarly to downstream flow, vertical (*v*) and lateral (*w*) flow components can be defined:

$$v' = v - V \tag{2.17}$$

and

$$w' = w - W \tag{2.18}$$

The average magnitude of the deviation from the mean for a given velocity reading reveals the 'intensity' of the turbulence for any of the three velocity components. Root-mean-square values are considered measures of turbulence intensity (Robert, 2003). For the downstream flow component, RMS is defined by:

$$RMS_u = \sqrt{\frac{[\sum(u')^2]}{N}} \tag{2.19}$$

where N is the total number of measurements (observations) made in a given output series (Robert, 2003). Similarly, expressions for the vertical and lateral flow components of the flow can be derived:

$$RMS_v = \sqrt{\frac{[\sum(v')^2]}{N}} \tag{2.20}$$

and

$$RMS_w = \sqrt{\frac{[\sum(w')^2]}{N}} \tag{2.21}$$

Equations (2.19), (2.20) and (2.21) can be combined to provide an expression called Total Turbulence Intensity or Turbulent Kinetic Energy (TKE) (Bradshaw, 1971; Clifford and French, 1993):

$$TKE = 0.5\rho(RMS^2{}_u + RMS^2{}_w + RMS^2{}_v) \quad (2.22)$$

TKE represents the energy extracted from the mean flow by turbulent eddies (Bradshaw, 1985; Robert, 2003). Until recently, the TKE method was not used extensively because of the difficulty in obtaining detailed and accurate turbulent measurements close to the bed and/or boundary layer in natural sand or gravel bed rivers (Dietrich and Whiting, 1989; Biron et al. 2004). The advancement in technology has led to the development of measuring devices such as the Acoustic Doppler Velocimeter (ADV), which has allowed detailed field measurements of turbulent velocity fluctuations in the three directions at high frequencies to be obtained (Biron et al. 2004).

Flow separation occurs when flow along a channel boundary develops an adverse hydrostatic pressure gradient, which becomes unstable and detaches from the boundary, which then forms a lateral zone of reverse flow called a recirculating eddy or wake (Tennekes and Lumley, 1994; Thompson, 2007). The separation area acts as a zone of high shear between the jet and recirculating eddy and is called a shear zone or 'shear layer'. The shear layer is characterized by smaller scale, periodic whirlpool like turbulent features called vortices. Constrictions along the bed surface of riffles and/or pools are capable of altering the patterns of sediment transport and the formation/maintenance of pools (Thompson, 2007). Near the downstream section of a pool unit, an upstream sloping section of the channel bed acts to influence the strength and location of

turbulence production (Thompson, 2004; Thompson, 2007). In this area of the pool exit slope, the decrease in flow depth acts to shorten vortices and decrease the angular velocities to satisfy conservation of angular momentum. Thompson (2007), stated that if sediment transport responds to these changes in the characterization of turbulence, then a feedback system between turbulence and topography should dominate the pool exit slope section.

The stretching of the vortex and the associated Reynolds stresses (discussed below) act to transfer energy from the larger scale vortices to the smaller scale vortices. This energy eventually leads to smaller vortices which are eventually dissipated by viscous stresses in the fluid (Tennekes and Lumley, 1994; Thompson 2007). Due to the fact that the vortices are in constant motion, the energy principle and fluid entrainment along the shear layer acts to create a narrow upstream zone of large vortices and a widening zone of energy dissipation in the streamwise direction. Therefore, this suggests that the characteristics of turbulence at any point in the flow are largely inherited from upstream characteristics. Therefore, the calculation of TKE can help to examine the intensity of turbulence as the more intense the turbulence is, the stronger the larger eddies are in comparison with the rest of the turbulence.

Small scale flow structures have been connected with sediment transport, however whether or not these short lived structures are of sufficient duration to directly affect the development of fluvial landforms (i.e., riffle-pool sequences) is still debatable (Ashmore et al. 2000). Structures in turbulent flows are central to turbulence production and to momentum exchange. However the connection of how these flows relate to the

morphological picture over rough boundaries still remains a controversial issue (Ashmore et al. 2000). It is widely known that coherent turbulent structures exist within the boundary layer. The main feature of turbulence over the boundary layer is bursting motions (sweeps and ejections) (Lapointe, 1992). Ejection and sweep motions on the river bed are only active a small fraction of the time but are responsible for most of the momentum exchange. These bursting motions may play a significant role and impact on the sediment transport processes. Figure 2.1, displays ejection events (fluid motions away from the boundary). These events are important for maintaining particles in suspension in the flow (Lapointe, 1992). Figure 2.1, also displays sweeps (downward fluid motions). Sweeps are faster fluid motions that may impact the movement of sediment on the bed surface (Lapointe, 1992). These structures are responsible for most of the turbulent energy production within a stream (Grass et al. 1991). The sweep and burst events are an examination of the instantaneous velocities measured parallel to *x* (downstream) and *z* (vertical) coordinates. These measured velocities allow for the identification of sweep and burst events based on the *Eulerian* 'burst detection scheme' of quadrant analysis (Lu and Willmarth, 1973).

The quadrant analysis allows for the identification of spatial and temporal positions on sweep and ejection events. Figure 2.1 displays four quadrants, of which quadrant 2 and quadrant 4 have been associated with sweep and ejection events, respectively (Robert, 2003). These quadrant events are responsible for the production of Reynolds stresses within the turbulent boundary layer. Reynolds stresses are another quantification of turbulent activity. Reynolds stresses are defined from the horizontal and

vertical flow fluctuations and the quantity is related to the exchange of momentum across a plane parallel to the mean flow direction. This momentum exchange gives rise to shear stress, τ_R (Reynolds Stresses) acting on the plane and are defined as:

$$\tau_R = -\rho\, u'v' \tag{2.23}$$

where u' and v' are the deviations from the mean for the horizontal and vertical flow velocity components respectively. The average product $-\rho u'v'$ is determined over a set time interval and is the Reynolds stress acting at that given point within the water column (Robert, 2003). The Reynolds method is widely accepted for obtaining accurate estimates of bed shear stress within natural rivers. For this study, Reynolds stresses will be determined by gathering point data at varying heights above selected positions along the study sites using an ADV.

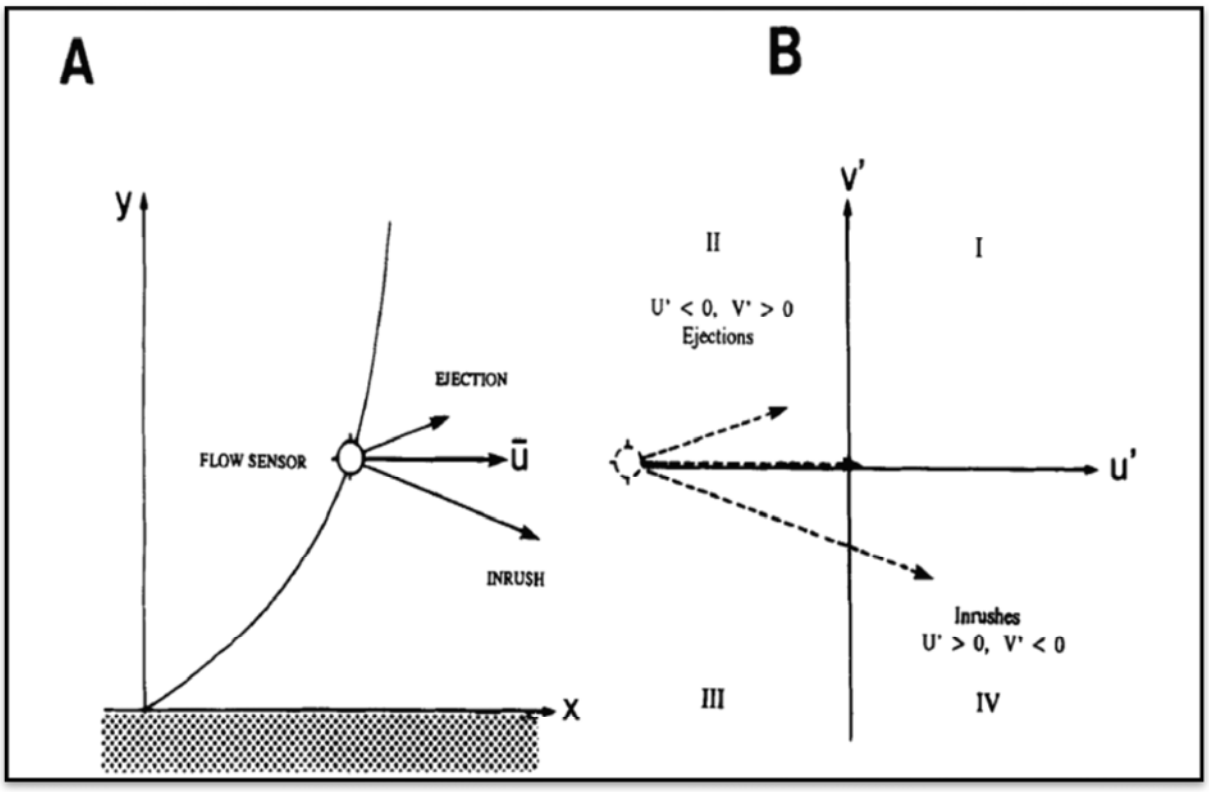

Figure 2.1: Eulerian Quadrant Identification (Lapointe, 1992). Panel A – bursting process relative to height above the bed. Panel B – quadrant analysis.

Numerous studies have utilized a quadrant analysis to observe turbulent fluctuations, where both horizontal and vertical flow fluctuations are considered in relation to upward or downward turbulent motions of varying intensities (Figure 2.1). Bursting motions from the bed have been shown to originate in the near wall region from alternating zones of low and high velocity streaks and sweeps (Robert, 1993). Sweeps can be defined as movements of fluid particles towards the boundary and ejections are defined as movement of fluid particles away from the bed and into the open flow. The transport of coarse bed material generally occurs during sweep and outward interaction flow periods. Further studies are needed to establish the link between the bursting

processes and the near bed region and the large scale flow structures within the boundary layer thickness (Robert, 1993).

Clifford et al. (1991), stated observations regarding the bursting process over smooth boundaries in flume laboratories may not be comparable to those rough boundaries observed over gravel bed rivers and therefore the bursting process may not occur over rough surfaces. However, Williams et al. (1991) observed that low-speed streaks were present over rough surfaces and concluded that turbulent flow structures can be observed over coarse grained river beds. Similarly, Drake et al. (1988) found that sweep transport events resulted in the entrainment of bed particles from areas typically 3 – 5 centimetres in diameter. They also observed that the sweep transport events were randomly distributed both spatially and temporally. These same events were shown to account for as much as 70% of total transport rate even though they occur only 9% of the time. Also, the instantaneous shear stress associated with the sweeps were on the order of three times the critical shear stress for initial entrainment (Drake et al. 1988). Finally, Drake et al. (1988) established that sweep events are associated with large scale turbulent fluctuations from the bed. Similarly, Robert et al. (1993) showed that turbulent fluctuations appear to be dominated by periods of 1 – 2 seconds and that there was a tendency for a decrease of the dominant frequency with an increasing height above the bed surface.

Researchers have indicated that the presence of flow turbulence and sediment transport in riffle-pool sequences may suggest that the *velocity reversal hypothesis* (VRH – to be discussed in section 2.4) is not necessary to explain the longitudinal variations in

surficial bed material size in riffles and pools (Clifford, 1993; Robert, 2003). As scientific understanding of riffle-pool sequences has developed, the interaction between riffle-pool morphology and sediment transport has been attributed to turbulence generation and decay (Clifford, 1993; Thompson and Wohl, 2009). For example, the varying channel morphologies between riffles and pools produce areas of different water depths, thus initiating flow accelerations and decelerations. This strongly impacts the turbulence generation and sediment transport around riffles and pools (Thompson and Wohl, 2009). Researchers have also noted that sediment transport conditions can occur where conditions are below the critical entrainment thresholds because turbulence creates instantaneous forces greater than the time-averaged values (Roy et al. 1999). The presence of turbulence structures at varying flow stages in riffles and pools may play a crucial role in determining riffle height and depth of scour in pools. For example, Sear (1996) found that riffles experience greater turbulent flows under base flow conditions. In contrast, pools do not experience the same level of near bed turbulence, therefore reducing the initiation of sediment entrainment. These turbulent structures lead to the riffle sections becoming tightly packed and interlocked and pool sections being poorly sorted (Sear, 1996). These differences lead to structured stable riffle regions which causes the need for higher critical shear stress entrainment thresholds to initiate sediment transport. Additionally, hypotheses for riffle-pool maintenance have suggested that flow converges on riffles at low flows which creates armouring, gradual incision and diminishing relief. During high flow periods, flow converges in pools, causing rapid scour.

Prior studies suggested that turbulent fluctuations in the near bed region scale in magnitude with grain size (D_{84} - particle size for which 84% of the material found on the bed is finer) and the periodicity is generally attributed to the vortex shedding from large particles, which is considered the dominant energy dissipation over gravel bed rivers (Levi, 1991; Clifford et al. 1992). Many studies have highlighted the relationship between flow turbulence, bed morphology and sediment transport (gravel) in fluvial environments (Drake et al. 1988; Williams et al. 1991).

2.3 Energy Expenditure

The only form of energy that is delivered to a river system is potential energy. Water flows downgradient (due to gravity) and potential energy is converted into kinetic energy. Kinetic energy is used in the transformation of channel form (e.g., bedload transport). Rivers are thought to be in a constant state of 'equilibrium'. On one hand the state of equilibrium can be defined between the water and the sediment supplied to the system and on the other hand channel morphology itself. In search for steady state conditions (state of equilibrium), rivers are considered stable and this is defined by a system in which the least amount of work is needed to perform and maintain the system (Keller and Melhorn, 1978). A river channel is thought to adjust its form in such a manner as to minimize its energy expenditure. The river adjusts its geometries in both the horizontal and vertical planes (i.e., width and depth respectively) to accomplish a reduction in energy loss per unit length or area (Keller and Melhorn, 1978).

Yang (1971), applied the aforementioned concept to rivers (reach scale) and introduced the 'Law of Least Time Rate of Energy Expenditure'. Yang (1971, 1987)

established that, generally rivers adjust their morphology to minimize the rate of energy dissipation. Energy dissipation is equivalent to the minimization of unit stream power. Examples of this included a river system instituting morphologies such as riffle-pool sequences and meanders in order to modify its channel to reduce the rate of energy expenditures, as both changes increase path length in different planes. Yang established this hypothesis because he postulated that rivers cannot adjust discharge, so the minimization of unit stream power implies that a minimization of energy slope occurs instead. Yang later showed that this hypothesis/principle could be used to help explain the formation and maintenance of riffles and pools. Furthermore, Yang suggested that the elongation of pools is likely the response of a river towards a tendency to minimize energy slope.

Similarly, Thompson et al. (1998) and Thompson (2001) also showed that pool length, turbulence production and secondary flow development are all linked in a complex feedback system. Secondary flow and turbulence production lead to head loss, so Thompson (2002) believed that this notion is a good enough reason to postulate that pool length can greatly influence energy slope. To support this belief, Thompson (2002) found that pools elongate at a rate 10 times higher than they deepen. Finally, because rivers tend to experience changes that minimize the rate of energy dissipation, adjustments in pool length with associated changes in turbulence generation may represent the primary morphologic response to imposed discharge conditions.

Overall, the differing lengths of pools represent a balance between the role of velocities and their ability to move sediment in and out of the pool unit and the tendency

for pool elongation, maintenance or formation as the system changes to reduce the time rate of energy expenditure. Yang's energy expenditure belief focuses on the mean conditions of flow and does not take into consideration the instantaneous forces associated with turbulence production and/or generation and sediment transport processes (Thompson, 2007).

2.4 Riffle-pool sequences

Riffles and pools are bed features generally found in coarse-grained rivers. However, they have been found in mountain streams, which are characterized by resistant channel boundaries, large roughness elements and irregular flow patterns (Harrison and Keller, 2007). They are commonly located along low to moderate slopes (<1%) (Clifford, 1993). Riffles and pools are found in both straight and meandering rivers, however they are more pronounced in meandering reaches (Knighton, 1998). Figure 2.2 displays the riffle-pool sequence as observed along a longitudinal profile. In this diagram it is evident that riffles are represented by high points in the bed topography, while pools are represented by low points in the bed topography (Keller, 1971; Robert, 2003). Under base flow conditions riffles are represented by faster flows, steeper water surface slopes and

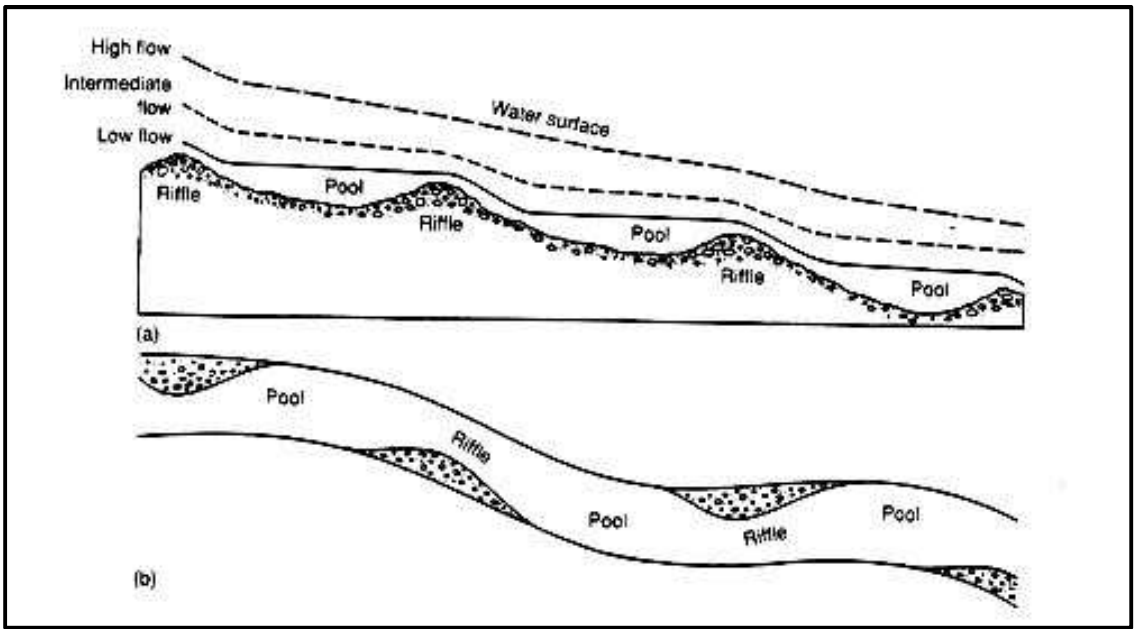

Figure 2.2: The riffle-pool sequence and bed features (Source: Dunne and Leopold, 1978).

Table 2.2: Bed and sediment transport characteristics of riffles and pools

Bedform	**Riffle**	**Pool**
Bed Topography	High	Low
Water Depth	Shallow	Deep
Water Velocity	Fast	Slow
Water Surface Slope	Steep	Moderate
Bed Material	Coarse	Fine
Cross-section Profile	Symmetrical	Asymmetric
High Flow	Fill	Scour
Low Flow	Scour	Fill

coarser bed materials (Table 2.2). Riffles are generally characterized by convergent flow and moderate transport competence (Clifford and Richards, 1992). In contrast, pools are associated by slower flows, moderate water surface slopes and finer bed material (Table 2.2) (Clifford and Richards, 1992; Robert, 2003). Pools are generally characterized by divergent flow and low sediment competence (ability to move sediment). The identification of riffles and pools and the riffle-pool sequences sometimes depends on river stage and discharge. In practice, problems arise in defining riffles and pools because there is a growing appreciation in the literature that the riffle and pool are part of a single bedform, named the bar unit (riffle-pool sequence) (Gregory et al. 1994).

Riffles and pools have a dominant wavelength spacing of 5-7 channel widths; however large variances in the measurements of this spacing have been reported in the literature because of various channel sizes and channel gradients present in rivers (Clifford, 1993; Carling and Orr, 2000; Robert, 2003). For example, Knighton (1984) stated that riffle-pool spacing can range from 1.5 to 23.3 channel widths, which an overall mean of 5.9 channel widths. However, his statements regarding spacing just confirm the tendency for riffle-pool spacing to on average fall within the range of 5 – 7 channel widths, which is remarkable given the fact that channel widths can range from a few meters to much greater than 100 m in natural settings (Gregory et al. 1994). Leopold and Wolman (1957) were the first to relate the riffle-pool sequence to stream width when they determined that wavelength was more directly dependent on width than discharge. After, Leopold et al. (1964) noted that the spacing of riffles and pools was 5 – 7 channel widths. Furthermore, Leopold et al. (1964) observed that straight (non-meandering)

channels generally had an undulating bed and alternate along its length between the deep portions and shallow portions, spaced more or less regularly at a repeating distance equal to approximately 5 – 7 channel widths. Keller and Melhorn (1973, 1978), stated that riffle-pool sequences are initiated at 3 channel widths in straight channels, however, the spacing approaches an equilibrium of 6 channel widths in meandering channels. As well, additional riffle-pool units may develop as sinuosity increases; it is said that additional units are established on the river bed in order to control the energy expenditure of the river. Carling and Orr (2000) stated that an actively meandering river should be subjected to greater scour and fill, creating variation in bed level adjustments.

Numerous publications regarding the spacing of riffles and pools are referenced in materials surrounding the riffle-pool sequence and/or gravel bed rivers. These numerous studies regarding the spacing of riffles and pools may have led to the false impression that the riffle-pools sequences are more stable than they really are (Gregory et al. 1994). However, several studies have found that because of the dependence of the riffle-pool sequence on the competence of flow to perform bedload transport and sort the supplied sediment in the stream channel, the characteristics of pools and riffles can be altered drastically by small or large changes in calibre of sediment loads (Milne, 1982; Gregory et al. 1994). These notions are becoming increasingly more significant in rivers that are surrounded by urban areas, as sediment and water supply are drastically altered by urbanization.

The height of riffles and depth of scour in pools have not been studied extensively. One of the few studies on this topic was conducted by Carling and Orr

(2000). They found that riffles rarely exceed 2 m in height (relative to the zero-crossing), with the majority of riffles being less than 1 m high (mean: 0.4 m). Their study also found that reach-average riffle height increased with an increase towards bankfull water depth and that riffle height is a constant proportion of the reach-average bankfull depth (Carling and Orr, 2000). Similarly, riffles were found to be symmetrical, which is in contrast to previous asymmetrical findings where riffles had longer stoss sides compared to the length of the lee side. Similarly, with respect to pools, Carling and Orr (2000) found that pools rarely exceed 2 m in depth (below the zero-crossing) with an average scour depth of 1 m. They also found that depths were only 1-2% of the pool length. Pool lengths were positively skewed and only a few pools were found to be greater than 100 m in length. Similar to riffles, Carling and Orr (2000) found that pools were symmetrical or had proximal upstream slopes shorter than the distal downstream slopes. This is in contrast to previous thought as pools were considered to be asymmetrical with longer proximal sections compared to the length of the distal sections. Carling and Orr (2000) concluded that the lack of preferred asymmetry means that there is no statistically significant difference in the distributions of stoss and lee side angles.

As previously stated (Table 2.2), bed material in pools is usually finer than that in riffles. The most widely known reason for this sediment sorting pattern is the VRH. The VRH states that the rate of change in velocity in pools is greater than that in riffles for flow conditions at or near bankfull capacity (Robert, 2003). It can also be shown that the velocity in pools under bankfull conditions may actually exceed the velocity in riffles. The VRH has been proposed by many researchers as being the dominant reason for riffles

displaying coarser bed material than that found in pools. VRH has also been suggested as the dominant reason to maintain bed morphology (Harrison and Keller, 2007). The higher velocity in pools likely leads to the movement of coarse material through the pool with deposition along the riffle where, under peak flow conditions, the average velocity or bed shear stresses could actually be lower than that observed along the pool units (Robert, 2003; Harrison and Keller, 2007). Velocities below the critical VRH cross over point display the opposite pattern. Generally, the finer bed material is still in motion along the riffles and deposited in pools where the velocity is lower than that found along the riffle sections (Robert, 2003).

However, researchers have shown that the VRH does not always occur in all river reaches. This is likely due to the flow intensity above riffles and pools and its variation with flow stage. Different river reaches have differing complexities of bed morphology, surface texture, sedimentary structures and associated bed-flow interactions (Carling, 1991; Clifford and Richards, 1992; Robert, 1997; Robert, 2003). Numerous studies including but not limited to Gilbert (1914), Keller (1971), Lisle (1979), Sear (1996), Robert (1997) and Milan et al. (2001) have shown that many rivers exhibiting riffle-pool sequences indeed do undergo a reversal in flow parameters. However, numerous studies have also documented a flow intensity that may converge between pools and riffles as discharge increases but not necessarily reverse (Harrison and Keller, 2007). Clifford and Richards (1992) stated that reversal may not occur in some field sites because of local variations and differing complexities in the riffle-pool morphology. Similarly, Booker et al. (2001) stated that a lack of a dataset containing spatially hydraulic data adds to the

difficulty in determining the maintenance of riffles and pools. As well as, Booker et al. (2001) stated that a data set or study which has high density (measurements per area) and high spatiality (measurements of carrying flow depth) of point measurements on a natural river is lacking. Additionally, they stated that a study at or near bankfull discharge has not been completed. The difficulty in observing scour in pools and flow reversal is due to the fact that high magnitude, low frequency flows do not occur often and that channel conditions during floods generally make field measurements impossible.

Finally, Carling and Orr (2000) showed that riffle-pool morphology is a function of stream gradient. Specifically, riffles and pools become longer and increasingly more asymmetric with reduced vertical expression as the channel gradient decreases.

2.5 Meander Morphology

Riffle-pool sequences and the degree of channel curvature both affect scour and sediment deposition patterns during both high and low flow events. In addition to channel geometry, pieces of wood, boulders and bedrock outcrops often create channel constrictions, which significantly alter the channel hydraulics (Thompson et al. 1999). In situations like this, riffle-pool geometry is controlled by constrictions where flow and sediment converged. The convergence of flow and sediment encourages scour and/or pool maintenance.

In addition to flow convergence, flow divergence and sediment transport characteristics, meander morphology is found to significantly control processes in rivers and is believed to be a fundamental component of fluid dynamics. According to Leopold and Wolman (1957), meandering is thought to be an inherent property of rivers. Meander

morphology may be an expression of bankfull discharge. Bankfull is the point at which the river can contain water in movement before it breaches the river bank walls and moves onto the floodplain. Meander wavelength, amplitude and radius of curvature are assessed at bankfull width.

In general, a meander wavelength, which is the distance between two successive meander bends (Figure 2.3), is typically 12 channel widths. The degree of curvature of a meander bend is measured by as the radius of curvature, which is defined as the radius of the circle of which the meander is an arc and the radius of curvature is generally found to have values between 2 and 3 channel widths. The third component of meander morphology is channel sinuosity. Channel sinuosity is a measure of the deviation from a straight channel and is defined as the ratio of the channel length to the path length of the channel. Generally rivers are considered meandering when a sinuosity of greater than 1.5 exists (Robert, 2003).

Flow and sediment transport dynamics along meandering channels are controlled by changes in the bed topography across the river and downstream along the channel (Knighton, 1998). The cross-sectional shape at the meander bend is generally asymmetrical, with the deeper portion of the channel being located along the outer bank and a shallow section extending from the inner bank towards the centre of the channel (Figure 2.4). The scour hole (pool section) generally is observed around the outside portion if the meander bends, whereas, the inner shallow section is an area of deposition referred to as a bar or a ‘point bar’.

The asymmetric channel cross-section in meander bends (due to sediment sorting via secondary circulation) favours the development of lateral sediment sorting along the bends, where coarse particles then to concentrate near the bottom of the pool section, with a gradual fining towards the inner bank (Robert, 2003). Sediment particles resting on the sloping surface are subject to drag forces, gravitational forces and velocity currents. The drag forces promote downstream movement and are proportional to the square of the particle diameter. The gravitational forces, promote downslope movement across the channel. The velocity currents promote secondary circulation (to be discussed in subsequent paragraphs). The gravitational force is proportional to the cube of the diameter (particle mass) and the near bed velocitiy forces the largest particles to be deflected downslope more directly than the finer ones due to their greater mass (Whiting, 1996; Powell, 1998; Knighton, 1998). Furthermore, finer particles tend to move inwards due to the influence of secondary circulation.

Secondary circulation in curved (meandering) rivers is caused by a combination of centrifugal forces and pressure gradient forces acting on the meander bend (Figure 2.4). The centrifugal force acting on the water flowing around the bend causes a build-up of water adjacent to the outer bank which is known as the ‘water super elevation’ (WSE). From Figure 2.4, it can be seen that the WSE results in as titling of the water laterally across the channel. The change in the WSE across the channel in the meander bend increases the average downstream velocity and the increase becomes more apparent as the ratio of radius of curvature over width decreases. The centrifugal forces acting on the flow in meander bends represent outward directed forces acting on the flow (Robert,

2003). Due to the curved motion and the buildup of water along the outer bank arises a force equal and opposite the mean centrifugal forces (inward force towards the inner bank). The balancing inward acting forces are a pressure gradient force. The result is a secondary circulation (spiral motion) cell being dominant over the thalweg (Figure 2.4). Figure 2.4 displays the characteristic pattern of secondary circulation, where the flow cell is oriented towards the outer bank, plunging along the outer bank and then oriented towards the inner bank in the vicinity of the bed (Allen, 1994; Powell, 1998; Robert, 2003).

A prominent feature of flow through meander bends are zones of high velocity that shift from the inside to the outside of the channel. Additionally, the zone of maximum bed shear stress gradually shifts toward the outside bank as the flow enters the central portion of the bend (Kighton, 1998; Robert, 2003). Furthermore, meander bends have longitudinal and lateral variations in bed material size which work in conjunction with riffle-pool sequences to form a characteristic bed material sorting pattern. In addition to secondary circulation, the tilting of the water surface

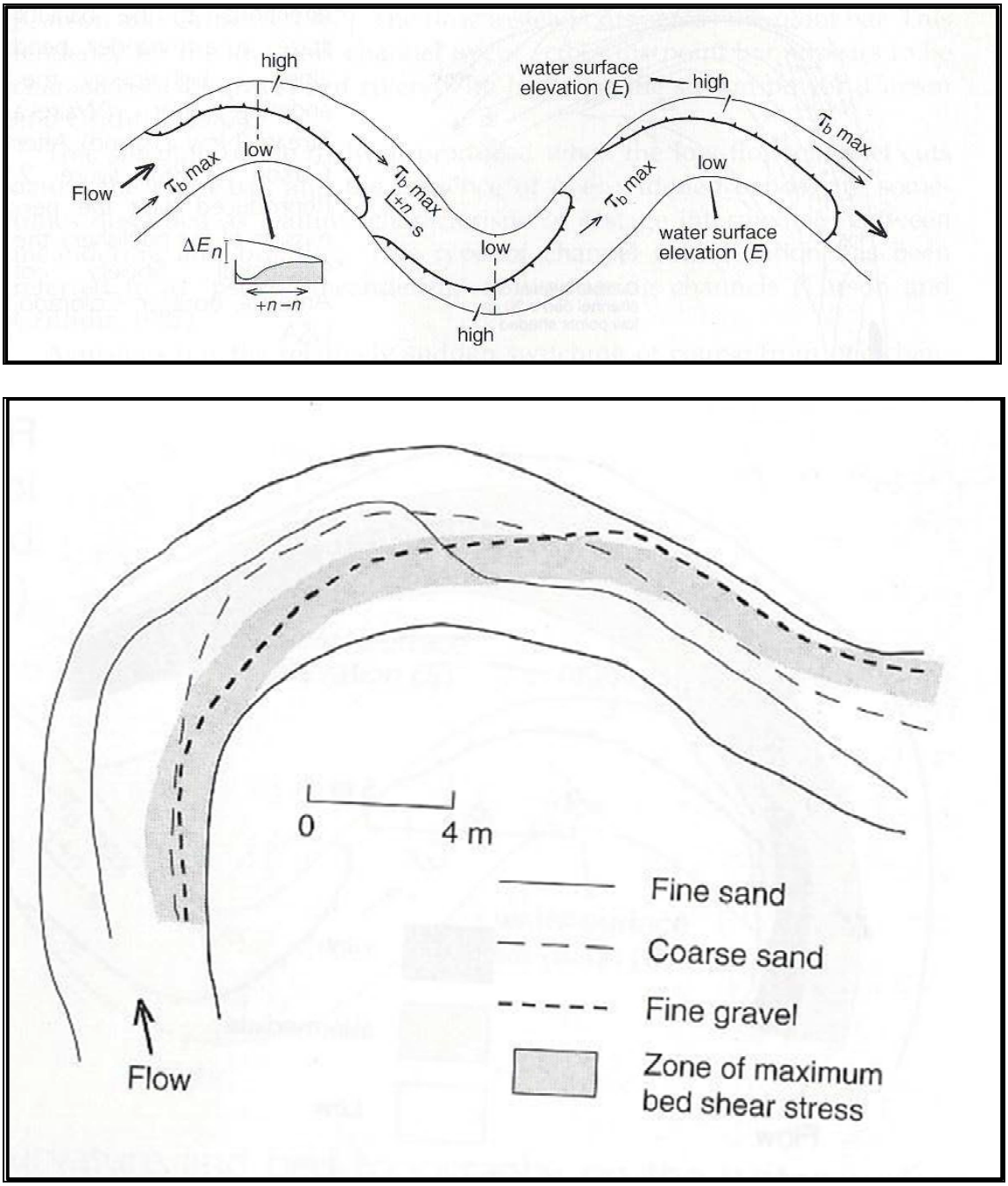

Figure 2.3: Meander Morphology (Dietrich, 1987; Powell, 1998; Robert, 2003)

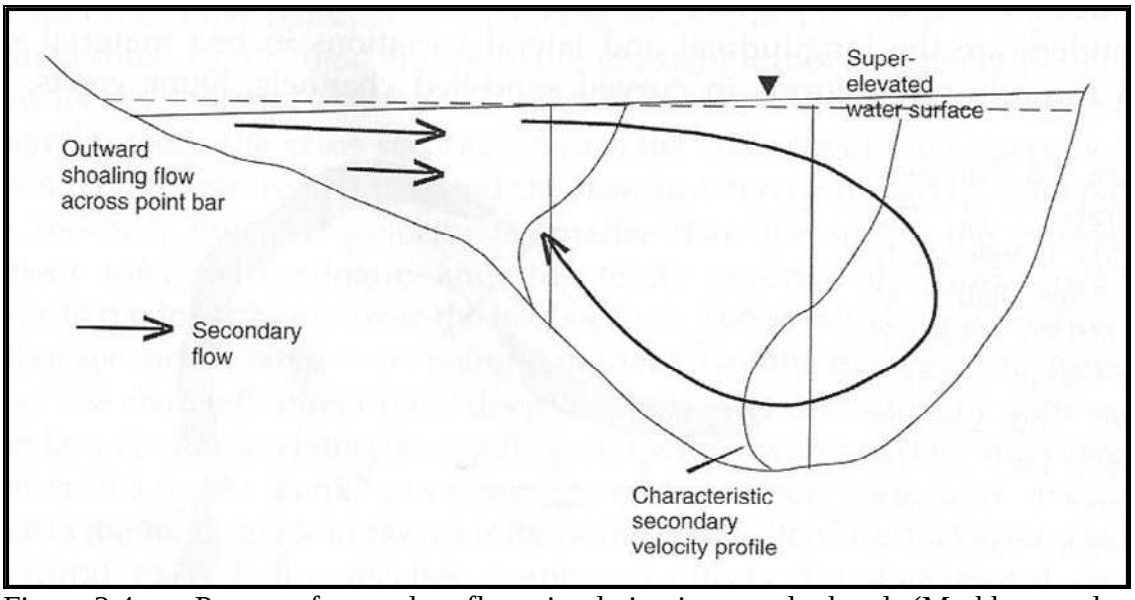

Figure 2.4: Pattern of secondary flow circulation in meander bends (Markham and Thorne, 1992)

generated by the curvature also generates large cross-stream variations in bed shear stress and the corresponding velocity (Robert, 2003). The centrifugal forces on the flow through a meander bends act to produce a zone of maximum bed shear stress that shifts from near the inside upstream bank to near the outside downstream bank (Dietrich, 1987; Robert, 2003). The riffle-pool sequence further enhances or alters the near-bed flow velocity as it increases the lateral or cross-stream variation in bed shear stress and promotes rapid shifting of the zone of maximum bed shear stress across the channel. In addition, fine and coarse sediments generally trade positions as they move through the meander bend. The trading of places between fine and coarse sediments results from the inward-acting secondary flow and the outward acting gravitational force. That is why large particles tend to move outwards under the influence of gravitational forces acting on the transverse slope, while smaller particles tend to be carried inward towards the shallower portion of

the channel, under the influence of secondary circulation (Powell, 1998). The cross-stream movement in opposite directions of coarse and fine sediment results in a switch in the cross-stream variation in bed material size. Upstream from the meander apex, the bed material size tends to become coarser inwards, whereas at the downstream end of the meander bend, the bed material size tends to be finer inwards.

The majority of research/studies completed on meandering rivers have been conducted on sand bed rivers. Many researchers argue that significant differences exist between gravel bed and sand bed rivers in terms of both meander geometry and flow and sediment transport processes (Carson, 1986; Carson and Griffiths, 1987).

2.6 Bedload Transport Flow/Sediment Transport Characteristics

Bedload transport in rivers is spatially and temporally extremely variable. A universal bedload transport equation has yet to be developed as there is no particular relationship between bedload and discharge. No relationship exists because bedload often moves in the form of pulses (intermittent stop and starts) and bedload and bed material calibre are spatially and temporally extremely variable. As well as hydraulic conditions are generally unsteady, velocity profiles are often nonlogarithmic and in gravel bed rivers, form drag is often associated with coarse bed roughness (Buffin-Belanger et al. 2000; Wohl and Thompson, 2000; Lawless and Robert, 2001; Hassan and Church, 2001; Dollar, 2002). Previous work on bedload transport in gravel bed rivers and more specifically riffle-pool sequences, suggested that transport could be defined in a series of phases. Phase I outlined a period where armour was broken up and Phase II outlined a period where transport occurred. These phases were then used to explain the cycles of

scour and fill in riffles and pools (Jackson and Beschta, 1982). However, later work by researchers (MacVicar and Roy, 2011) demonstrated that sediment transport in gravel bed rivers was best described as 'partial mobility'. Partial mobility is best described as a condition where some sediment grains on the river surface are in transport, while others remain immobile. The notion of partial transport has been accepted by many (Ashworth and Ferguson, 1989; Lisle, 1995; Church and Hassan, 2002; Wilcock and DeTemple, 2005; MacVicar and Roy, 2011) through a broad range of flow conditions and it has been stated that it must be incorporated into models of sediment transport and scour and fill in riffle-pool sequences.

Bedload transport is difficult to measure, although in most recent decades the use of bedload traps and tracer pebbles/clasts as well as other methods have been frequently utilized (Sear et al. 2000; Hassan and Church, 2001; Habersack, 2001; Dollar, 2002). Much of the difficulty involved in the prediction of bedload transport rates is due to the complexity and irregularity of natural coarse grained river bed surfaces (Robert, 2003). More specifically, problems arise because of the wide range of particle sizes, the effect that bedforms play on shear stress partitioning and bedload movement. Also, the high spatial variability of local traction forces exerted on the bed due to various grain sizes, changes in flow gradients, bed undulations as well as various river bed features including but not limited to meander bends and bars cause high complexity (Robert, 2003). Previous research on bedload transport within gravel bed rivers has come to recognize that partial bed material transport occurs rather than continuous movement of the majority of clasts. As well, research has found that the majority of bed material remains

in place for extended periods of time because of the presence of small-scale bed structures (Dollar, 2002). Similarly, Hassan and Church (2000) have shown from experimental work on gravel bed rivers that bed material transport is extremely sensitive to bed surface structure and/or grain size on the river bed. Hassan and Church (2000) found that structure has been shown to carry between 17% and 47% of the stress, bed grains >50% and river load <4%. Hassan and Church (2000) also found that the threshold of initial motion within structures (or pebble clusters) occurs at 4.5 times the shear stress associated with the average initial motion. The value Hassan and Church (2000) reported substantially higher than values commonly calculated in laboratory flumes and they stated that the primary reason for an increased value was likely due to bed structure and grain/clast packing.

Wohl and Tompson (2000) found that riffle-pool sequences exhibit spatial differences in the turbulent structure that likely control bed topography by influencing bedload transport. Booker et al. (2001) stated that nearbed velocities and bed shear stresses commonly decreased on riffles and increased in pools with increasing discharges toward bankfull. They also stated that secondary flow routes the near-bed flow over the downstream end of the riffles and into the pool-head away from the pool centre. They also suggested that the VRH is insufficient to explain the maintenance of riffle-pool sequences and therefore maintenance has to be related to the changes in spatial hydraulic patterns (Booker et al. 2001; Dollar, 2002).

The majority of bedload transport equations use some form of the threshold of initial motion to account for bedload transport rates. More specifically, this means that

most equations assume that the rate of bedload movement is a function of the 'excess' shear stress or excess steam power (Robert, 2003). Below are the two most common expression used in bedload transport equations, where transport rate (I_b) can be either a function of excess shear stress or excess stream power (Knighton, 1998):

$$I_b = f\ (\tau_0 - \ \tau_c) \tag{2.24}$$

or

$$I_b = f\ (\omega - \ \omega_c) \tag{2.25}$$

where subscript *c* refers to the critical stage and f indicates that it is a functional relationship (Robert, 2003). Using stream power measurements, Bagnold (1977, 1980 and 1986) showed that in addition to excess stream power, the bedload transport rate can be seen as an inverse function of the relative roughness and/or ratio of flow depth (d) to grain size (D). Bagnold further revised his initial stream power expressions for bedload transport to include a wider range of particles sizes to include gravel bed rivers (Robert, 2003). The expression for bedload transport Bagnold defined is expressed as:

$$I_b\ \alpha\ (\omega - \ \omega_c)^{\frac{3}{2}}\ (\frac{d}{d_r})^{-\frac{2}{3}}\ (\frac{D}{D_r})^{\ -\ \frac{1}{2}} \tag{2.26}$$

where d_r and D_r are arbitrary references values of flow depth and grain size, respectively (Robert, 2003).

In order to understand riffles and pools in terms of their flow characteristics and sediment transport behaviour, spatial characteristics must be understood and taken in consideration. Bedload transport, scour and fill patterns are strongly linked to channel morphology (Richards, 1976). Riffle units generally act as sources and sinks for sediment; at lower discharges, sand-sized particles move over a stable gravel bed surface

in the riffle regions and settle on top of the coarser sediments at the base of pools. As discharge increase the bedload transport in pool exceeds the rate in riffles (i.e., initiation of VRH), which acts to uncover the coarse deposits in the pool units. From numerous studies, it has been understood that the interaction between morphology and sediment transport has been attributed to turbulence generation and dissipation along the riffle-pool sequence. Areas of rapid change in depth or width, initiate flow acceleration and deceleration, which substantially impacts the turbulence generation and therefore the associated sediment transport. Therefore, it is critical that any study examining riffle and pool units must take into consideration turbulence generation, sediment transport characteristics and riffle-pool morphology in order to full understand and appreciate the processes at work and draw accurate hypotheses regarding riffle and pool maintenance and evolution.

SECTION THREE: METHODOLOGY

3.1 Research Objectives

There has been limited research on the three dimensional flow structures of riffle-pool sequences, more specifically on how they influence depth of scour in pools and deposition height on riffles. This study emphasizes the turbulence structure of riffle-pool sequences at two study sites within the Rouge River, Toronto, Ontario. By obtaining three-dimensional data using an ADV and by assessing the bathymetry using survey techniques this studies aim was to identify the depth of scour in pools and deposition height on riffles at varying flow stages at the two study sites within the Rouge River. By using two differing study sites, data could potentially be examined to see if differences exist between straight and meandering reaches (Study Site 1 versus Study Site 2). Finally, bed and sediment transport characteristics at both study sites 1 and 2 can be evaluated using various bed sediment collection techniques.

A field-based project was initiated and three-dimensional velocities and turbulence intensities were measured with an ADV. Sediment sorting and transport patterns were observed by introducing a combination of painted tracer pebbles, permanent bedload traps and handheld bedload samplers.

3.2 Study Site

The Rouge River consists of approximately 430 km of defined river and stream channels in its watershed (TRCA, 2007). Over the past few decades, urbanization and

various development projects have been occurring in the upstream regions of the Rouge River watershed. The Rouge River has adapted to such urbanization practices by altering its stream network (TRCA, 2007). These alterations have led to destabilization and consequently have led to enlargement and channel adjustment as a result of hydrologic channels.

Study sites 1 and 2 (Figures 1.1) are situated in the Lower Rouge River (Strahler Stream Order = 5) near the Sheppard Avenue East and Meadowvale Road intersection, Toronto, Ontario. The Lower Rouge River was chosen because of its relatively un-urbanized area in comparison to the Upper Rouge River or the Credit River. Site 1 and 2 differ because site 1 is represented by a straight section pool-riffle-pool sequence and site 2 is represented by a meander bend pool-riffle-pool sequence. This description of the study sites is better illustrated by the topographic and bathymetric surveys depicted in subsequent sections. The analysis of two study sites rather than a study composing of any greater number of sites was chosen because of the complexity of measurements being made at each study site (to be further discussed in subsequent sections). Due to such complexity and density of measurements, it would not be logistically possible or feasible to compare the turbulence structure and sediment transport characteristics at more than two study sites.

Site 1 and 2 (Figures 1.1) were free from obstructions such as logs, boulders, bridges, weirs and other flow confining structures which can result in back water or surge and vortices. Sites 1 and 2 were also remote from tributary confluences to avoid the influences from merging flows. The selection of a 10 m transect increment was based on

field visit experience, orthoretified image interpretation and topographic survey data. The choice of an equal distance approach for transect selection is preferred over a target specific (i.e., pool entrance/exit slope, riffle entrance/stoss side) approach, to keep variables consistent between site 1 and site 2. Also, the choice of an equal distance approach was chosen without reference to channel form and will be used as the basis for a stratified random sample design. The choice of an equal distance approach also allows the sections (transects) to represent the range of channel characteristics between riffles and pools.

3.3 Cross-Section Placement

Site 1 encompassed seven transects, permanently placed at 10 m intervals downstream. The initial transect was placed at the midpoint of the first pool (defined by the greatest depth). Site 2 also had seven transects, permanently placed at 10 meter distances downstream. Cross-sections were measured perpendicular to the center line of the channel. Each cross-section was permanently fixed into the ground using survey stakes. Two survey stakes were hammered into the bank at the end of each cross section. Each survey stake was connected using nylon rope to enable the identification and marking of verticals (permanent measurement points) to be used for measurement. The nylon rope was tied as tight as possible to each survey stake to minimize sagging and to ensure the placement of verticals was as accurate as possible. Each cross-section and each vertical along each cross section was surveyed using a Total Station for both site 1 and 2.

3.4 Flow Measurements

Discharge measurements were obtained using a Sontek Flow Tracker Handheld ADV. Along each transect (Site 1 and 2) approximately 10-15 verticals were established depending on the bank width of the particular transect in question. Verticals were marked along each transect for both sites using fluorescent tree tags in order to maintain consistency and ensure measurements were made at the same point each time. Discharge measurements were made once weekly from the end of April 2010 until July 2010. Measurements were conducted for durations of 1 minute at each sampling point, in order to obtain accurate flow measurements.

Depending on the depth in question along the specific transect for site 1 and 2; the number of flow measurements varied. If water depths were 0.3 m or less, one flow measurement was taken at each vertical on each cross section for sites 1 and 2. If water depths were greater than 0.3 m, flow measurements were taken at 0.2*d* and 0.8*d* (where *d* is flow depth) at each vertical on each cross section for sites 1 and 2. Stream discharge was calculated by determining the product of Qi (discharge). Q_{Total} was calculated by determining Qi for each vertical by using the following equation:

$$Qi = Wi \times Vi \times Di \tag{3.1}$$

where Vi is the velocity measurement in metres per second (m/s), Wi is the width in meters (m) and Di is measurement or reading depth (m). Q_{Total} was then calculated for each transect by summing the vertical Qi measurements:

$$Q_{Total} = \sum Qi \tag{3.2}$$

The discharge Q for each site was then calculated by taking an average of the Q_{Total} measurements for each transect. Q was therefore defined as:

$$Q = \frac{(\sum Q_{Total})}{N_t} \quad (3.3)$$

where N_t is the number of transects located at the site (7 per site).

Flow measurements were made using a Sontek ADV. The ADV unit had a three dimensional (3D) down looking sensor that measured flow in the u (streamwise), v (lateral) and w (vertical) directions (Figure 3.3). The unit measures flow in a small sampling volume (less than 0.25 cm^3) and allows for measurements 5 cm away from the sensing element (Figure 3.3). The sensor was mounted on a 40 cm stem and was able to measure velocities at heights above the bed as low as 5 mm. The ADV unit also allowed measurements to be made in varying temperatures (0ºC – 40ºC). The ADV unit also allowed for sampling rates ranging from 0.1 to 25 Hz. A sampling frequency of 20 Hz was used. This sampling rate was used to maximize the data output in the sampling time frame of one minute.

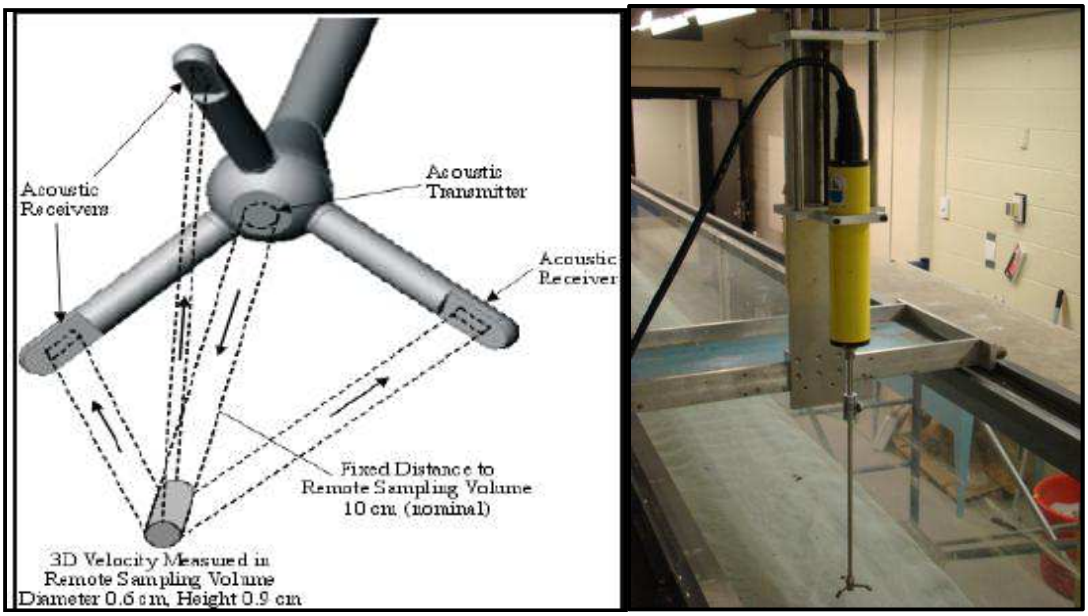

Figure 3.3: Acoustic Doppler Velocimeter (ADV) sensor probes and sampling volume (www.sontek.com) (left); Sontek ADV unit (right).

The use of an ADV, which measures flow in three-dimensions, enables a spatially-detailed characterization of velocity fields at different flow stages during the study (Sawyer et al. 2010). The use of the ADV will also allow for a better understanding of the instantaneous forces that are responsible for sediment entrainment (Nelson et al. 1995; Thompson, 2007).

A few limitations existed with respect to using the ADV during the study. Turbulence measurements could only be taken at one vertical at one time. When attempting to investigate spatially distributed phenomena, quite often flow is unsteady due to a changing hydrograph, thus work had to be performed quickly under high flow/changing hydrograph situations (Booker et al. 2001). Additionally, the orientation of the ADV with respect to transect position or perpendicular to the flow institutes a certain amount of error in the measurements. If the position of the tripod is not perpendicular to

the flow or completely level the horizontal and vertical measurement readings could be in error. To limit the amount of error prior to each measurement a self-check with respect to being parallel to each transect and perpendicular to the flow was performed. Additionally, the tripod had a level bull's-eye built on it to ensure that the instrument was level on the river bed. To further ensure that the unit was level a portable level meter was also used prior to set up at each vertical.

For both sites 1 and 2 (7 transects each), ADV measurements were taken at 3 – 5 verticals along each transect. Not every vertical for sites 1 and 2 could be measured due to: 1) time frame to level tripod, 2) 1 minute sampling times (at varying heights) and 3) computer configuration (file organization). To compute multiple measurements points on 10-15 verticals on each transect was not be possible in one measurement day and would therefore lead to unreliable and inconsistent results if sample periods had to be extended to more than one day. The ADV was mounted on a custom-built tripod, which was constructed out of stainless steel and aluminum (Figure 3.5). The tripod was designed to permit velocity profiling by vertically traversing a mounting platform on three rods (Figure 3.5). The same verticals used for the calculation of discharge were used for the flow measurements using the ADV. At each vertical, attempts were made to obtain point velocity profiles, similar to those outlined in Thompson and Wohl (2009), with probe heights above the bed of 1 cm, 3 cm, 5 cm, 10 cm and 20 cm. If the flow depth was greater than 20 cm, measurements were made every 10 cm after the 20 cm reading until the water surface was reached or until the maximum allowance permitted by the tripod. In locations where the water depth was not great enough to obtain all four-point velocity

profiles, as many readings as possible were taken. Point velocity profiles were not taken closer than 1 cm to the bed, because of concerns of the probe head becoming damaged due to bedload transport and/or clast outcrops.

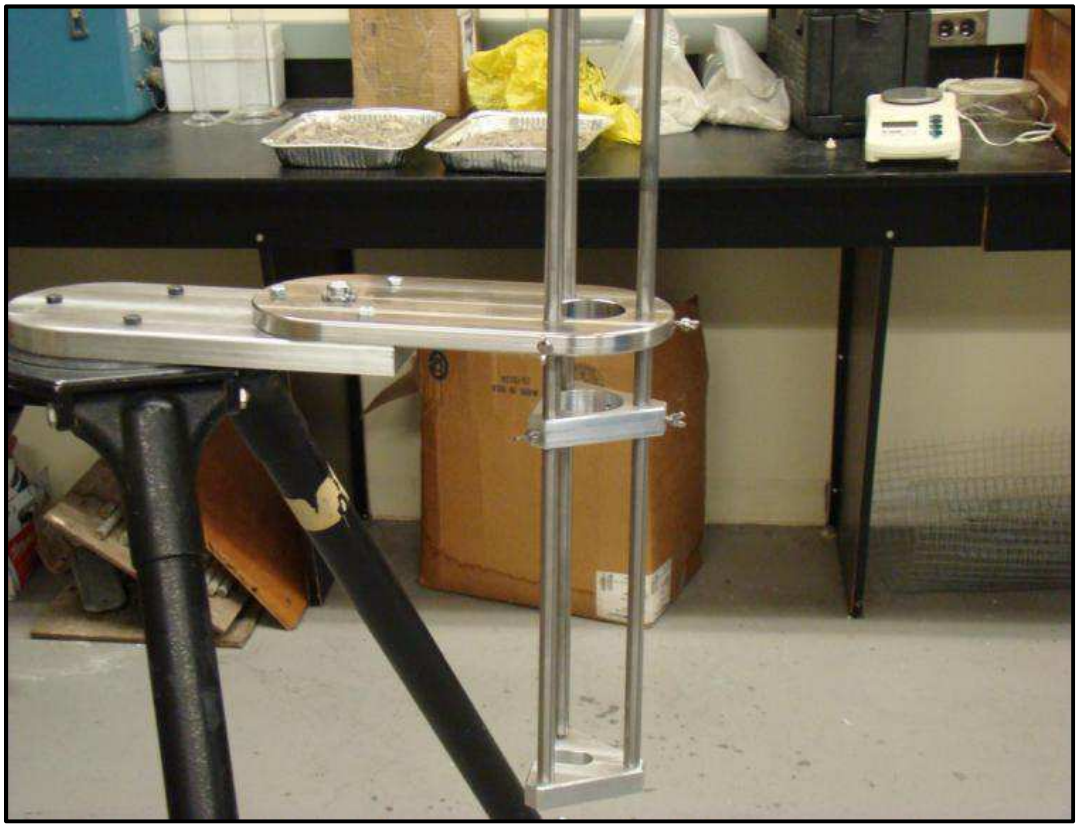

Figure 3.5: Stainless steel and aluminum custom built ADV tripod

Three-dimensional ADV point velocity profiles were collected weekly at site 1 and 2 from the end of April 2010 until July 2010. Due to time constraints, energy supply issues and the complexity of measurements, it was not possible to obtain ADV measurements more frequently than once weekly.

The recording time at each point was approximately 60 seconds. Detailed measurements were taken once a week at each Site at specified verticals along each transect. Buffin-Belanger and Roy (2005) observed that recording lengths shorter than 60 seconds were not adequate for turbulent flow characterization in river channels. Also, the 60 second recording time was used because of the ability of the ADV to pick up minute changes in the flow during the measurement period. In order to capture 175 velocity profiles (maximum of 35 verticals/site × 5 point depths) work had to be performed quickly because of the concern that the discharge may change over the sampling time or over the course of the measurement day. As well, the 60 second recording time was used because of concern regarding battery power supply. A 20 Hz sampling rate was used with a maximum lateral maximum velocity range of 250 cm s^{-1}.

For signal quality, the ADV uses signal-to-noise ratio (SNR) to determine how well the flow is seeded. Seeding refers to amount of particles in the flow that the ADV signals can bounce off of. The higher the SNR value, the better the flow is seeded with particles, therefore the more reliable the data is. The ADV uses and provides a correlation statistic to display the quality of the data. The closer the correlation value is to 100% the more reliable that data is and the less noisy the data will be. The ADV has some uncertainty with its technology. The primary reason for uncertainty comes from the need to input the salinity and temperature values. If these measurements are not taken accurately, the measurements will be biased. Doppler noise is another form of uncertainty. Sontek states that Doppler noise can be estimated at 1% of the maximum velocity range at a sampling rate of 25 Hz and an SNR above 15 db. Lane et al. (1998)

described the importance of signal processing on the velocity files to remove data corrupted by communication errors, low signal-to-noise ratios (SNR) and low correlations. Lane et al. (1998) also stated that a lower limit of 20 db be used for SNR values and a lower limit of 0.70 for the correlation values. However, based on field experience this study used a lower limit of 15 db for SNR values and a lower limit of 0.30 for the correlation values. Palmer (2002), stated that an SNR value of 15 db only causes an estimated 1% of uncertainty due to Doppler noise in the maximum velocity range. Martin et al. (2004) found that the low correlation values were attributed to an increase in turbulent flows over rough boundaries (i.e., riffle sections). They found that data comprised of low correlations could accurately be used to determine average velocities above the bed. Martin et al. (2004) concluded that a correlation filter as low as 40% could be used provided that 70% or more of the data remained after filtering. To minimize the output errors, the velocity profile data will be filtered with a low-pass filter to a frequency of 5 Hz, as described in the WinADV post processing program developed by Sontek Systems. After post processing the data, it was found that only 5 - 10% of the measurements taken during a 60 second time period were removed due to not meeting the lower limits of filtering the data. Examination of turbulence production and dissipation (turbulent energy) was determined by calculating TKE (as discussed in previous chapter). The value of TKE represents the energy extracted from the mean flow by motion of the turbulent eddies (De Serres et al. 1999). Patterns of TKE at mid to high-flow periods should provide a better estimate of greatest sediment entrainment potential in comparison to cross-section or time-averaged values of flow or shear stress (Thompson and Wohl,

2009). As well, areas represented by low values of TKE should be representative of areas of sediment deposition.

As well, Reynolds stresses (turbulent stresses) represent the degree of momentum exchange at a given point in the flow. Reynolds stresses were also calculated from the 3D ADV output readings. Reynolds stresses are defined from the horizontal and vertical flow fluctuations. The product of $u'v'$ (as discussed in previous chapters) was of great interest in this study as it was related to the exchange of momentum across a plane parallel to the mean flow direction. For the purpose of this study, Reynolds stresses were calculated for comparison purposes only.

3.5 Sediment Sampling

The bulk sediment sampling method was used. A bottomless 35L pail (12" diameter) was used as a standard sampling device to excavate the sample(s) from the bed. The bed material from the inside of the cylinder was removed. The advantage of using this method was that a volumetric sample was obtained over a wide range of particle sizes as well as a large sample volume. The ISO standard ISO 4364-1977(E) outlined in Mosley and Tindale (1985) stated that the recommended number of bulk samples should be taken at every other vertical along each cross section. A bulk sample was taken using this standard at site 1 and 2 along each cross section. At each vertical on each cross section, the armour layer was first removed from the cylinder and placed in a bag labelled with its cross section number and vertical number. In rivers that are low to moderately sloped, the river goes under a period of low flows where bed sediment is re-arranged to create an armour layer (Tan and Curran, 2011). The smaller sediments (sands) are

transported downstream leaving the larger clasts exposed, which is defined as the 'armour layer'. Figure 3.6 depicts the armour layer and the sub-surface layer which is commonly observed on the riffle section of river beds:

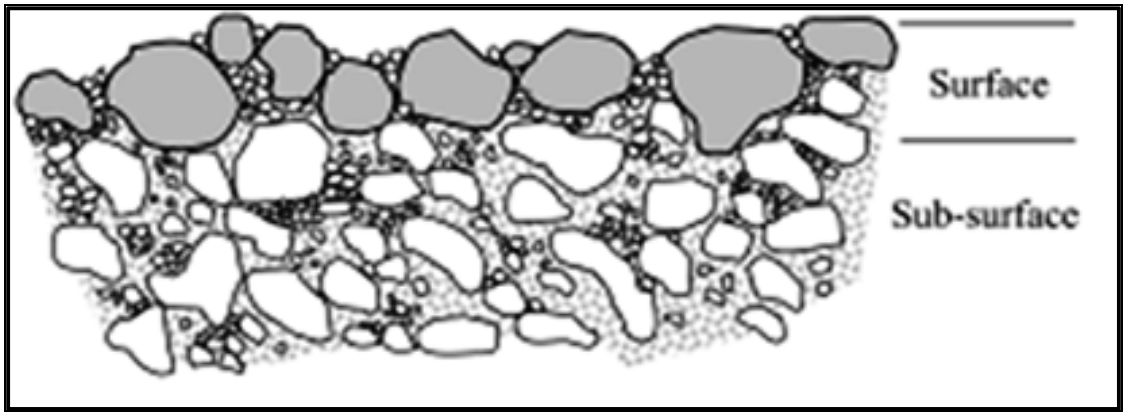

Figure 3.6: Typical armour layer and sub-surface layer schematic of gravel bed rivers (Tan and Curran, 2011).

The sampling depth of the armour layer was equal to the diameter (intermediate B-axis) of the largest particle located in the cylinder sampling area. At each vertical, the sub-pavement samples were removed using a trowel at the same sampling space as the armour material and put in a separate bag labelled with its cross section number and vertical number. The depth of the sample removed was equal to the depth of the largest particle diameter removed from the overlying pavement sample. To characterize the beds of the study sites, bed material sampling was made once during the study period, during a low flow event in May 2010.

In the laboratory, the samples were air dried and then sieved through U.S. Sieve Sizes 2.50", 2.00", 1.50", 1.25", 1.00", 7/8", 3/4", 5/8", 3/8" and a 0.19" (#4 US Sieve) for grain size analysis. Samples that were too large to be sieved were measured based on

their b-axis and weighed. At each site, grain size parameters D_5, D_{16}, D_{50}, D_{84} and D_{90} were calculated. Cumulative frequency curves for both surface and bulk samples were made for each site.

It was also important to characterize the bed material on the riffles and pools separately in order to understand when particles resting on the river bed are entrained by the flow. This was especially important to this study because particles entrained by the flow at site 1 and 2 will either add or detract to riffle height and depth of scour in pools.

In order to assess sediment transport characteristics at site 1 and site 2 both indirect and direct methods were used. Tracer particles were used to provide an indirect measure of bedload-transport competence during changes in the stream hydrograph during the study. Tracers are defined as marked particles (e.g. painted, magnetized and radio transmitters) that are implemented into the river bed in order to characterize the movement of sediment in rivers (Hassan and Ergenzinger, 2003). Painted tracer particles and tracer movement provided the opportunity to study the general characteristics of sediment movement under various flow stages at the study sites. The average particle distances were recorded for each tracer found.

The size and location of the deposited tracer particles were recorded in order to hopefully provide an accurate measure of stream competence for the riffles and pools at both sites. After a storm event, tracers were recovered and their location was recorded in an attempt to provide a good estimate of the maximum stream competence of flow events during the study period. The tracers were used in conjunction with the Helley-Smith portable sampler (discussed in subsequent section) as tracers are an ideal way to detect

the motion of the coarsest particles on the stream bed which are usually larger than those caught in portable samplers. Tracer particles implemented at site 1 and 2 were painted with one of four fluorescent spray paints. The spray paint colours represented the starting locations of the clasts. On each tracer clast, a unique identification number was indicated by permanent marker which served to represent the tracer pebble clast size and weight. The tracer particles were placed in a 2 meter diameter area with approximately 100 tracer particles in each location. The tracer particles used were those obtained from the aforementioned bulk sediment sampling procedure.

Limitations to using tracer particles may have included particles which were more mobile than natural sediments because of differences in structural position and imbrication (Laronne and Carson, 1976). Milan et al. (2001) found that tracer clasts tend to move from riffle to riffle and tracer particles scoured from the head and centre of pools were deposited on the pool exit slope and riffle head. Milan et al. (2001) also found that bars and riffles collected the majority of the deposited clasts, while the pools only accumulated a small fraction of the introduced tracers after initial motion and re-deposition. Furthermore, it was found that the mean distance travelled for each tracer particle was highest for tracer clasts originating on pool-entrance slopes and the mean distance travelled decreased for tracers originating at the centre of pool, pool-exit slopes and riffles (Sear, 1996).

The starting position of each tracer particle was surveyed using the total station (see tracer maps in subsequent section). After a flow event of interest (rain event), the painted rocks were recovered and the transport distances were surveyed using the Total

Station. After each storm event the morphological and sedimentological environment for each clast was recorded, prior to replacing the clasts on the bed surface.

Additionally, a Helley-Smith bedload sampling device was used during the study period. The modified Helley-Smith sampler with a 76.2 × 76.2 mm nozzle was used (Figure 3.7). The sampler was designed to collect particle sizes less than 76 mm at a maximum velocity of 3.0 m/s (Gomez, 1991). The Helley-Smith sampler was used due to its practical reasons such as ease of use and portability.

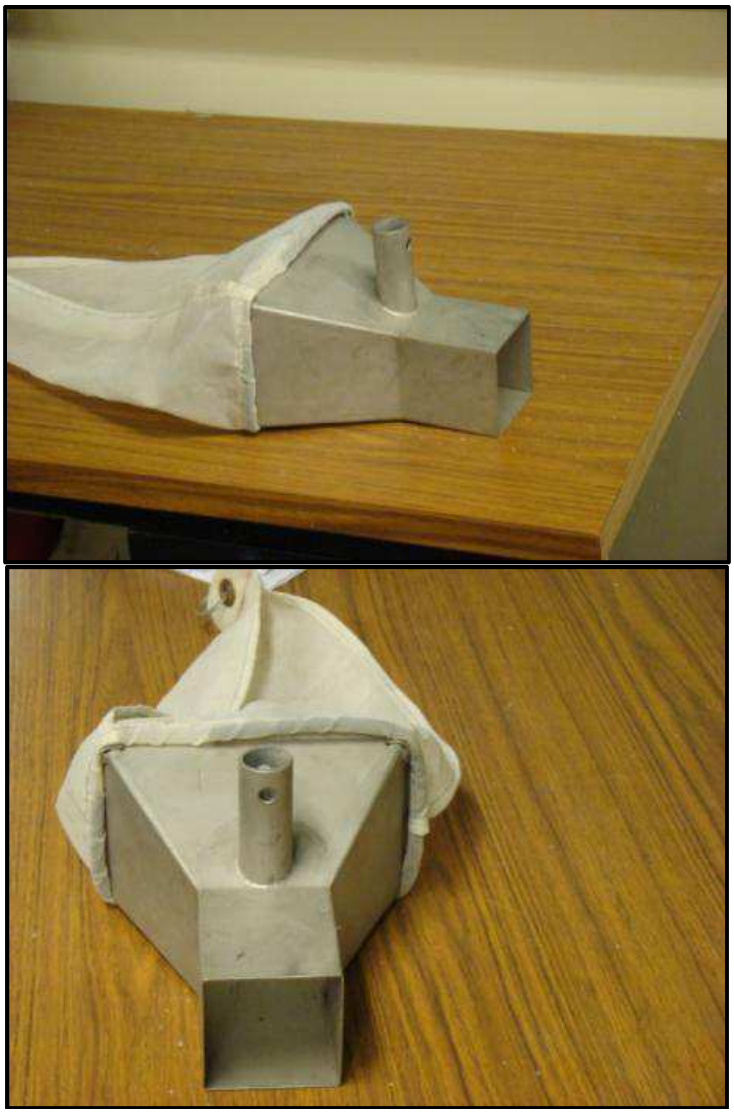

Figure 3.7: Modified Helley-Smith bedload sampler

Bedload transport rates vary spatially and temporally, even during constant flow conditions. Dietrich and Whiting (1989) established that sampling times ranging from several minutes to an hour are required to estimate the particle size distribution of the bedload accurately. Due to time constraint limits at the field sites, each bedload sample along each transect at site 1 and 2 was placed for a sampling time of approximately 10

minutes. A 10 minute sampling interval was chosen to ensure that the change in flow hydrograph during high flow periods was minimized during bedload sampling. As well, the Helley-Smith sampler was not designed for long sampling times (Bunte et al. 2004). Bedload samples collected by the Helley-Smith sampler were also sieved and grain size distributions were determined based on Φ classes (see subsequent sections for results).

Bedload transport sampling at site 1 and 2 occurred sequentially. Two bedload samples were taken along each transect (14 total transects = 28 bedload samples) at both sites for each flow stage or change in flow stage from April to July, 2010. De Vries (1973) suggested that 10 bedload samples were required to provide an acceptable estimate if the mean bedload transport rate at a study site. Similarly, Carey and Hubbell (1986) concluded that little reliance could be placed on any mean value that was derived from less than 5 bedload samples. Furthermore, Nesper (1937) observed that 10-15 sequential samples were required to provide an acceptable indication of the mean bedload transport rate and 30 samples were required at high transport rates.

Three bedload traps were also deployed on the riffle section at site 1 and site 2. The traps were checked periodically or after each storm event to observe the flow capacity of the river over the riffle section for a specified time period. Each trap was built out of a 20-L open face plastic bucket and installed/buried into the riffle section so that the opening of the bucket was flush with the river bed/bar. The bedload traps are designed to catch material with particles sizes ranging from 4-90 mm. The benefit that bedload trap has over the handheld sampler is that the data obtained from the bedload trap is usually considered exact (Hicks and Gomez, 2003). Trap efficiencies are

considered to be 100% as long as the opening is wide enough to prevent the overpassing of moving particles. Bedload traps are also very beneficial because they will permit the ability to continuously monitor and measure all the bedload that passes through the measuring section in a given time period that is a lot greater than handheld samplers (Hicks and Gomez, 2003).

Samples were taken periodically from the trap or after a flow event of interest. Samples were then taken back to the laboratory, where they were weighed and sieved for grain size analyses.

3.6 Topographic Surveys

Bathymetry and topography surveys of site 1 and 2 were completed in order to assess the variability in riffle height and depth of scour in pools and to characterize the study sites within the basin. Detailed surveys were completed for each flow stage exhibited at site 1 and 2 and/or every two weeks during the study period. Surveys were completed using a total station (Figure 3.8). The strategy was to survey immediately after all floods or high discharge events that were significant enough to enable sediment transport, preferably at the same time as the mapping of the tracer clasts, however, this was not always possible because of the frequency of floods during the latter half of the study. Additionally, surveys were also troublesome to complete in the latter half of the study due to dangerously high water levels and discharge.

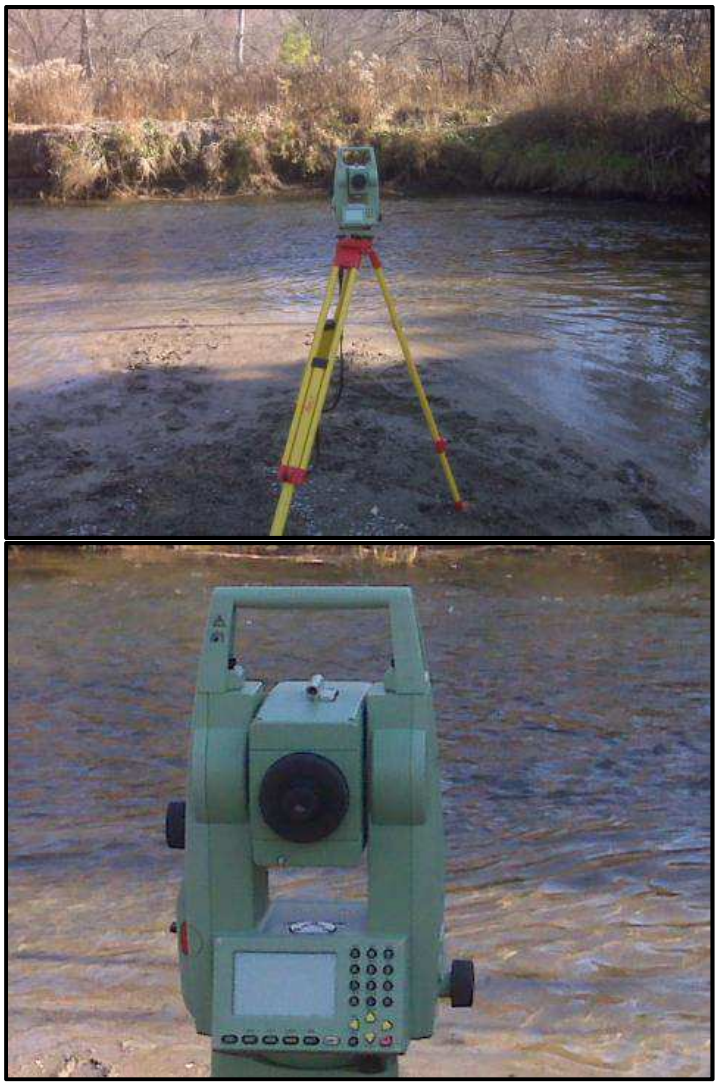

Figure 3.8: Total station survey equipment (left); Total station unit (right).

Each detailed survey consisted of approximately >1000 survey points (point density of 2 points/m^2) at both site 1 and 2 (Figure 1.1). High density survey points were needed in order to assess the rate of change in riffle height and/or depth of scour in pools at both sites. At each survey point, water depth measurements were recorded in order to assess water depth (to be used in post-processing). Water depths were measured using the survey rod; a 1.0 m measuring stick was taped to the survey rod and water depth

measurements were recorded for each survey point taken. A customized wood footing was fabricated to fit on the end of the survey rod to ensure that the survey readings were taken consistently in terms of depth into the bed. Additionally, individual boulders, bedrock outcrops and breaks in slope were surveyed extensively, in order to gain a detailed as possible representation of the river bed(s). In July 2010 a detailed survey of the valley including the floodplain was completed in order to show site 1 and 2 in the valley reach. Maps of bed topography and calculated flow characteristics were created of the bed morphology measurements using GIS (Geographic Information Systems) software (ArcMap 8.2). A deterministic approach via spline interpolation and the optimization method of natural breaks Jenks was used for bed topography maps. Furthermore, spline interpolation was performed with barriers in order to control the surface behaviour of the bed maps. The river banks edges (bankfull width) were used to define the barriers and to limit the input points to those surveyed within the river bed.

To identify riffles and pools, an average bed height was taken along each transect using interpolation from the spline bathymetric maps created in ArcMap 8.2. From the interpolated survey data bed slope was calculated. To calculate bed slope, the average height along each transect was computed in order to determine the slope of each reach (Site 1 and Site 2).

3.7 Additional Measurements

A YSI 30 STC (Figure 3.9) (salinity, temperature and conductivity) was used to measure the temperature and salinity of the water for each site. Measurements were taken on each field day at each field site and for each vertical (site 1 and 2). Temperature and

salinity measurements were critical for the calibration of the ADV prior to 3D measurements. The ADV unit was very sensitive to changes in temperature and salinity; therefore it was critical that the ADV was calibrated with proper salinity and temperature values. As previously discussed, changes in temperature and salinity result in changes in the speed of sound, which affects the ADV velocity measurements (Sontek, 1997). For example, a change in temperature of 5°C results in a change in the speed of sounds of 1%; a change in salinity of 12 ppt results in a change in the speed of sound of 1%. Furthermore, if the speed of sound used by the ADV is in error by 1%, the resulting velocity readings will be in error by approximately 2% (Sontek, 1997).

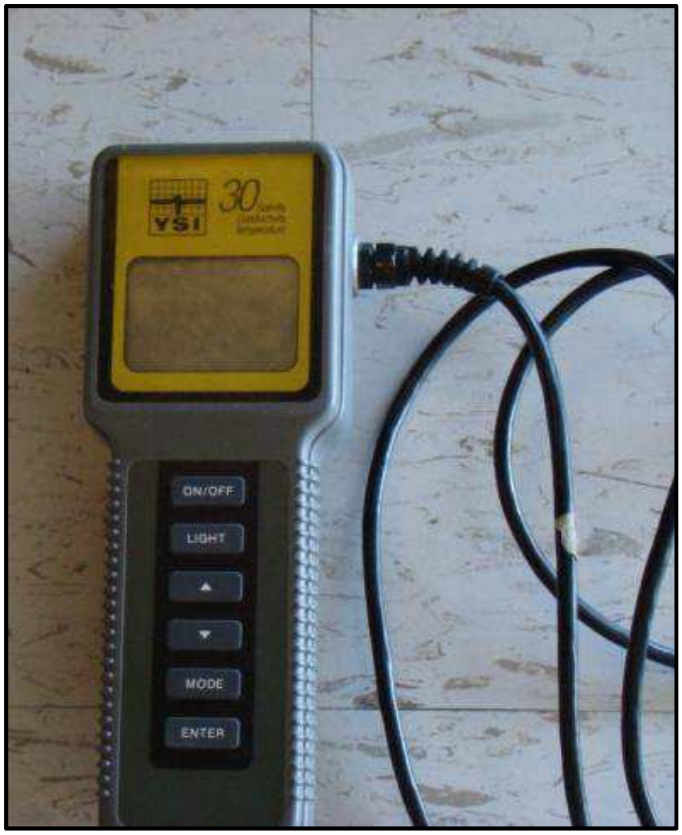

Figure 3.9: YSI 30 STC Instrument

Bank material present in a river represents a significant source of sediment or component of the bed material load (Knighton, 1998). However, the source of the sediment supplied by the banks to the river is not uniform downstream throughout the river; rather it exhibits great spatial and temporal variability. The spatially variability in bank erosion rates is controlled by the longitudinal and vertical variation in grain size, moisture content, organic matter content, vegetation, channel sinuosity, angle of internal friction and shear stress applied on the bank (Robert, 2003). Flow erosion on the banks is caused by the water flowing producing a drag force on the river banks, which in turn may initiate the entrainment and detachment of particles. Mass failure depends on the processes of weathering. Mass failure of bank material relates to its bulk mechanical properties, where the shear resistance or shear strength is a function of friction, cohesion and effective normal stress (Thorne, 1998). One common cause of bank erosion is the rapid immersion of dry banks and repeated wetting and drying cycles (Thorne, 1998). These cycles lead to cracking which result in reduced shear strength and therefore an increased likelihood of erosion. Mass failure is also related to flow erosion. This occurs when the flows scour the bed beneath the bank, which leads to increased bank height, bank angle and eventually instabilities that lead to mass failure (Thorne, 1998). River bank material tends to gradually become finer as you move up from the river bed to the floodplain. Generally, cohesive materials are covered by non-cohesive sand or gravels which causes a vertical stratification, which tends to increase erosion near the bottom on the bank. This eventually leads to undercutting which subsequently collapses the bank into the river (mass failure) (Robert, 2003).

Both field sites had examples of mass failure occurring on their outer banks. These mass failures contribute a great deal of sediment into the riffle-pool sequence, therefore influencing riffle height and potential fill or depth of scour in pools. It was therefore crucial to sample the material in these outer banks to determine their spatial variability in terms of grain size.

A sediment corer (Figure 3.10) was used to obtain bank sediment samples. At site 1 and 2 core samples will be taken at the top of the bank and laterally into the bank. Samples were taken from transects 1, 3, 5, 9, 11 and 13 at sites 1 and 2. Sediment samples were taken once over the studied period and were analyzed in the laboratory in order to characterize the amount of sand, silt and clay found in the banks. The purpose of characterizing the bank sediment samples was for descriptive purposes. Soil profile horizons were established and vegetative influences were noted at each site.

Figure 3.10: Handheld sediment corer unit (left), sediment core (right).

SECTION FOUR: RESULTS

4.1 Sediment Distribution

Sediment sampling was undertaken at Site 1 and Site 2 of the Rouge River to characterize the type of sediment (i.e., grain size and Unified Soil Classification System - USCS) and to quantify how sediment size affects the flow properties. Grain size is the most significant parameter to consider when dealing with sediment transport processes. Bulk sediment properties refer to the volume of various material on the bed or banks of a river. The grain size of bed sediments is commonly identified by D_{10}, D_{30} and D_{60}, where the subscript 10, 30 and 60 refer to the percent for which the valued percent of the sampled material is finer.

When examining the sediment characteristics and distribution patterns along riffle-pool sequences it is important to look at the individual transect regions in order to identify the differing bed characteristics along riffles and pools. The sediment size distribution for the river bed (armour layer) by 'Percent Passing by Weight' and 'Percent Retained by Weight' is shown in Figures 4.1 – 4.7 and Figures 4.8 – 4.14 for Site 1 and Site 2 riffle and pool transect sections respectively.

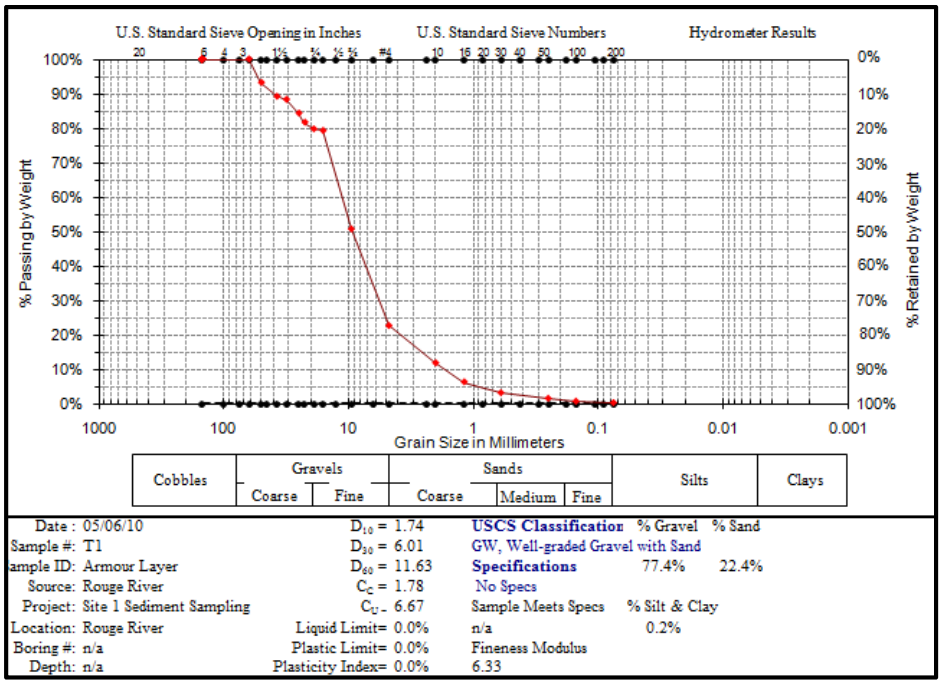

Figure 4.1: Site 1 - Transect 1 - Grain Size Distribution and USCS Sediment Classification.

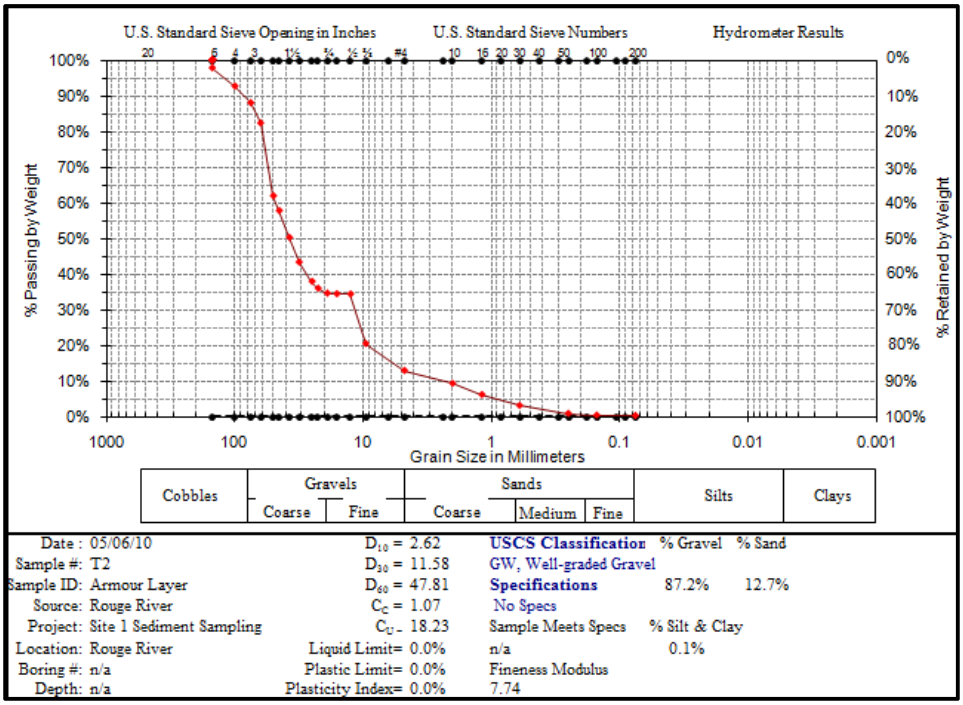

Figure 4.2: Site 1 - Transect 2 - Grain Size Distribution and USCS Sediment Classification.

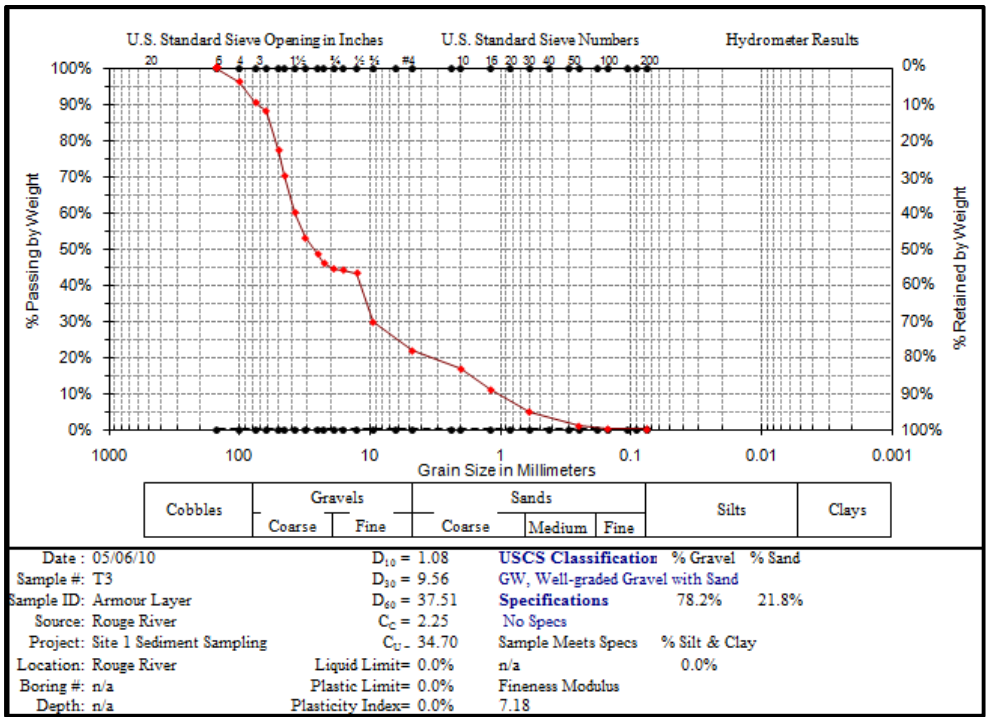

Figure 4.3: Site 1 - Transect 3 - Grain Size Distribution and USCS Sediment Classification.

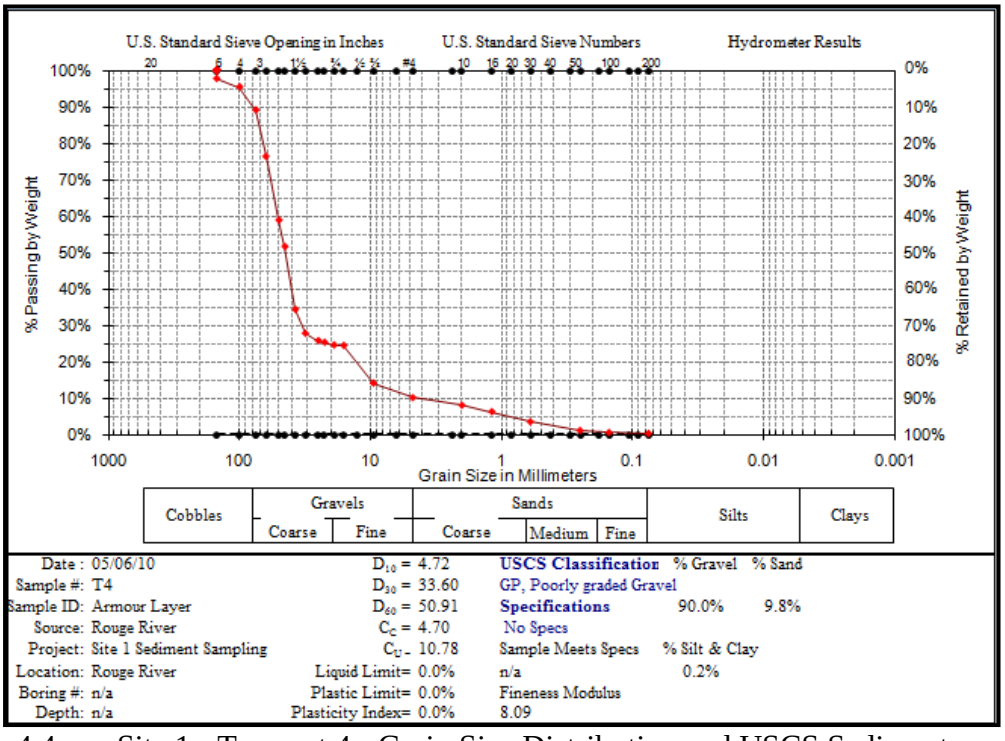

Figure 4.4: Site 1 - Transect 4 - Grain Size Distribution and USCS Sediment Classification.

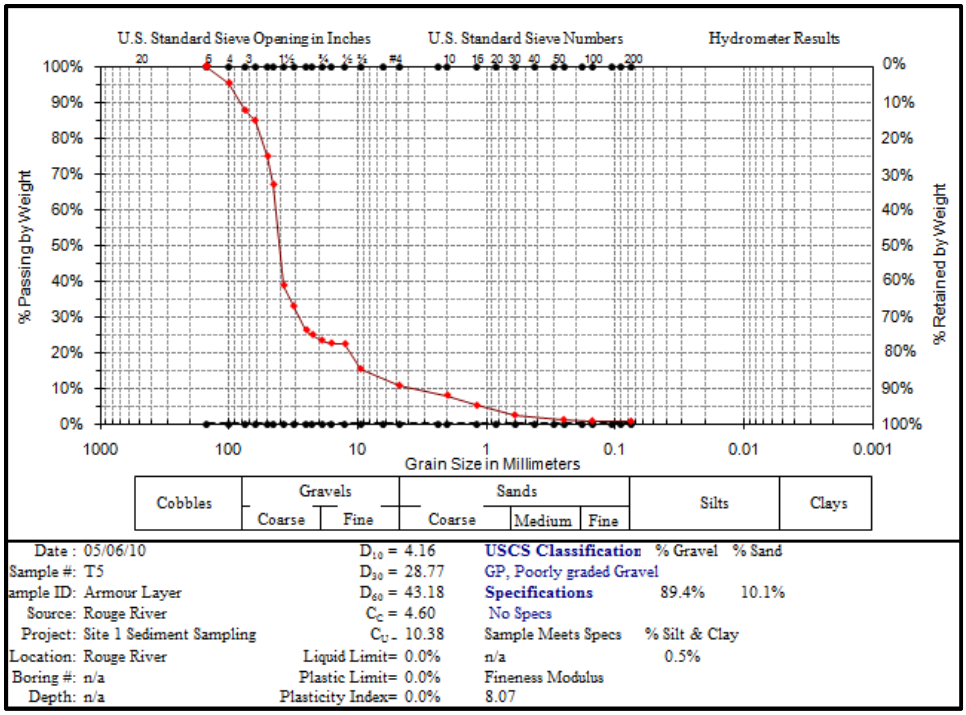

Figure 4.5: Site 1 - Transect 5 - Grain Size Distribution and USCS Sediment Classification.

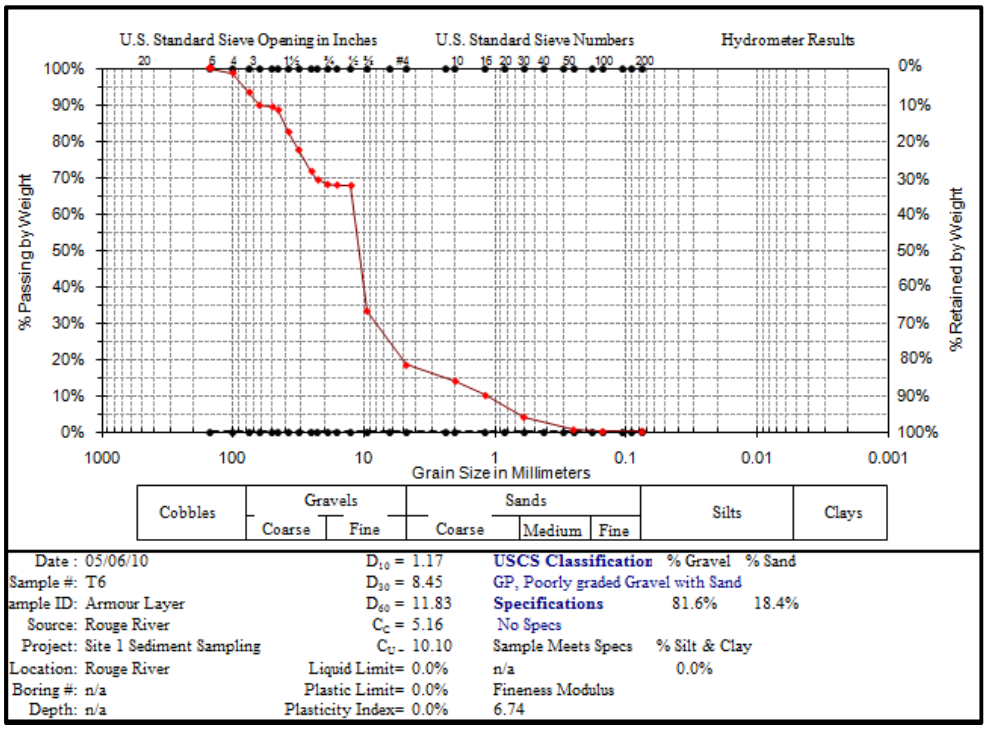

Figure 4.6: Site 1 - Transect 6 - Grain Size Distribution and USCS Sediment Classification.

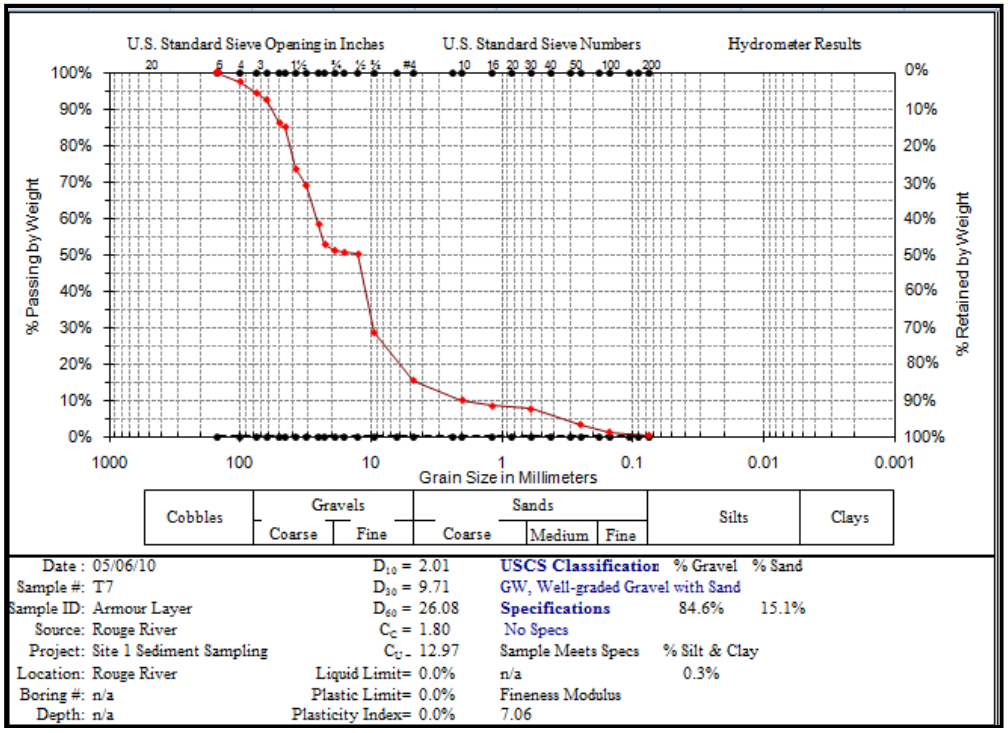

Figure 4.7: Site 1 - Transect 7 - Grain Size Distribution and USCS Sediment Classification.

It is evident from Figures 4.1 – 4.7 that gravel dominates the individual bulk sediment (armour layer) collected from transects 1-7 riffle and pool regions. From the grain size distribution curves, gravel material represents approximately 77 – 90% of the weight of a given bulk sample collected from the Rouge River. The remainder of the bulk sample material collected from the armour layer was comprised of a combination of sand, silt and clay materials. The grain size distribution curves and sediment characteristics for Site 2 are as follows:

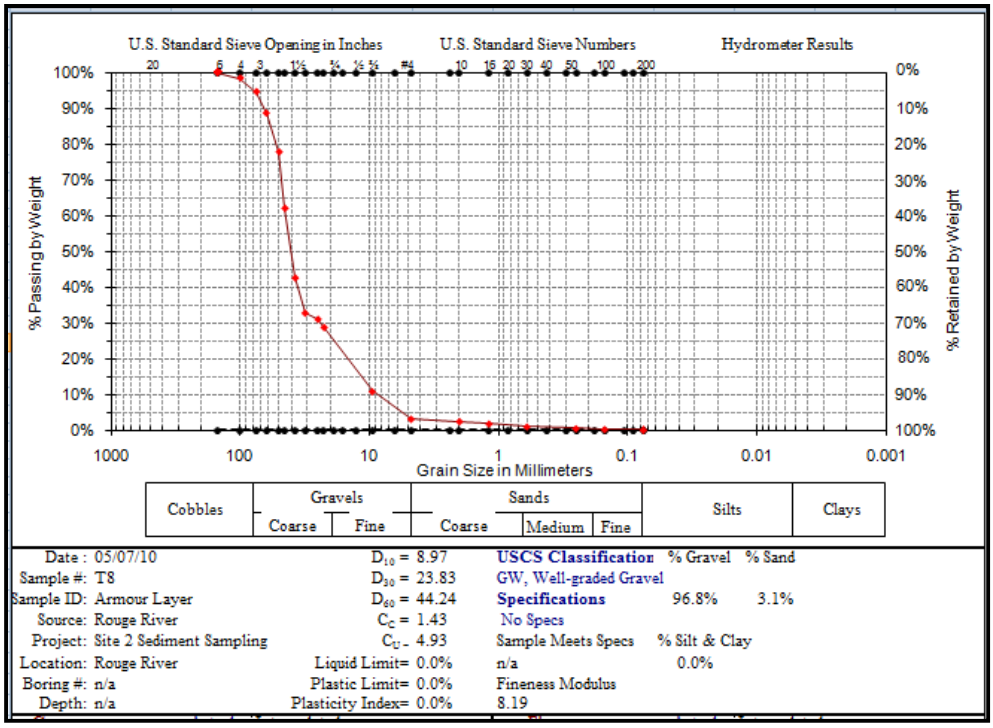

Figure 4.8: Site 2 - Transect 8 - Grain Size Distribution and USCS Sediment Classification.

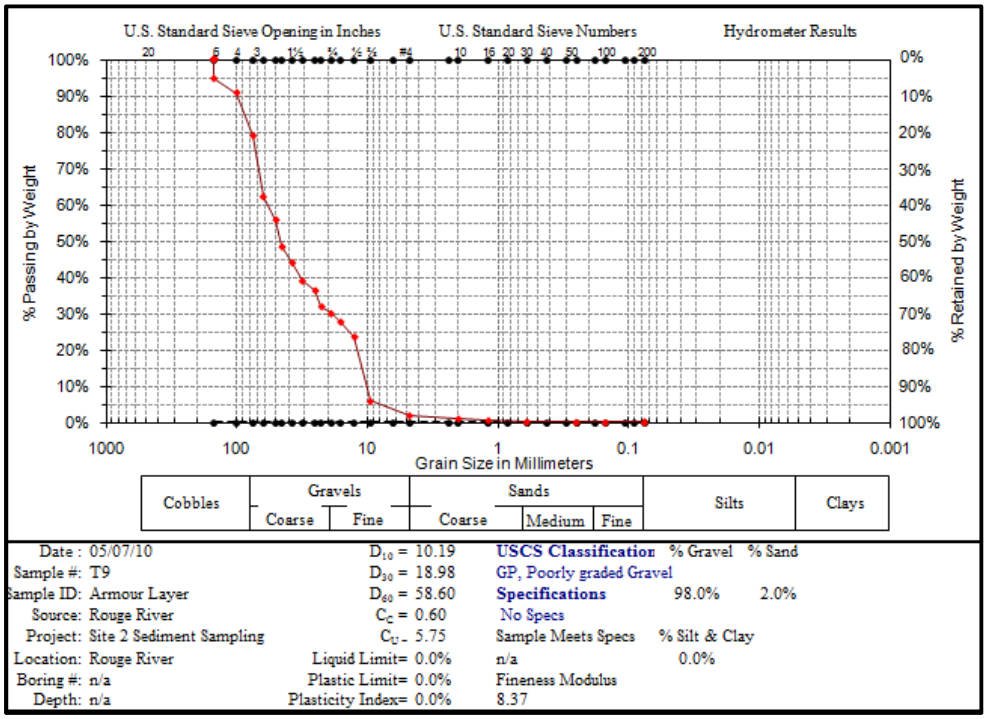

Figure 4.9: Site 2 - Transect 9 - Grain Size Distribution and USCS Sediment Classification.

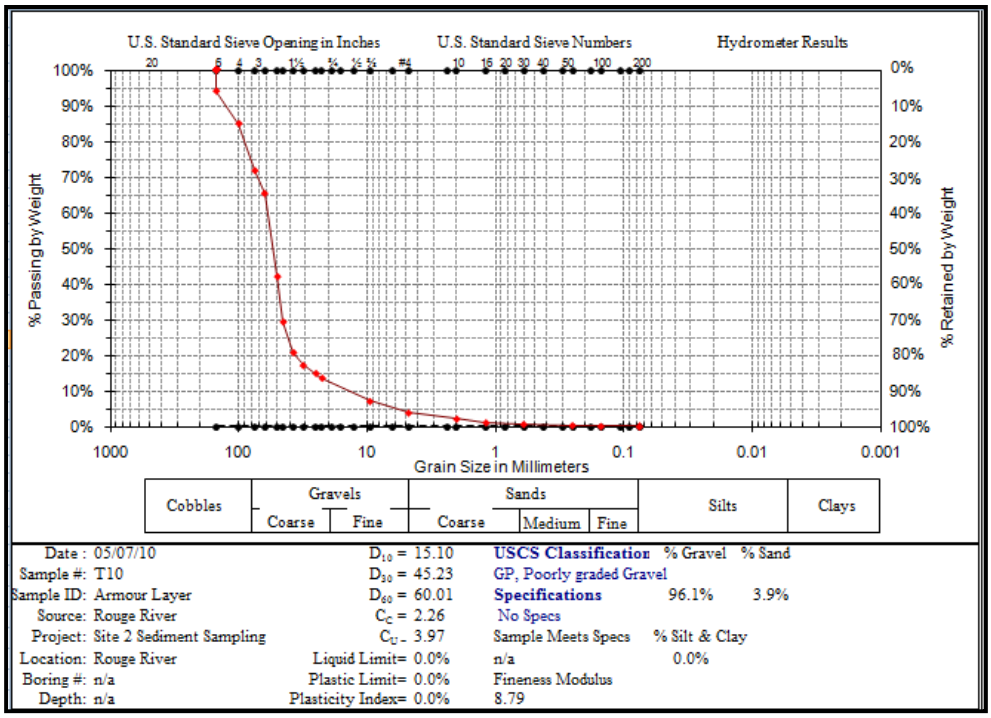

Figure 4.10: Site 2 - Transect 10 - Grain Size Distribution and USCS Sediment Classification.

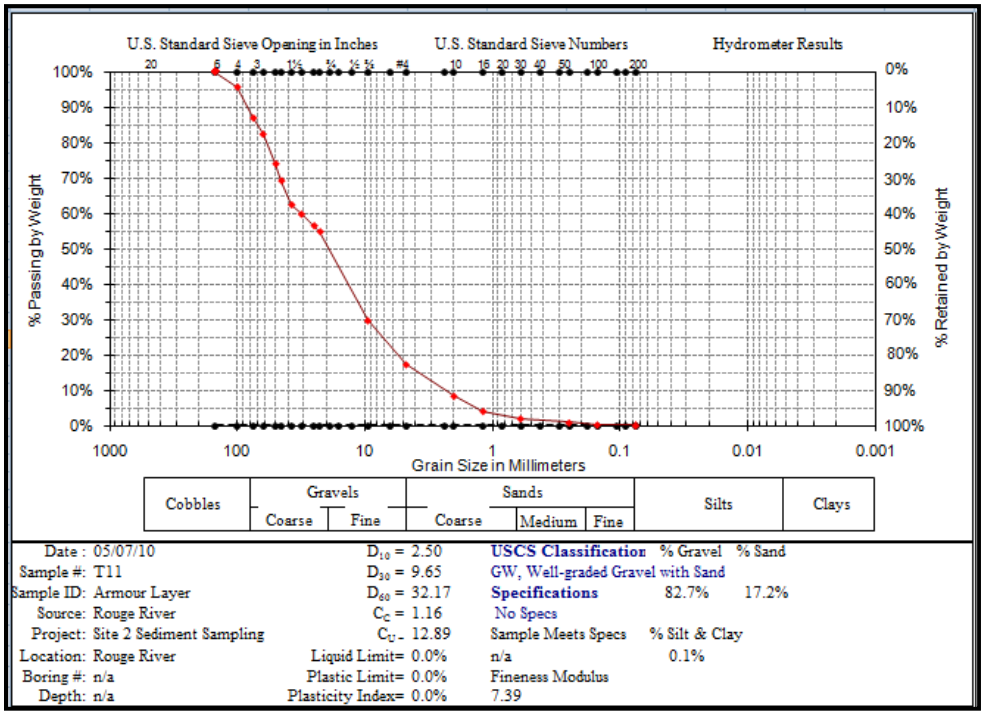

Figure 4.11: Site 2 - Transect 11 - Grain Size Distribution and USCS Sediment Classification.

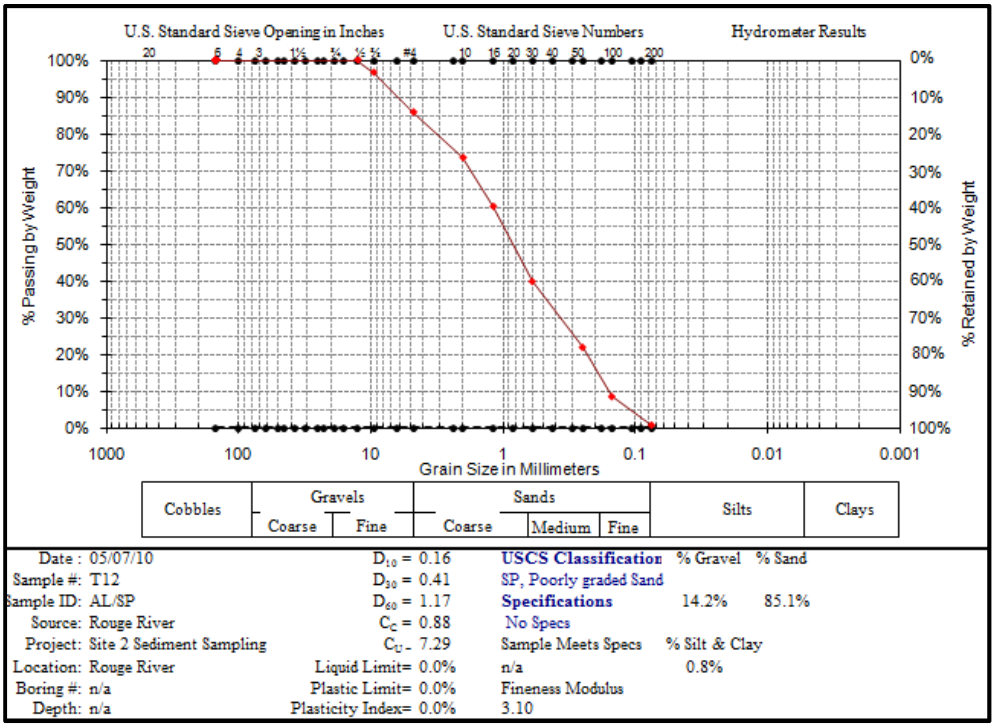

Figure 4.12: Site 2 - Transect 12 - Grain Size Distribution and USCS Sediment Classification.

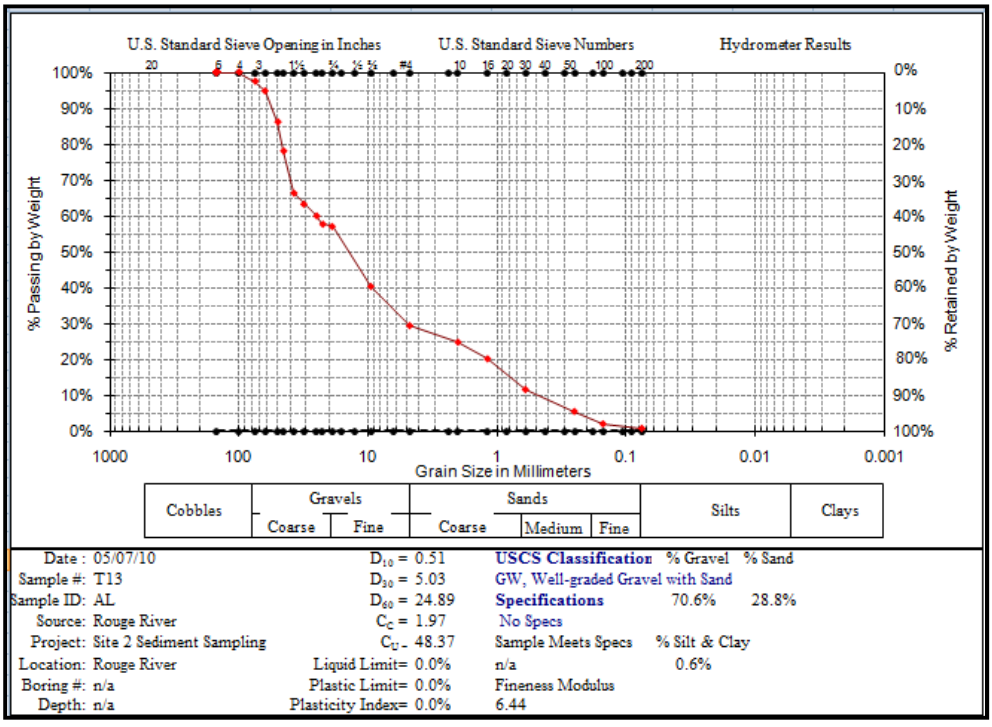

Figure 4.13: Site 2 - Transect 13 - Grain Size Distribution and USCS Sediment Classification.

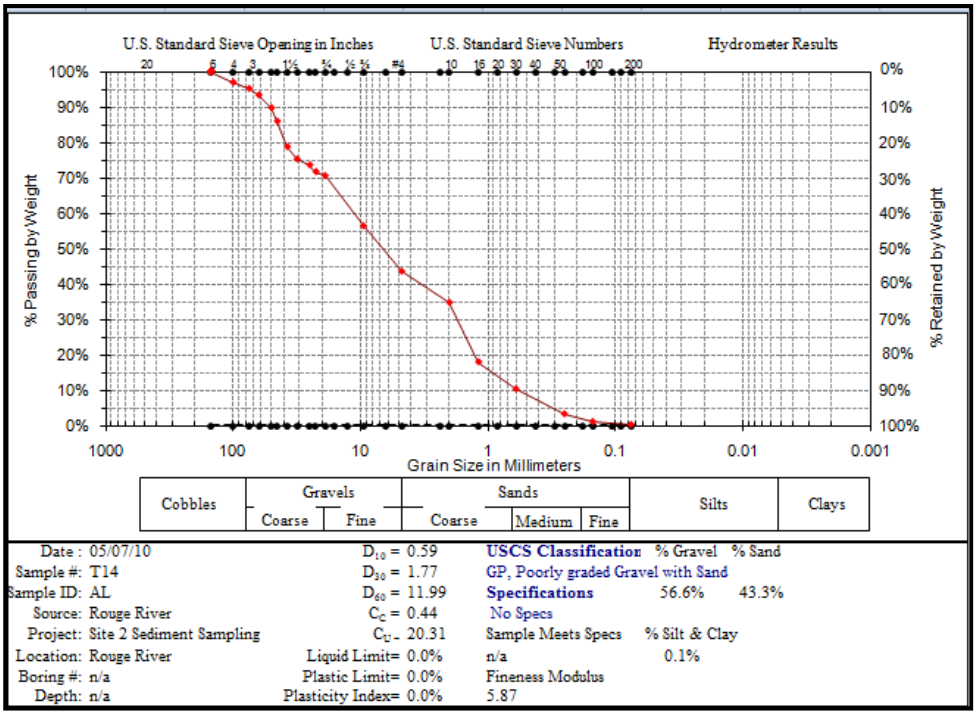

Figure 4.14: Site 2 - Transect 14 - Grain Size Distribution and USCS Sediment Classification.

It is apparent from Figures 4.8 – 4.14 that gravels dominate the armour layer individual bulk sediment samples collected from the riffles regions. Gravel represented approximately 83-98% of the bulk weight of the samples. The remained of the material in the armour layer riffle regions was comprised of sand, silt and clay. From Figures 4.12 – 4.14 the bulk samples were comprised of approximately 14-71% of gravel, 29-85% sand and 0.1-0.8% silt and clay.

In addition to armour layer samples were obtained from Site 1 and Site 2, sub-pavement samples were taken along each transect to characterize the surficial bed materials along the riffle-pool sequences and Site 1 and Site 2. Site 1 sub-pavement samples revealed that the samples were comprised of approximately 17-68% of gravel,

34-81% sand and 0.2-2% silt and clay. Site 2 sub-pavement samples revealed that the samples were comprised of approximately 14-72% gravel, 27-85% sand and 0.1-1.2% silt and clay.

Figure 4.15 and Figure 4.16 show the overall sediment characterization of Site 1 and Site 2. The bulk sediment sampling method was used because it provided an aerial representation of the sediment distribution for Site 1 and Site 2 (Figure 4.15 and Figure 4.16) with no bias. The advantage of using this method was that a volumetric sample was obtained over a wide range of particle sizes and a large sample volume. At each vertical on each cross section (transect), the armour layer was first removed to a sampling depth of equal to the diameter (intermediate B-axis) of the largest particle located in the cylinder sampling area. Following the removal of the armour layer, the sub-pavement layer was removed to the same depth as the armour layer. For both Site 1 and Site 2 (Figure 4.15 and Figure 4.16), the sediment size distribution deviates from the typical 'S-shape' curve commonly observed for coarse grained rivers. The deviation from the typical 'S-shape' curve that is commonly observed for coarse grained rivers may have important impacts on the local flow conditions that were observed for Site 1 and Site 2 (Figure 4.15 and Figure 4.16). The sorting index is the ratio of D_{84}/D_{16} (Robert, 2003). The advantage of the bulk sediment sampling method is that it captures the smaller fraction of sediment found on the river bed, which also play a critical role on local flow conditions in rivers. The median D_{50} size was approximately 25 mm for Site 1 and Site 2. The sorting index, based on the ratio of D_{84}/D_{16} for Site 1 and Site 2 was 13.26 and 53.39 respectively (Figure 4.15 and Figure 4.16). These numbers are very important and

suggest that greater bed heterogeneity exist over Site 2 than Site 1 and that local flow conditions are likely different and have different characteristics due to local differences in bed heterogeneity. For both Site 1 and Site 2, the USCS classification characterized the bed sediments as GW (Well-graded Gravel with Sand).

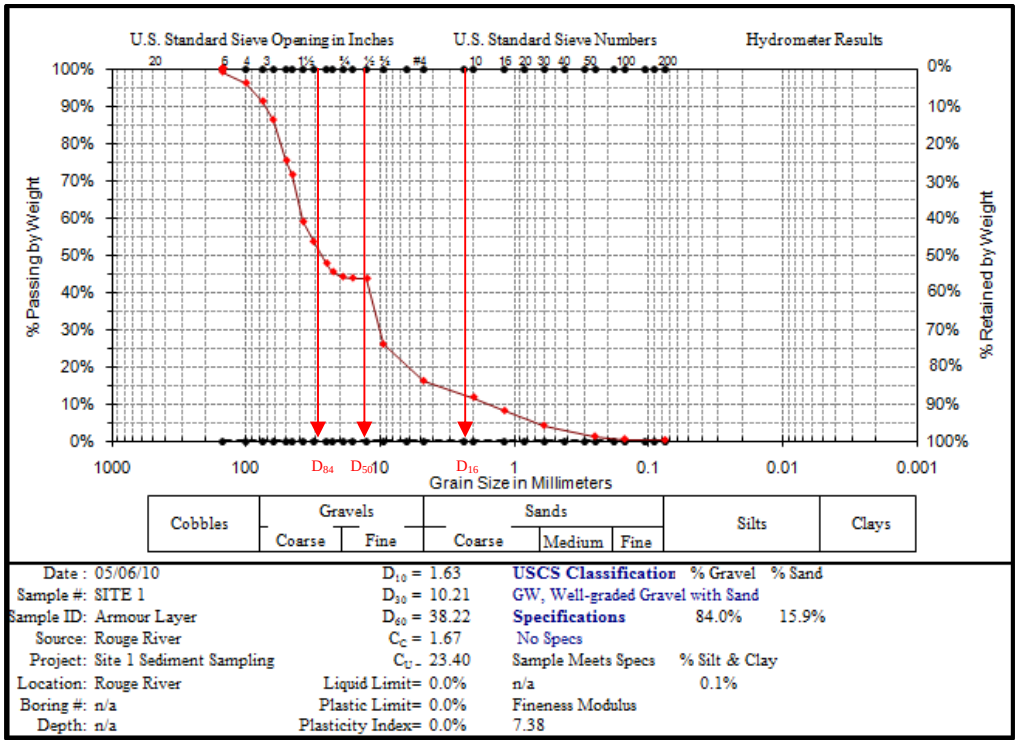

Figure 4.15: Site 1 – Overall Grain Size Distribution and USCS Sediment Classification.

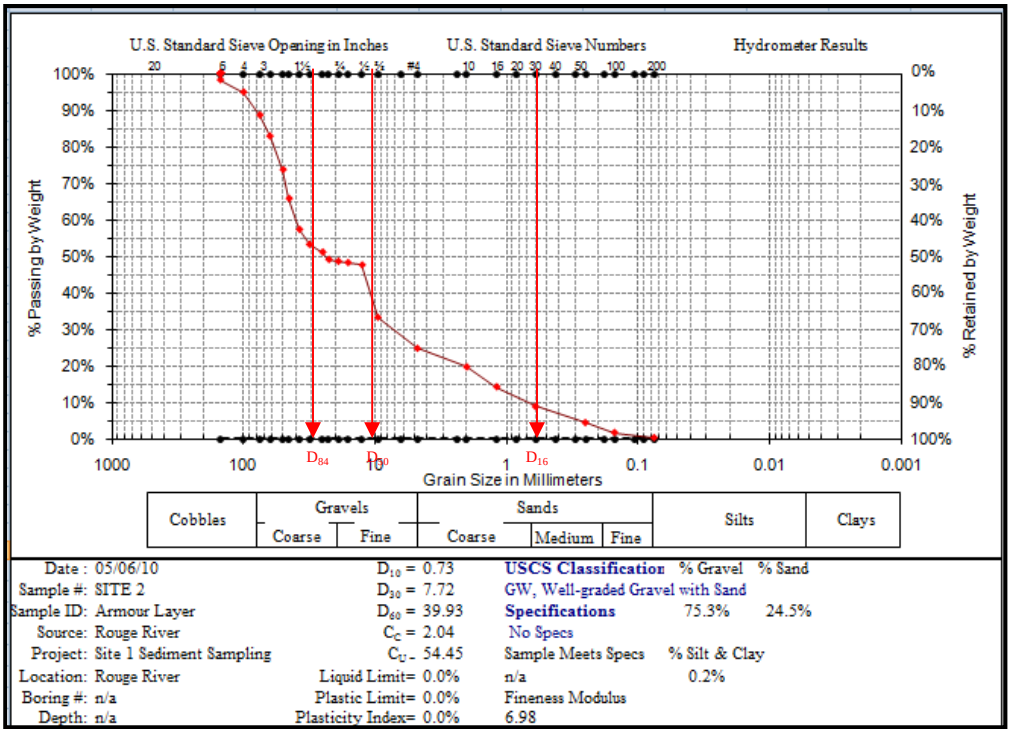

Figure 4.16: Site 2 – Overall Grain Size Distribution and USCS Sediment Classification.

Sediment analysis including bedload traps, handheld sampling and tracer pebbles was employed at both Site 1 and Site 2. Unfortunately during the study period, Site 1 experienced numerous events of vandalism including the removal of bedload traps and tracer pebbles. Even though handheld sampling continued at Site 1, due to the incomplete data set for bedload trap data and tracer pebbles, only Site 2 data will be evaluated for sediment analysis. Handheld sampling was completed along select transects and the bedload traps are depicted in Figures 4.17 - 4.20 for Site 2.

Figures 4.17 through 4.20 display sediment loads captured after a peak flow event in the bedload traps located at Site 2.

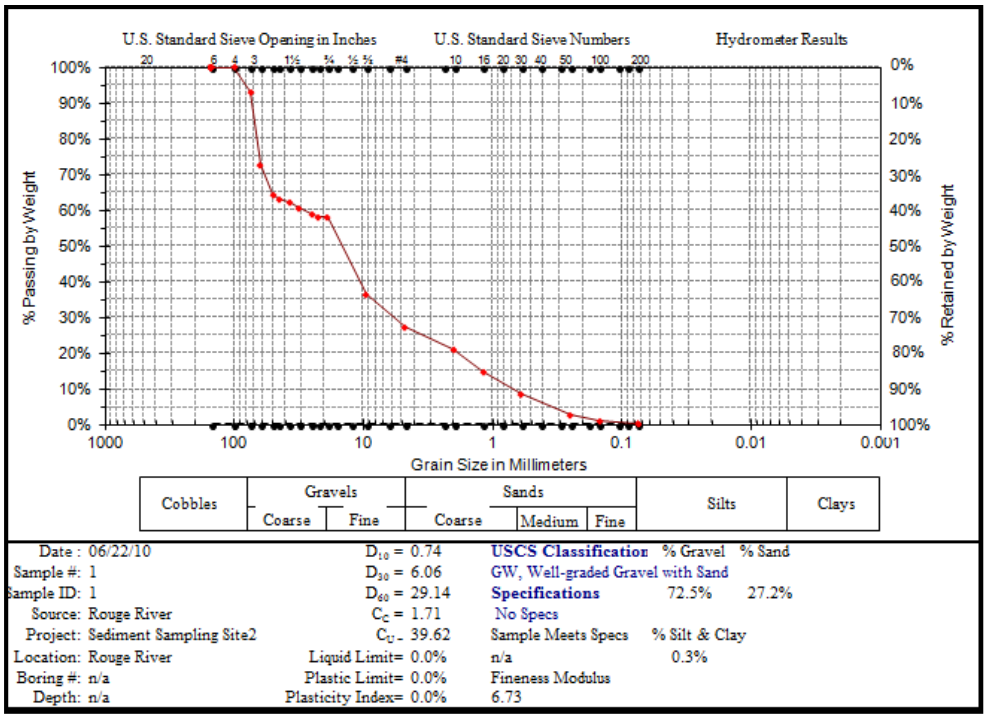

Figure 4.17: Site 2 – Bedload Trap #1 Data – June 22, 2010

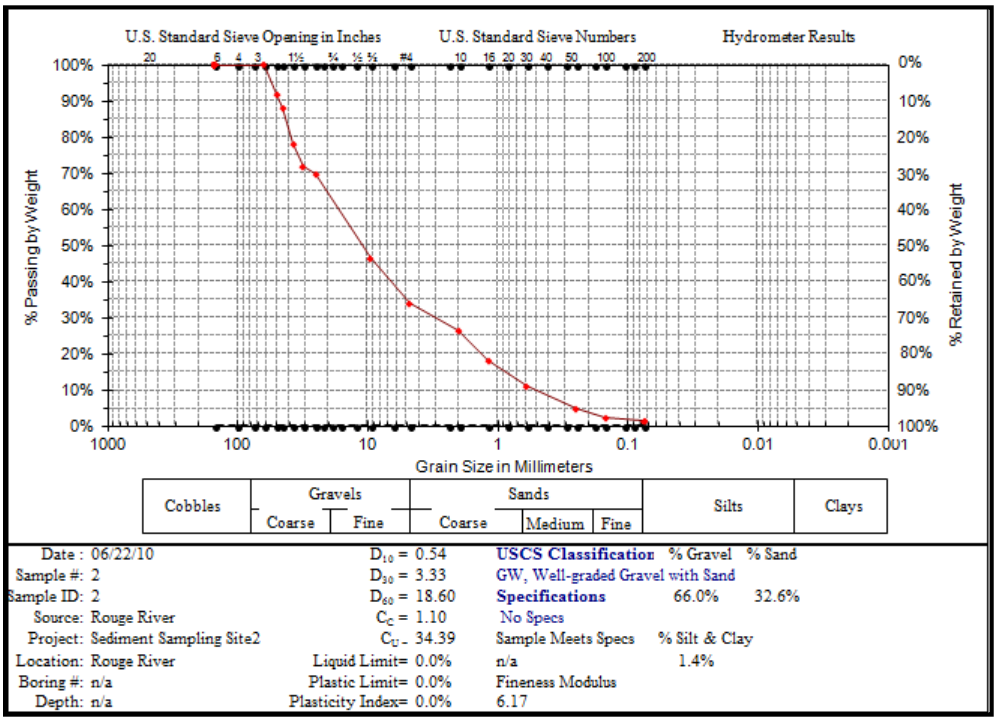

Figure 4.18: Site 2 – Bedload Trap #2 Data – June 22, 2010

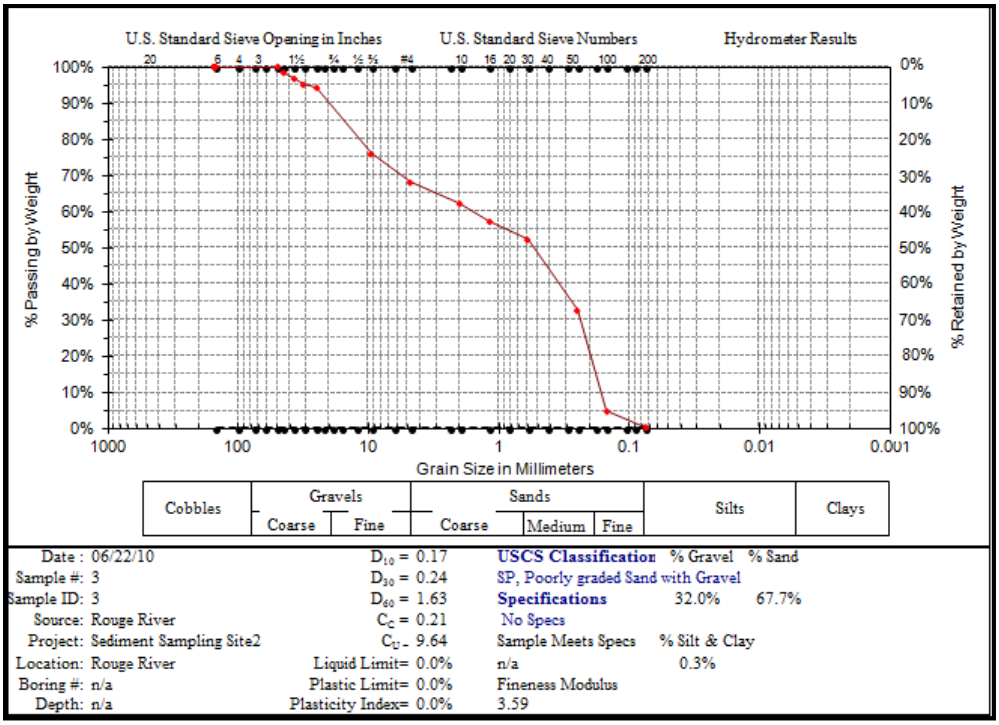

Figure 4.19: Site 2 – Bedload Trap #3 Data – June 22, 2010

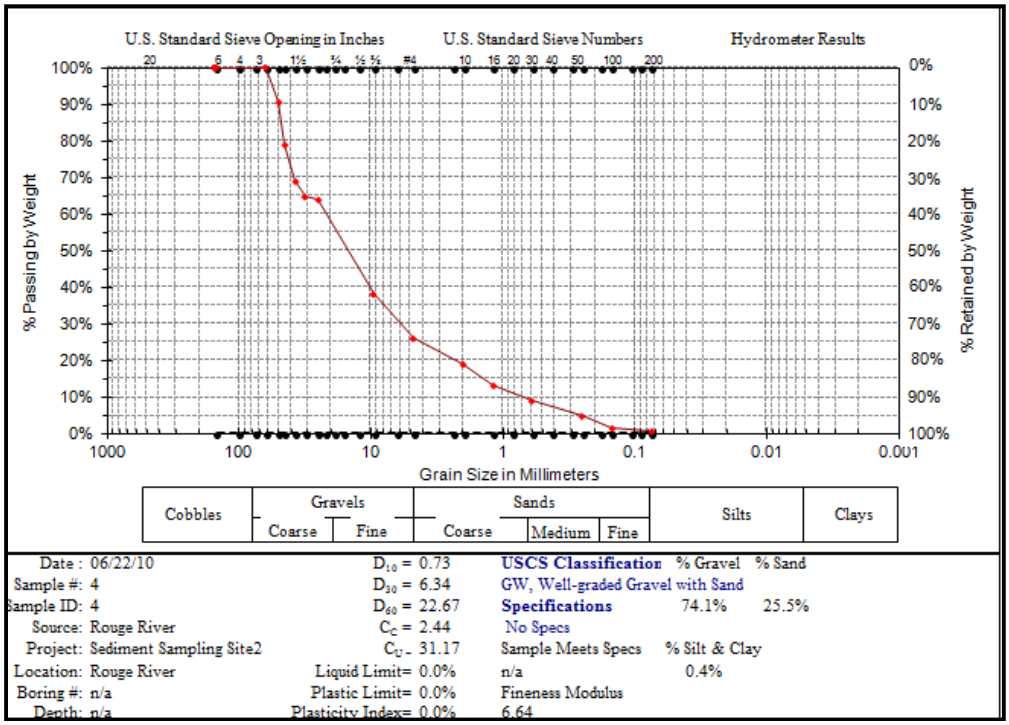

Figure 4.20: Site 2 – Bedload Trap #4 Data – June 22, 2010

From Figure 4.17 and 4.20, trap #1 was strategically placed near the riffle exit slope in an effort to evaluate the sediment moving out and/or through the riffle section. Trap #2 was placed on the upstream side of the point bar in an effort to collect sediment moving out of the riffle section and into the pool centre. Trap #2 and #3 were strategically placed on the point bar adjacent to the pool centre and adjacent to the pool exit slope respectively. Under lower flow events in the beginning of the study period (April and May 2010), the bedload traps remained relatively empty during non-peak flow events. June 16 – July 1st exhibited frequent periods of elevated discharge due to storm events (as expressed later in Figure 4.31). For example, the total sediment load captured in traps 1 – 4 on June 22, 2012 (Figures 4.17 – 4.20) was 13,174 g, 17,826 g, 13,753 g and 13,674 g respectively. The % of gravel and D_{60} values for traps 1 – 4 were 73% and 29 mm for trap #1, 66% and 19 mm for trap 2, 32% and 2 mm for trap 3, and 74% and 23 mm for trap 4. From Figure 4.16 (Armour Layer Sediment Classification for Site 2) it is evident that the armour layer is fully mobile during peak flow events. It is interesting to note that traps 1, 2 and 4 clearly exhibited armour layer gravels moving during sediment transport, whereas trap 3 primarily captured sand. This shows that even under high flow events, secondary circulation via the meander bend still evacuated sand out of the pool centre and toward the point bar, where as coarser gravels are evacuated out of the riffle exit slope, thought the pool centre or over the point bar.

This is further supported by the data collected via handheld sampling just after peak flow events in April and June 2013 (Figures 4.21 – 4.32):

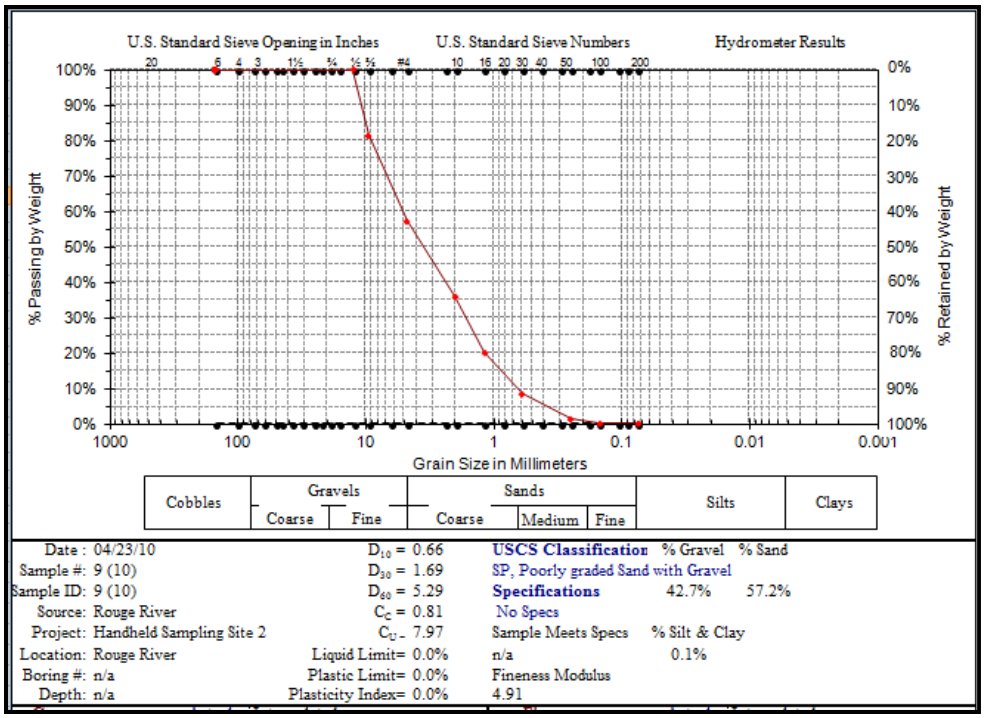

Figure 4.21: Site 2, Transect 9, Vertical 10 – Handheld Sampling – April 23, 2010

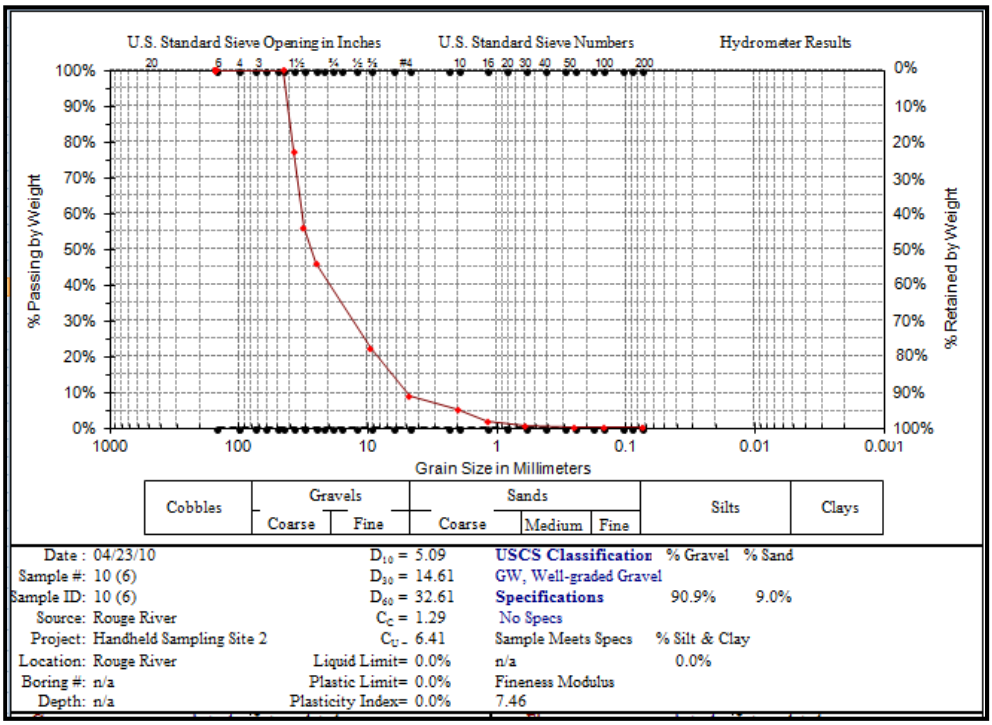

Figure 4.22: Site 2, Transect 10, Vertical 6 – Handheld Sampling – April 23, 2010

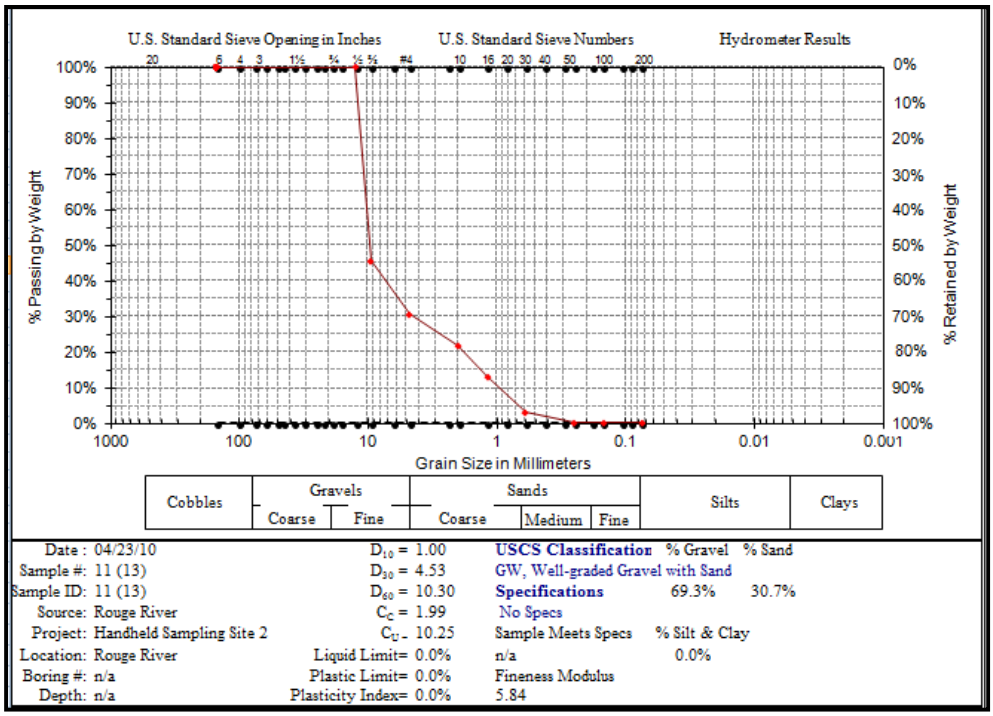

Figure 4.23: Site 2, Transect 11, Vertical 13 – Handheld Sampling – April 23, 2010

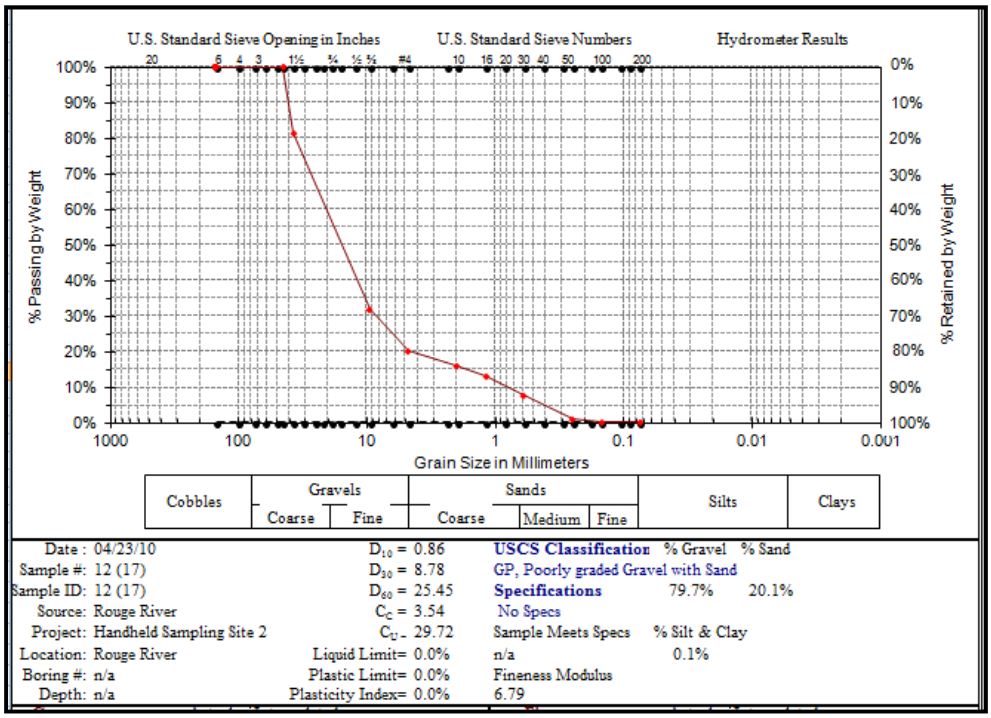

Figure 4.24: Site 2, Transect 12, Vertical 17 – Handheld Sampling – April 23, 2010

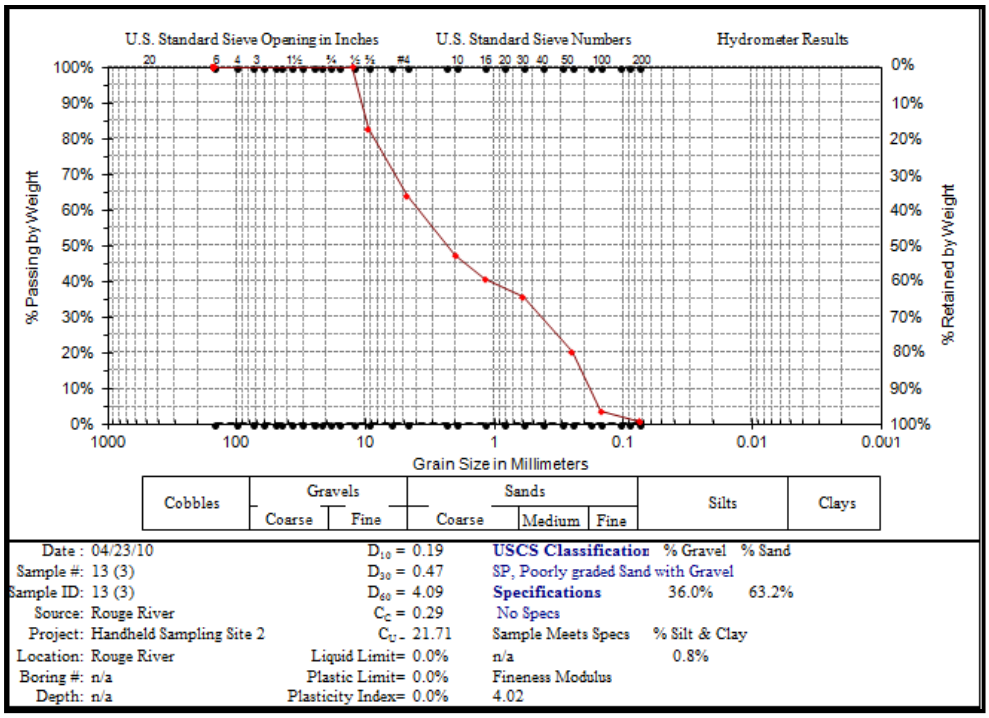

Figure 4.25: Site 2, Transect 13, Vertical 3 – Handheld Sampling – April 23, 2010

Figures 4.21 – 4.25 exhibit handheld samples taken along the riffle section (Transects 9 & 10) and the pool section (Transects 11, 12 & 13). Under lower flow conditions, the majority of sediment being transported is coarse sands and fine gravels. To further this point, the total sediment captured in the handheld sampler from transects 9, 10, 11, 12 and 13 was 312 g, 797 g, 380 g, 427 g and 158 g respectively. Figures 4.26 – 4.30 exhibit samples taken along the same transects during high flow events in June 2010:

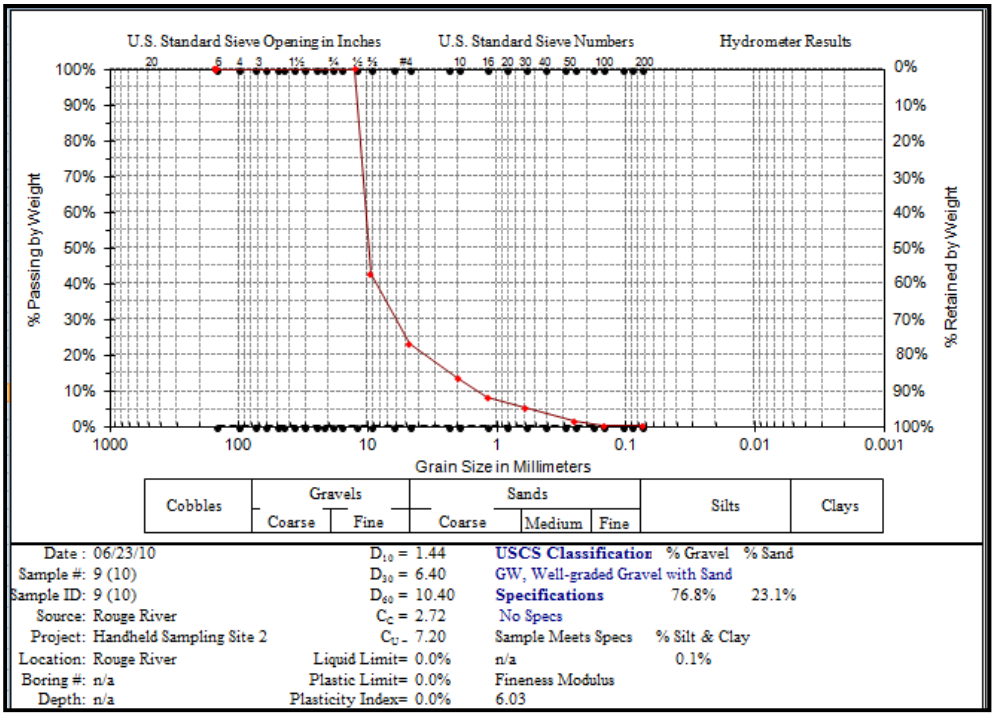

Figure 4.26: Site 2, Transect 9, Vertical 10 – Handheld Sampling – June 23, 2010

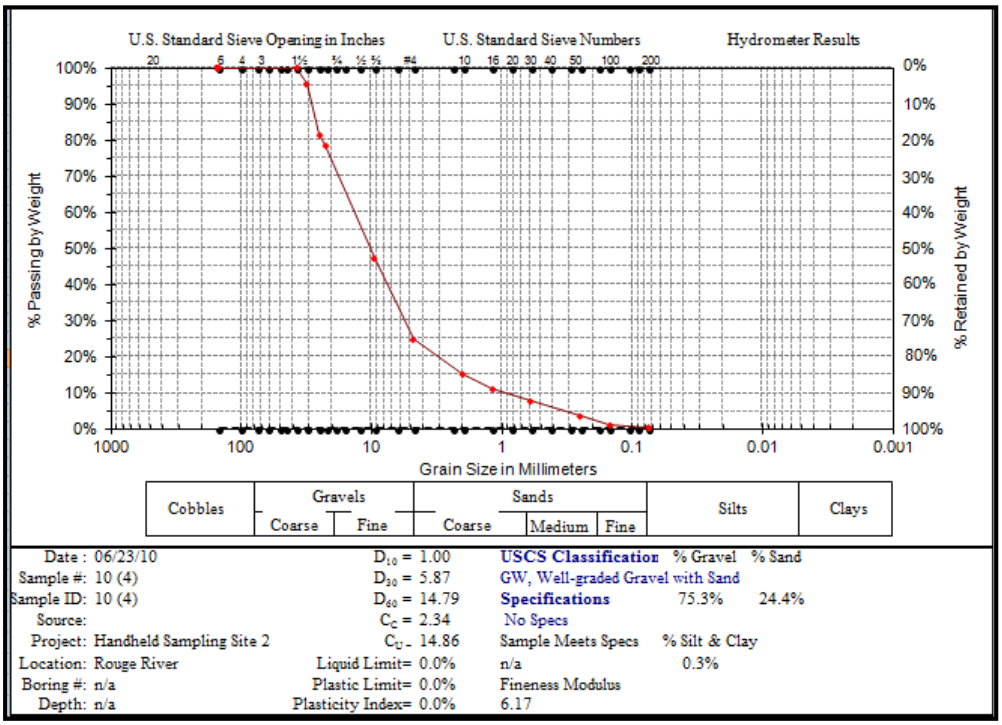

Figure 4.27: Site 2, Transect 10, Vertical 4 – Handheld Sampling – June 23, 2010

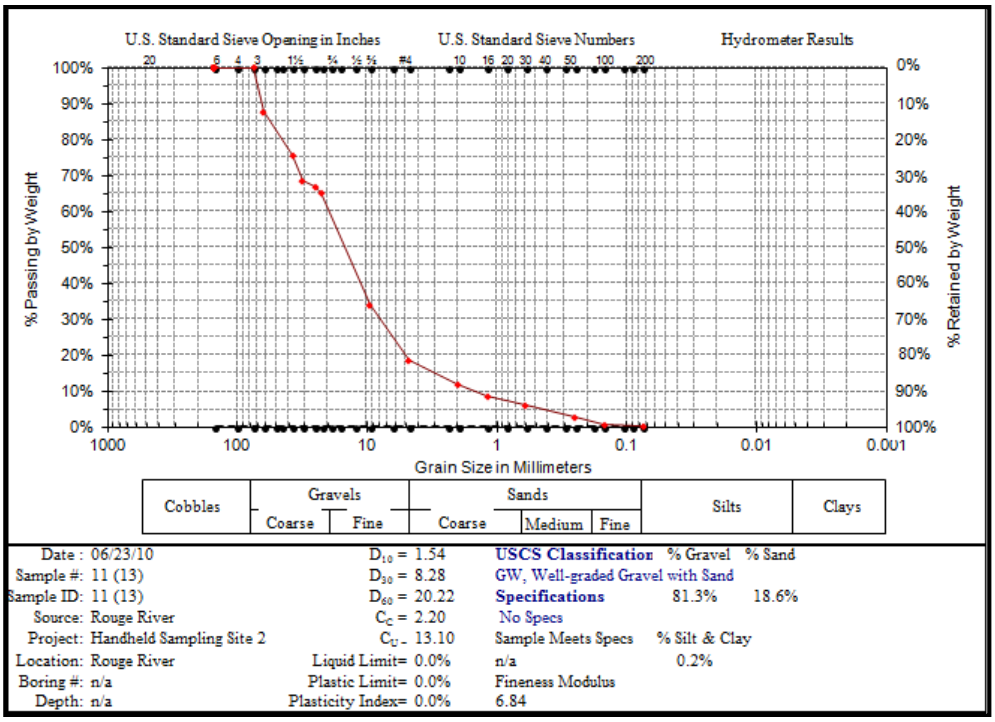

Figure 4.28: Site 2, Transect 11, Vertical 13 – Handheld Sampling – June 23, 2010

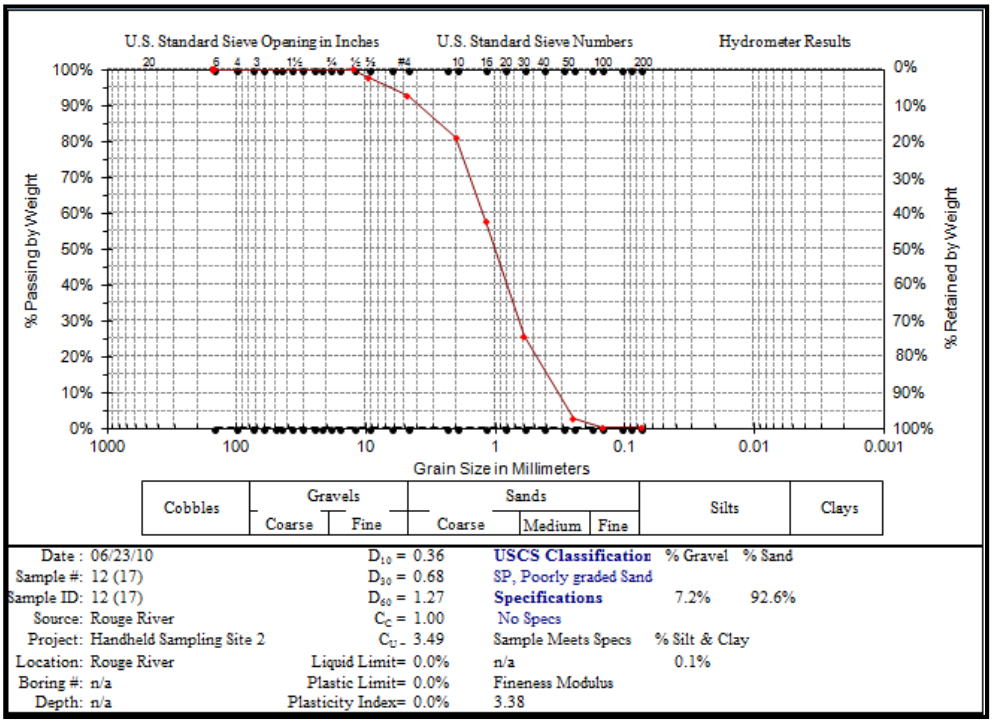

Figure 4.29: Site 2, Transect 12, Vertical 17 – Handheld Sampling – June 23, 2010

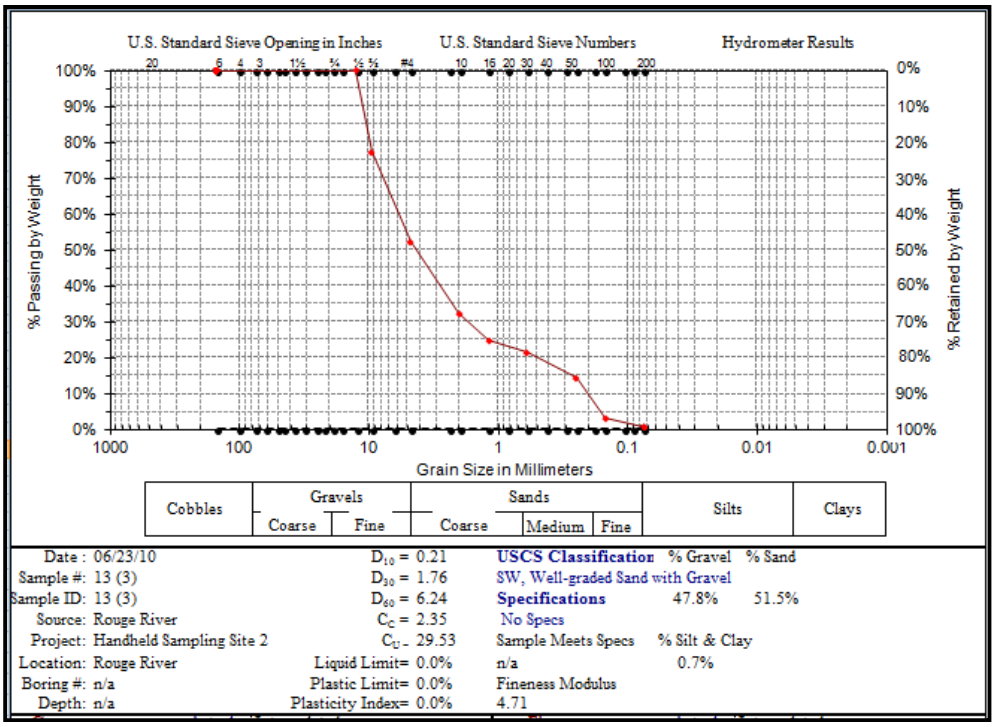

Figure 4.30: Site 2, Transect 13, Vertical 3 – Handheld Sampling – June 23, 2010

In contrast to Figures 4.21 – 4.25 (sampled under low flow), Figures 4.26 – 4.30 exhibit samples taking during higher flow events. This is supported by the volume in transition during this time period. Transects 9 – 13 had a D_{60} and total volume (g) of 10 mm and 623 g, 15 mm and 1701 g, 20 mm and 1996 g, 1 mm and 1594 g, and 6 mm and 212 g respectively. A rise in discharge (as expressed later in Figure 4.31) during this time period results in an increase in sediment volume being transported but no clear increase in the size of the gravel being transported. The three highest areas of sediment transport based on volume were the riffle exit slope (Transect 10 & 11) and pool centre (Transect 12). It is interesting to note that the D_{60} of sediment moving out of the riffle section was 20 mm and only 1 mm for the pool centre. Therefore, even under higher flow events, it

appears as if the pool still acts as an area of sediment deposition for coarser material (gravels) and an area of sediment evacuation for fine materials (sands).

4.2 Flow Properties and Bed Morphology

Flow parameters for Site 1 and Site 2, as well as the channel slope are provided in Table 4.1 and Table 4.2 respectively. More specifically, the discharge (*Q*), Reynolds numbers (*Re*), Froude numbers (*Fr*), Darcy-Weisbach friction factor (*f*) and average bed shear stress (τ_0) were calculated multiple times each month during the study period.

Average bed hear stress is defined in section 2.1 equation (1), Reynolds stresses are defined in section 2.2 equation (2.22) and discharge (*Q*) is defined in section 3.4 under equation (2.27). More specifically, Froude number (*Fr*) distinguishes between subcritical flows, which are Fr <1 and supercritical flows, which are Fr>1. In natural settings such as the Rouge River, flows should be turbulent and subcritical. The Darcy-Weisbach friction factor (*f*) suggests that as flow stages increases, the value of *f* decreases. The value of *f* is related to relative roughness which is a function of depth over grain size (d / D_{50}).

It can be seen from Table 1 for both sites and each measurement date that the river flow was fully turbulent and subcritical. From Figure 4.31 the discharge over the study period showed significant variations for both Site 1 and Site 2, with drastic increases in discharge toward the latter half of the study period. The *Re* show a dramatic increase over the study period at both sites as discharge increased towards the latter half of the study. Average *Fr* remained quite steady throughout the study period for both sites.

Additionally, there appears to be no difference in *Fr* between the two sites. The *f* values show an inverse relationship with *Q*, in that as *Q* increase *f* tends to decrease for both sites and as *Q* decreases, *f* tends to increase for both sites. Table 4.2 displays the variation in slope over the study period and difference in slope between the two study sites. It is clear that that slope for all measurement periods for Site 2 was greater than that of Site 1 during the study period. Slope was determined by interpolating survey data in GIS and obtaining an average bed height along each transect.

Table 4.1: Flow properties of Site 1 and Site 2, Rouge River, April – June 2010.

	Q (m^3/s) Site 1	Q (m^3/s) Site 2	Re ($x10^3$) Site 1	Re ($x10^3$) Site 2	Fr Site 1	Fr Site 2	f Site 1	f Site 2	τ_0 (Nm^{-2}) Site 1	τ_0 (Nm^{-2}) Site 1
April 23	0.94	0.83	127.20	85.10	0.25	0.31	8.70	7.93	30.51	35.91
April 27	0.69	0.66	90.30	73.20	0.23	0.25	6.07	15.15	21.63	30.29
May 7	0.94	0.73	110.50	72.20	0.23	0.27	6.87	10.21	34.08	31.70
May 14	4.05	3.67	260.10	249.30	0.34	0.33	2.17	7.02	50.03	52.47
May 28	0.80	0.72	92.20	80.40	0.21	0.23	5.17	8.67	17.66	27.12
June 9	1.32	1.50	188.80	128.00	0.25	0.28	7.96	8.40	23.98	28.08
June 16	2.78	3.61	307.70	318.40	0.38	0.35	1.78	8.27	27.12	31.32
June 23	4.10	4.44	500.50	396.80	0.40	0.33	0.54	3.79	32.84	44.31
June 29	3.76	3.73	403.70	333.80	0.39	0.36	0.51	5.45	26.62	33.30

Table 4.2: Slope variation of Site 1 and Site 2, Rouge River, April – June 2010.

	Slope*	
	Site 1	**Site 2**
April 23	-0.0088	-0.0109
April 27	-0.0069	-0.0112
May 7	-0.0102	-0.0117
May 14	-0.0102	-0.0117
May 17	-0.0064	-0.0107
May 28	-0.0064	-0.0107
June 9	-0.0067	-0.0087
June 16	-0.0064	-0.0087
June 23	-0.0062	-0.0085
June 29	-0.0054	-0.0075

*Slopes are negative as they reflect a downward gradient (downstream).

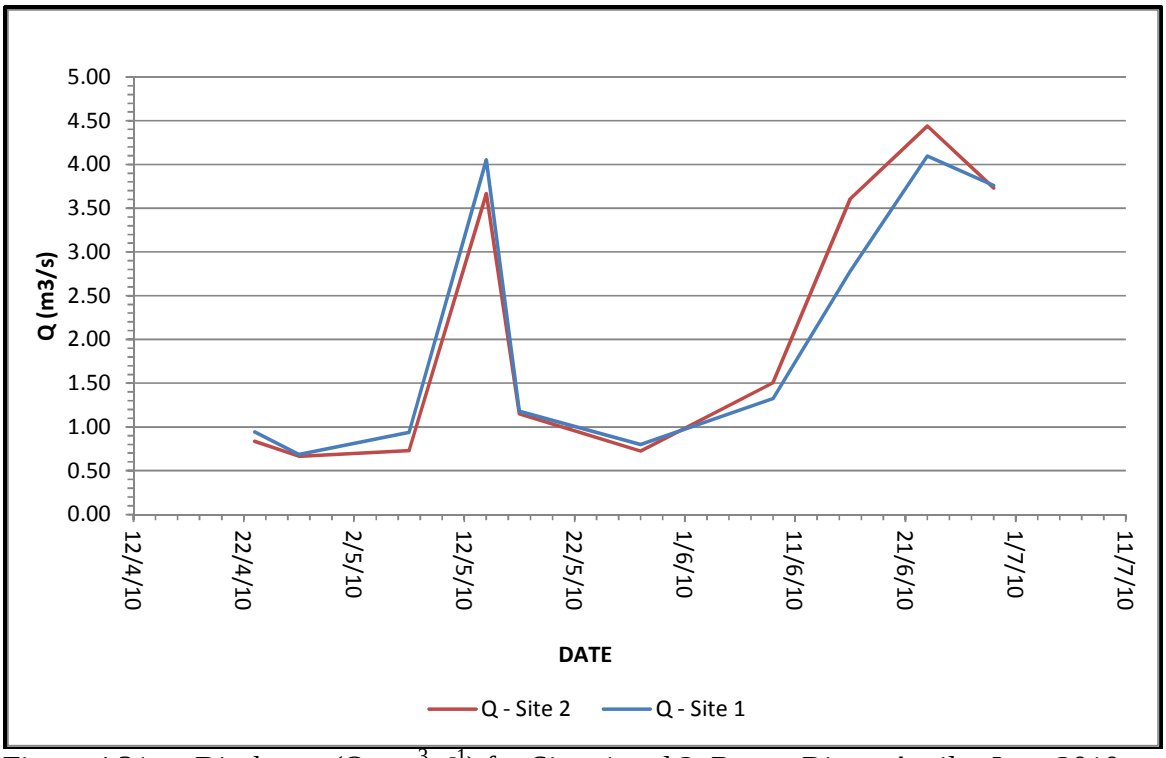

Figure 4.31: Discharge (Q - $m^3 s^{-1}$) for Sites 1 and 2, Rouge River, April – June 2010.

For supplemental purposes water level data was obtained from the Toronto and Region Conservation Authority (TRCA). Water level data is referenced based on an arbitrary instrument point (located near the Twyn Rivers Bridge – north of the Study Sites) within the water column. From Figure 4.32 and Figure 4.33 it is evident that water levels during the study period (April to June 2010) exhibited frequent fluctuations when compared to 2009 data that was also supplied by the TRCA. The fluctuations observed in Figure 4.33 are indicative of frequent precipitation events that occurred during the study period that led to significant rises in discharge. It is possible that the 2010 study period data may be an anomaly as the 2009 data exhibits less frequent rises in water level and hence discharge.

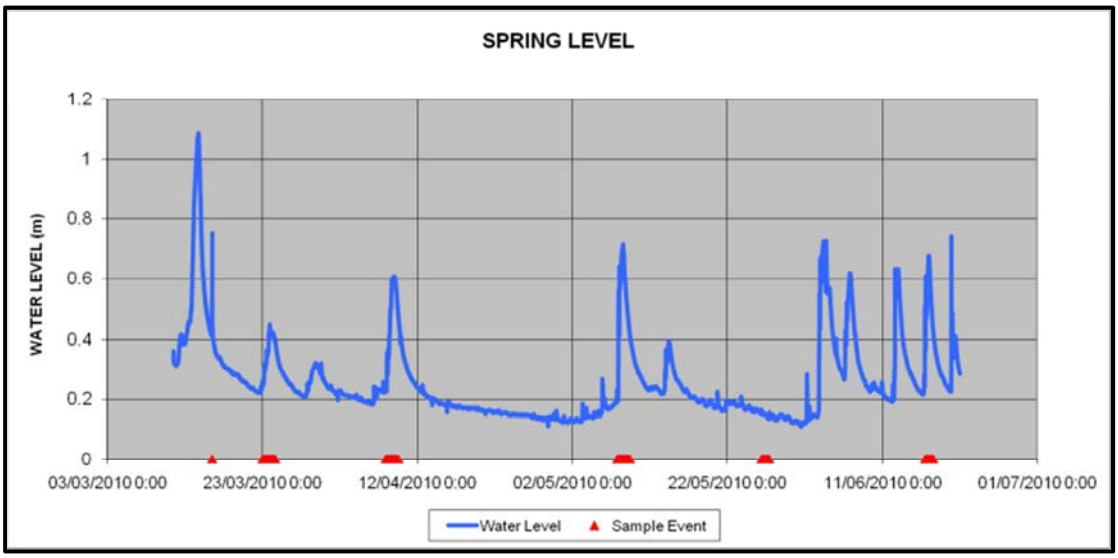

Figure 4.32: Spring Water Level data for 2010 from the Twyn Rivers Bridge, Rouge River, located upstream of the study sites.

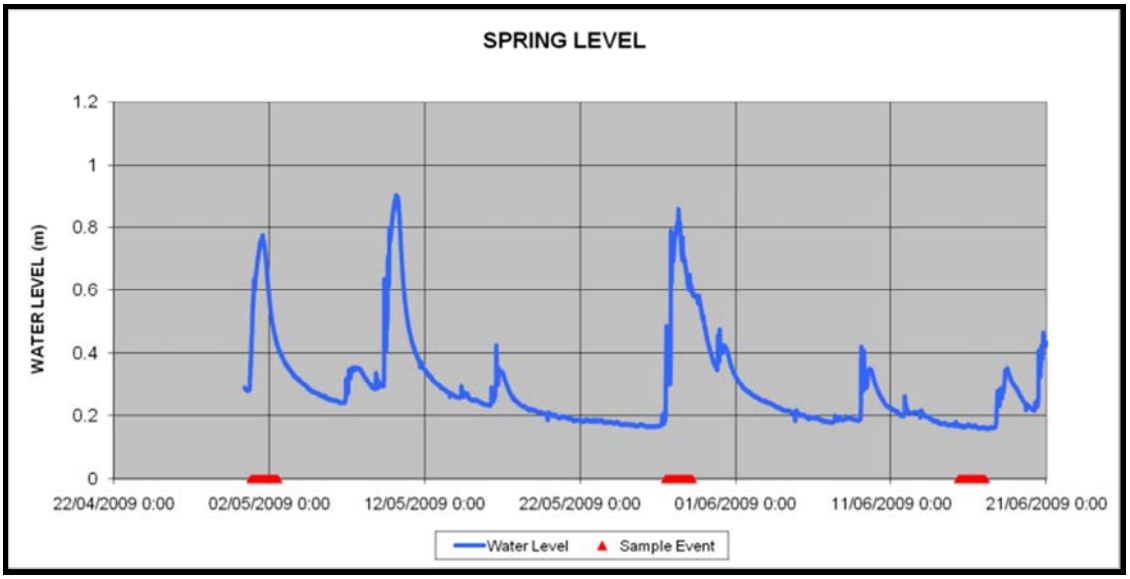

Figure 4.33: Spring Water Level data for 2009 from the Twyn Rivers Bridge, Rouge River, located upstream of the study sites.

For comparison purposes Site 1 and Site 2 were broken down into zones in order to assess the study sites. The zones (areas of importance) were chosen in order to assess the flow parameters, sediment yields, as well as turbulence statistics for this study. Zones were chosen based on visual analysis of bathymetry maps in terms of identifying areas of scour and fill at both Site 1 and Site 2 over the study period. Comparisons for each site were kept to two or three zones as any greater number is beyond the scope of this study; the zones are displayed in Figure 4.34 – 4.35 and 4.36 – 4.37. For Site 1, zone 1 is represented by transect 1 and transect 2; these transects are represented by the pool centre section and the pool exit slope respectively. Zone 2 for Site 1 is characterized by a riffle entrance slope (Transect 3), the riffle crest (Transect 4) and the riffle exit slope/pool entrance slope (Transect 5). Zone 3 is characterized by the pool centre (Transect 6) and the pool exit slope (Transect 7). For Site 2, zone 1 is represented by transect 8, transect 9 and transect 10; these transects are represented by the pool exit slope/riffle entrance slope, riffle crest and riffle exit slope respectively. Zone 2 is characterized by the pool entrance slope (Transect 11), pool centre (Transect 12) and the pool exit slopes (Transect 13 and Transect 14).

Figure 4.34 through Figure 4.37 display interpolated bed elevations for Site 1 and Site 2 for the months of April and June. The interpolated bed elevations for the month of May for Site 1 and Site 2 are not present here; for the sake of running a visual comparison analysis of bed topography the beginning and end of the season or a low and high flow event respectively will suffice.

Figures 4.34 and 4.35 bathymetry maps for Site 1 indicated that bed topography over the study period generally exhibited minor changes. Zone 2 exhibited change, while zone 1 and zone 3 had the most notable changes. Zone 2 which is characterised by the riffle entrance slope (Transect 3), riffle crest (Transect 4) and riffle exit slope (Transect 5) exhibited significant chnage, whereby riffle height from deposition increased over the study period. This is interesting as the riffle region appeared to be a zone of accumulation after high flow discharge events subsided. This could be deceiving, however, as under low flow events the flow is diverted around and beside the bar, through a narrower channel where flows are increased and potential sediment evacuation could occur. Then under high flow events, the bar is submerged and acting as a point of sediment evacuation, thus zone 2 could potentially be an area of sediment transport under many varying flows. Noticeable change is evident in zone 1 as the deepest part of the pool region (pool centre) shifted downstream and became shallower through the study period toward the high discharge events. Similarly, in zone 3, the deepest portion of the pool section shift slightly downstream and more toward the centre of the channel through the study period and towards higher discharge events. The shift of the deepest portion of the pool section toward the centre of the channel is interesting as it proves that the position of the centre of the pool is a function of channel curvature. During lower discharge, the channel is slightly obstructed and diverted around the bar, thus increasing the channel curvature and complexity of the flows.

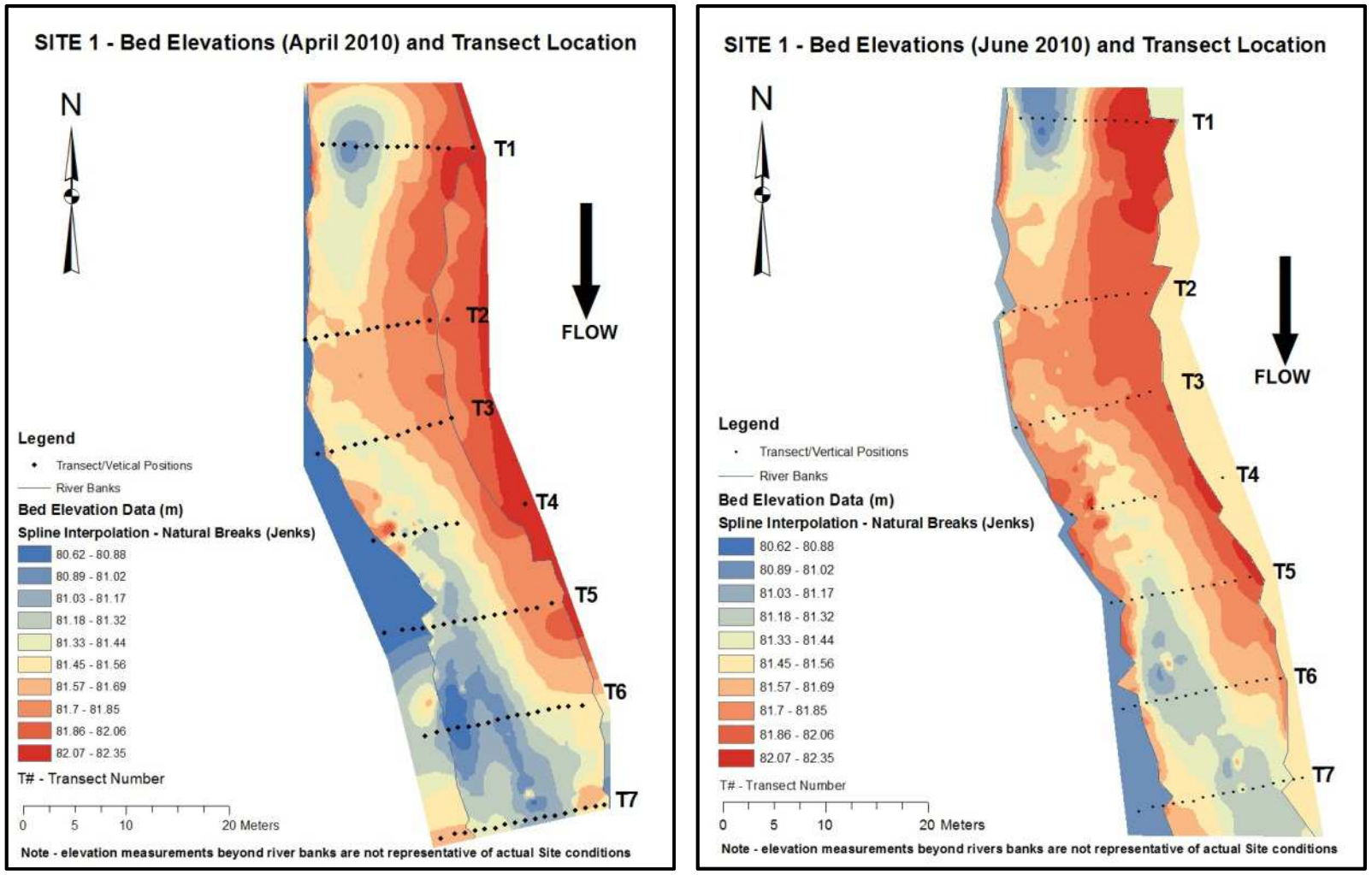

Figure 4.34 – 4.35: Interpolated bed elevations (NAD 1983 UTM Zone 17N), transect location and bedload trap location for Site 1, April 2010 and June 2010.

The maps of bed topography for Site 2 indicate that bed topography over the study period generally exhibited minor changes (Figures 4.36 and 4.37). The most notable changes are observed in the pool centre section (Zone 2), as the pool is noticeably shallower at the end of the season (by approximately 10 cm). Additionally, the spatial extent of the deepest part of the pool section is somewhat narrower and shorter, as well its position has shifted downstream. The same observations that apply to the deepest part of the pool section, also apply to the bar across the channel. Additionally, noticeable change is observed in the riffle section (Zone 1), transect 9, where average riffle height across the transect is noticeably higher at the end of the season. A calculation of average riffle height revealed that the riffle section in June was approximately 30 cm higher than it was at the beginning of the study period. It is interesting to note that zone 1 for the higher flow period at the end of the study period appears to be an area of sediment accumulation (represented for greater/darker redness) within the zone. Areas where scour zones or holes once existed at the beginning of the study period have now been filled with sediment as bedload transport had occurred. Figure 4.38 and Figure 4.39 clearly exhibit how sediment is moved throughout the riffle and pool sections during high flow and peak discharge events.

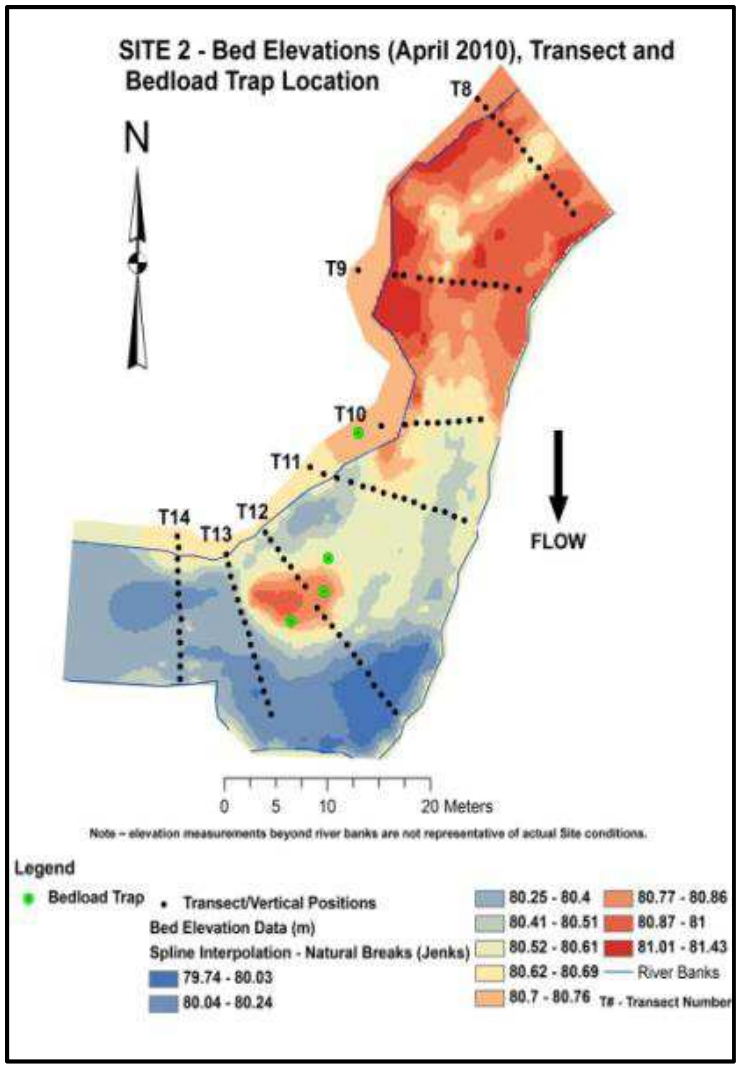

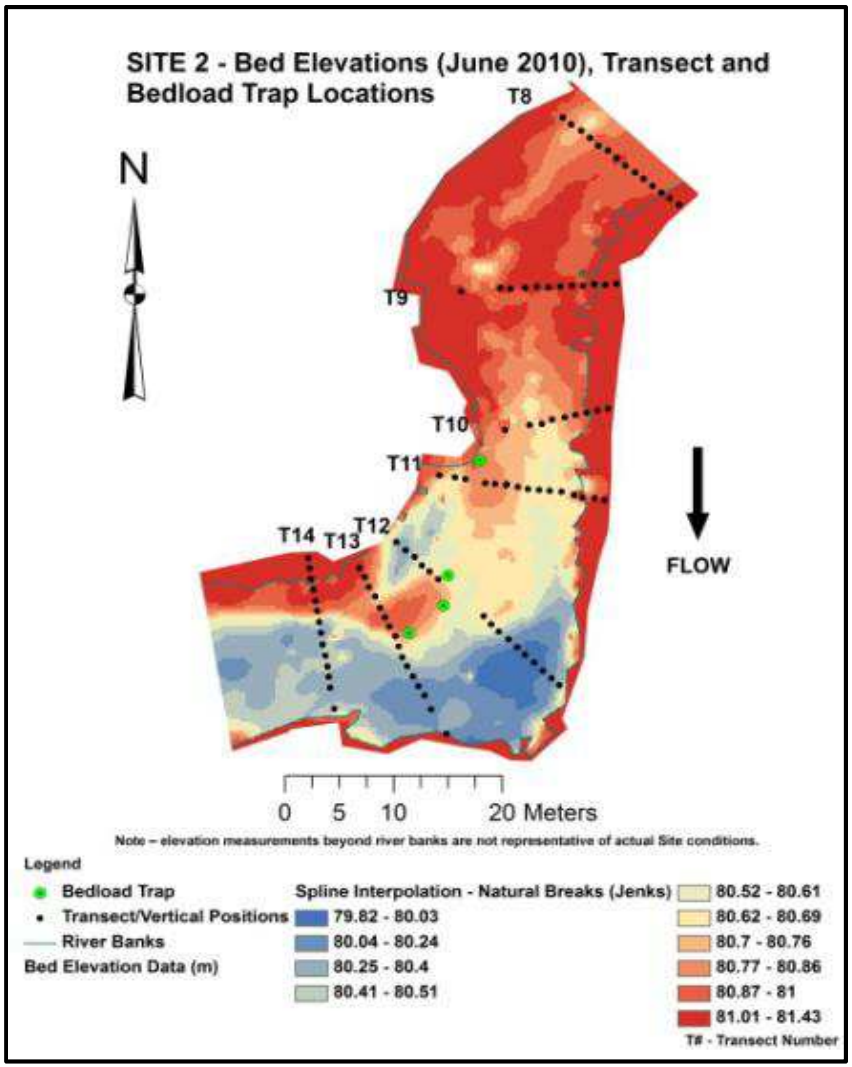

Figure 4.36 – 4.37: Interpolated bed elevations (NAD 1983 UTM Zone 17N), transect location and bedload trap location for Site 2, April 2010 and June 2010.

Figures 4.36 through 4.37 are important in terms of comparison due to drastically different flow regimes that were occurring. The April 2010 data was taken during a period of relatively lower/base flow conditions. In contrast, the June 2010 data was taken immediately after a multitude of storms (high-flow events) that occurred in the month of June. From the TRCA water level data (Figure 4.32) it can be seen that June had seven (7) high flow events in the month of June.

4.3 Mean Turbulent Flow Characteristics

4.3.1 Site 2 – Zone 1

The flow properties and statistics for Site 2, zone 1 are displayed in Figures 4.40 through 4.45 for low flow, moderate flow and high flow events.

Under low flow conditions (April 2010 and May 2010), the average downstream velocity profiles for Site 2, Zone 1 (Transect 8 - pool exit slope) exhibits a characteristic velocity profile with average velocities increasing with height above the bed and reaching a maximum average velocity near the water surface. The maximum average downstream velocities observed during low flow conditions were approximately 40 cm s^{-1}. Under high flow conditions (June 2010), the typical average downstream velocity profile is observed, however, the maximum velocity above the bed roughly doubled to approximately 80 cm s^{-1}.

Similar to downstream average velocity, the turbulence intensities and Reynolds stresses also increased from low flow to high flow for the pool exit slope section. During lower flow conditions (April 2010 and May 2010), the Reynolds stresses ranged from

approximately 6 dyn cm^{-2} (N m^{-2}) in April to 40 dyn cm^{-2} in May. It interesting to observe that under roughly similar average downstream velocities and discharges, the Reynolds stresses are approximately six times higher in the pool section in May 2010 than they were in April 2010 at 20 cm above the bed. Additionally, a spike of Reynolds stresses under lower flow conditions was observed at approximately 5 cm above the bed. The spike in Reynolds stresses or momentum exchange that was observed very close to the bed, likely plays a crucial role in bed sediment transport processes in the pool exit slope. Under higher flow conditions (June 2010), Reynolds stress were similar in magnitude (approximately 40 dyn cm^{-2}) to that of May 2010, however, the maximum momentum exchange was observed approximately 5 cm above the bed, likely indicative of sediment and bedload transport characteristics.

The turbulent intensities also display a similar profile to that of the Reynolds stress profiles with spikes in turbulent intensity observed near the bed surface (approximately 5 cm above the bed) and approximately 20 cm above the bed. Similar to the Reynolds stress profiles, the turbulent intensities observed were higher in magnitude during May 2010 than they were in April 2010. However, during the higher flow events (June 2010), the turbulent intensity increased to approximately 250 g $cm^{-1}s^{-2}$ As well, under higher flow conditions, the zone of maximum turbulent intensity was located over a larger range with maximum values occurring from approximately 5 – 15 cm above the bed.

It is interesting to observe that the pool exit slope seems to be linked closely with increases in discharge. Furthermore, an increase in discharge appears to also mean an

increase in Reynolds stresses and TKE above the bed. Under higher flow conditions, the magnitude of Reynolds stresses and TKE increases dramatically.

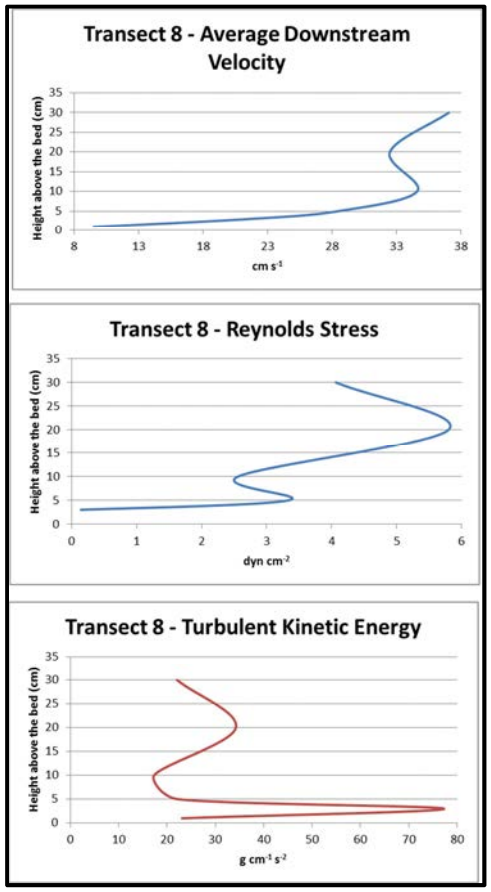

Figure 4.40: Cross channel averages of downstream velocity, Reynolds stresses and turbulent kinetic energy for zone 1, transect 8 – April, 2010

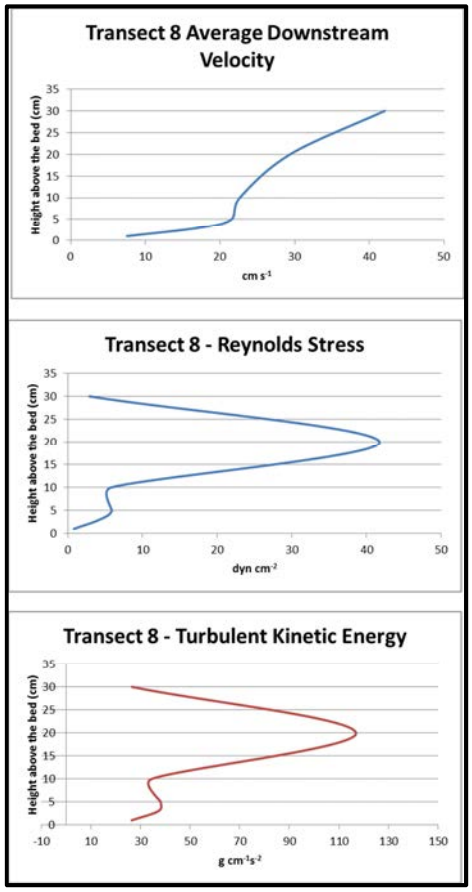

Figure 4.41: Cross channel averages of downstream velocity, Reynolds stresses and turbulent kinetic energy for zone 1, transect 8 – May, 2010.

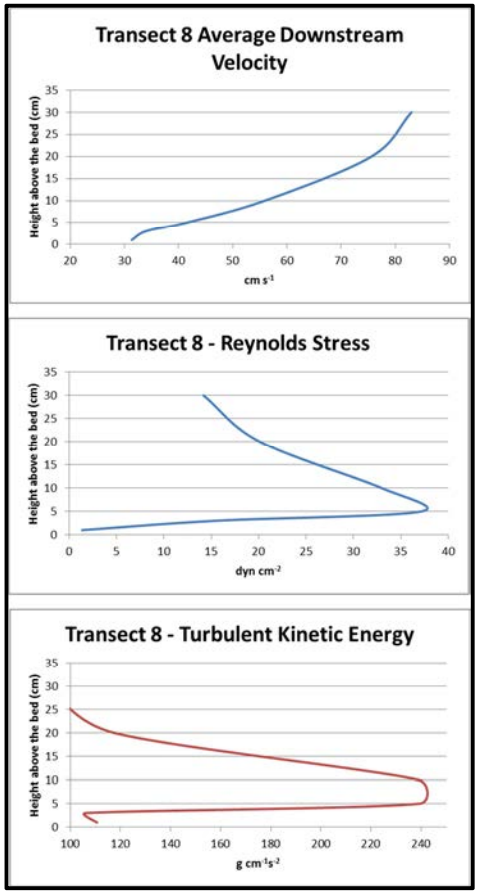

Figure 4.42: Cross channel averages of downstream velocity, Reynolds stresses and turbulent kinetic energy for zone 1, transect 8 – June, 2010.

Zone 1 Transect 9 represents the riffle crest region of Site 2. The downstream average velocities under low flow conditions (April 2010 and May 2010) exhibited a typical profile for downstream velocity and maximum values ranged from approximately 50 – 60 cm s^{-1}. Under high flow conditions in June 2010, the maximum average downstream velocity nearly doubled to approximately 120 cm s^{-1}.

The Reynolds stresses for lower flow conditions April and May 2010 were observed to be very similar with maximum values of momentum exchange occurring approximately 5 cm above the bed and having maximum values of approximately 20 dyn cm^{-2}. A sharp decrease in momentum exchange is also observed at heights greater than 5 cm above the bed (toward the water surface). It is clear that riffle regions exhibit momentum exchange very close to the river bed surface in a concentrated zone approximately 5 cm above the bed. Under high flow conditions (June 2010), it is observed that the riffle region exhibits maximum Reynolds stress values nearly three (3) times higher (60 dyn cm^{-2}) than May 2010. The increased momentum exchange values observed during the high flow periods are likely the reason why riffle regions act as a sediment evacuation zone in the riffle-pool sequence.

Similar to Reynolds stresses, the turbulent intensities increased with increasing discharge. Maximum turbulent intensities values ranged from approximately 350 g $cm^{-1}s^{-2}$ (April 2010) to 550 g $cm^{-1}s^{-2}$ (May 2010). Under high flow events (June 2010), the maximum turbulent intensity values reached an approximate value of 500 g $cm^{-1}s^{-2}$. It appears as if the TKE over the riffle section reaches a maximum value during a

rising discharge but does not continue to increase linearly as the discharge continues to rise.

When comparing the pool exit slope/riffle entrance slope (Transect 8) with the riffle crest (Transect 9) it can be noted that the maximum observed Reynolds stresses do not appear to change over the two areas. The turbulent intensities over the riffle crest regions are approximately two (2) to seven (7) times greater than those maximum values observed over the pool exit/riffle entrance slope section.

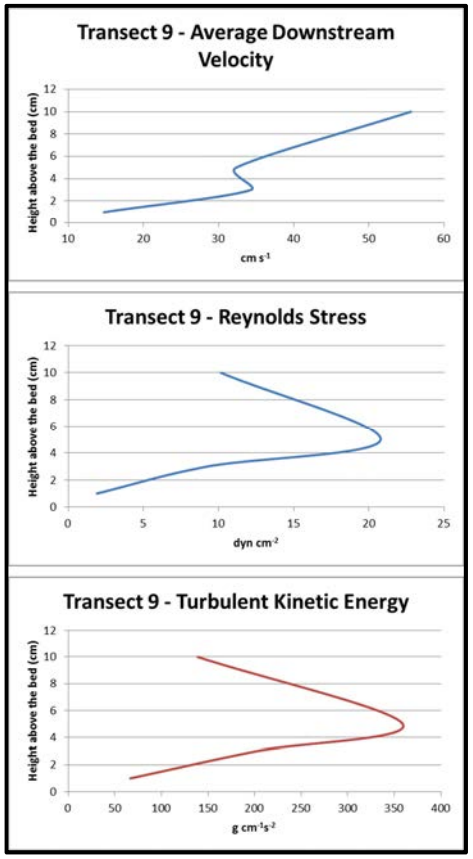

Figure 4.43: Cross channel averages of downstream velocity, Reynolds stresses and turbulent kinetic energy for zone 1, transect 9 – April, 2010.

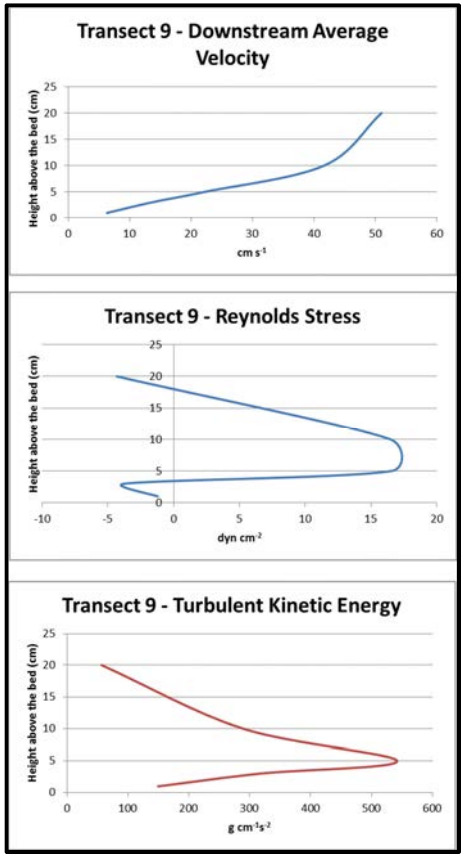

Figure 4.44: Cross channel averages of downstream velocity, Reynolds stresses and turbulent kinetic energy for zone 1, transect 9 – May, 2010.

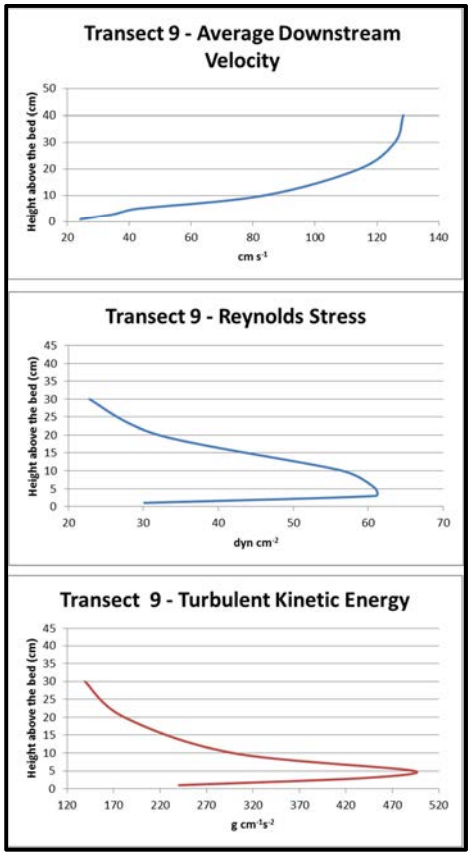

Figure 4.45: Cross channel averages of downstream velocity, Reynolds stresses and turbulent kinetic energy for zone 1, transect 9 – June, 2010.

4.3.2. Site 2 – Zone 2

The flow properties and statistics for Site 2, zone 2 are displayed in Figures 4.46 through 4.51 for low flow, moderate flow and high flow events respectfully.

Zone 2, Transect 12 represents the deepest portion of the pool (pool centre) for Site 2. Although the typical velocity profile for downstream velocity exists, it is apparent that under lower flow conditions (April 2010) that maximum velocity in pool sections is significantly slower when compared to the maximum velocity over riffle sections. The maximum velocity is approximately <20 cm s^{-1}, confirming the notion that pool sections act as sediment deposition areas for finer particles. In contrast, the downstream velocity profile for May 2010 was almost linear from the river bed, with velocities reaching values of approximately 25 cm s^{-1} at 40 cm above the bed. If recorded values could have been taken at heights >40 cm above the bed, it is likely that the observed velocity profile would be similar to that of the typically observed profile (e.g. Figure 4.45). Due to limitations in the equipment, readings could not be performed for heights greater than 40 cm above the bed. The tripod could only be built to a certain size that could be manageable for movement on the river bed. Due to this limitation the ADV could only be traversed to a maximum of 40 cm above the bed. Interestingly, in June 2010 the velocity in the pool section near the bed did not increase as dramatically as that observed in the riffle section of Zone 1. Maximum values observed were equal to that of May 2010 with a maximum value of approximately 25 cm s^{-1} at 25 cm above the bed. This observation is

interesting as the data suggests that downstream velocity near the bed in pool sections does not increase with a rise in discharge.

Similarly, unlike riffle sections observed in zone 1, the maximum values for Reynolds stresses and TKE are not as clear near the pool bottom; rather the maximum values are observed approximately at >20 cm above the bed. Reynolds stresses and turbulent statistics observed were fairly low with maximum values smaller than 10 dyn cm^{-2} and approximately 60 g $cm^{-1}s^{-2}$, respectively. The momentum exchange and turbulent energy is likely influenced by the secondary circulation of flows associated with meander bends, creating steeper velocity gradient in the velocity profile. However, as the discharge increased in May 2010, the Reynolds stresses were at a maximum of approximately 7 dyn cm^{-2} at 10 cm above the bed. A noticeable spike in Reynolds stresses of 4 dyn cm^{-2} was also observed at 4 cm above the bed. This spike in momentum near the bed is likely an observation of sediment transport and evacuation of sediment out the pool centre. The profile of TKE is linear with maximum values of approximately 110 g $cm^{-1}s^{-2}$ being observed at 40 cm above the bed. In June 2010, an interesting observation is that the downstream velocity and the degree of Reynolds stresses and TKE actually decreased with an increasing discharge. Reynolds stresses were observed to only be a maximum of 4 dyn cm^{-2} 5 cm above the bed and turbulent statistics were observed to only be a maximum of 30 g $cm^{-1}s^{-2}$ at 5 cm above the bed. Both Reynolds stresses and TKE drastically decreased with height above the bed after 5 cm in height. It appears that momentum exchange and TKE are confined to a zone immediately above the bed; however, it is likely that a change in river pattern may have affected the results and

patterns observed. June 2010 was marked by periods of heavy rainfall and drastically increasing discharges as illustrated in Figure 4.19 and 4.20. An important visual observation made while at the study site was that flows took a more direct route as the rising water levels breached the inner bank of the meander. This caused a reduction in the radius of curvature of the meander bend, which likely affected the associated secondary flow characteristics (channel form became more straight than meandering).

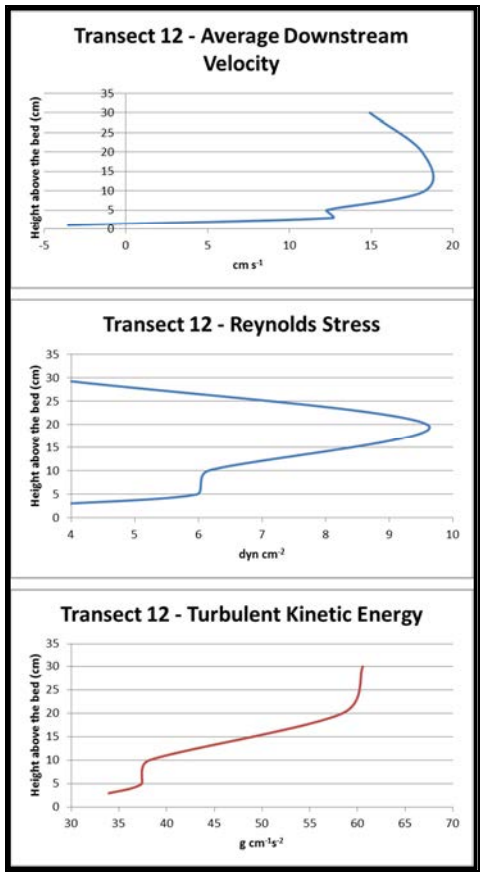

Figure 4.46: Cross channel averages of downstream velocity, Reynolds stresses and turbulent kinetic energy for zone 2, transect 12 – April, 2010.

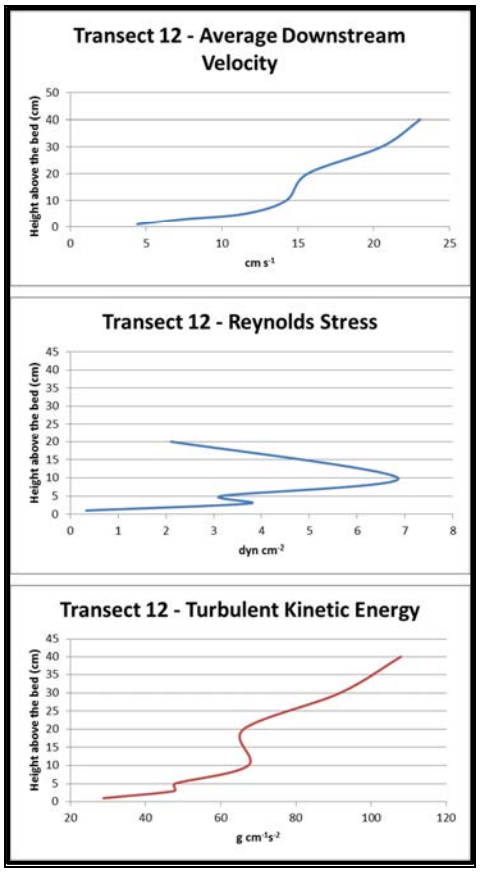

Figure 4.47: Cross channel averages of downstream velocity, Reynolds stresses and turbulent kinetic energy for zone 2, transect 12 – May, 2010.

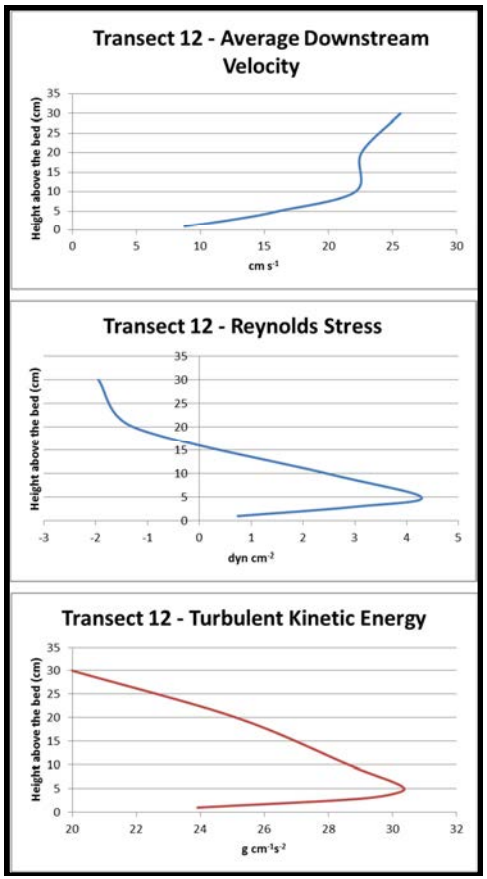

Figure 4.48: Cross channel averages of downstream velocity, Reynolds stresses and turbulent kinetic energy for zone 2, transect 12 – June, 2010.

Zone 2, Transect 14 is represented by the pool exit slope region of Site 2 (Figure 4.49 - 4.51). Downstream velocities under lower flow conditions (April 2010) were observed to be a maximum of approximately 25 cm s^{-1}. Under slightly higher flow conditions/discharges in May 2010 and June 2010, the maximum downstream velocity was observed to be approximately 35 cm s^{-1} and 80 cm s^{-1} respectively.

The Reynolds stresses for the pool exit slope region appear to be linked to increasing discharge. For example, under lower flow conditions (April 2010) the Reynolds stresses observed were almost non-existent with maximum values of approximately 3 dyn cm^{-2} at 10 cm above the bed; whereas under higher flow conditions, May 2010 and June 2010, the maximum Reynolds stresses observed were approximately 10 dyn cm^{-2} and 22 dyn cm^{-2} at 10 cm above the bed. Similarly, the maximum observed TKE for May 2010 and June 2010 was approximately 65 g $cm^{-1}s^{-2}$ at 5 – 10 cm above the bed and approximately 170 g $cm^{-1}s^{-2}$ at 5 cm above the bed. It appears that the pool exit slopes act as a zone of higher momentum exchange and turbulent statistics as the flow depth and the discharge increase. This observation may further fuel the notion that pool sections act as a zone of section evacuation under higher flow conditions and deposition under lower flow conditions.

Overall, the patterns and linkages between downstream velocity, momentum exchange and turbulence statistics with respect to location (i.e., riffle or pool section) appear to be highly influenced by localized events or effects along the bed. In most instances, an increase in discharge was represented by an increase in downstream velocity, and also an increase in momentum exchange and turbulent kinetic energy. Due

to localized events occurring in such a small scale it is very difficult to find a pattern of distinct differences other than the obvious higher downstream velocity, Reynolds stresses and TKE in riffle sections compared to pool sections. The most noted differences occurred at Transect 12 (meander bend) from April to June 2010. An apparent shift in the degree of momentum exchange and turbulent kinetic energy towards the bed as discharge increased (near bankfull discharge) was observed from the June 2010 profiles. The apparent shift towards the bed may be significant in supporting the theory of velocity reversal whereby pool sections act as a zone of sediment deposition during low flow periods and as a zone of sediment evacuation during high flow (near bankfull discharge) events. Additionally, the change in the data from April to June 2010 could be due to a change in channel pattern. Through visual on site analysis and documentation, it was observed that the channel pattern and degree of sinuosity changed significantly after the high flow events in June 2010. Under low flow conditions in April and early May 2010, Transect 12 was characterized as a meander bend. However, under high flow and near bankfull conditions the flow pattern of the reach around Transect 12 changed from a meandering section to a relatively straight section. The change from meandering to straight section would have affected the flow characteristics around this transect significantly. Under meandering conditions, the flow patterns around Transect 12 were highly influenced by the secondary circulation and centrifugal forces, both of which are commonly observed in meander sections. However, under high flow conditions the flow patterns around Transect 12 would not have been influenced by these forces as the river reach become rather straight.

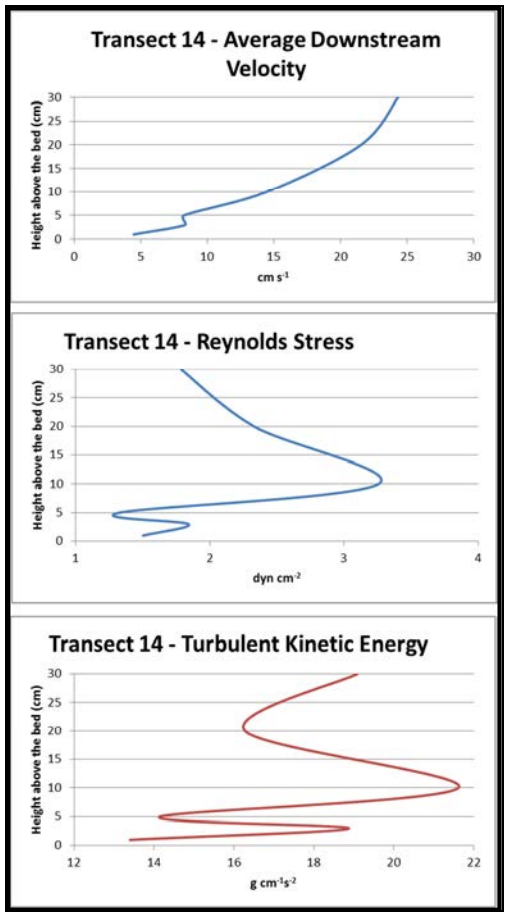

Figure 4.49: Cross channel averages of downstream velocity, Reynolds stresses and turbulent kinetic energy for zone 2, transect 14 – April, 2010.

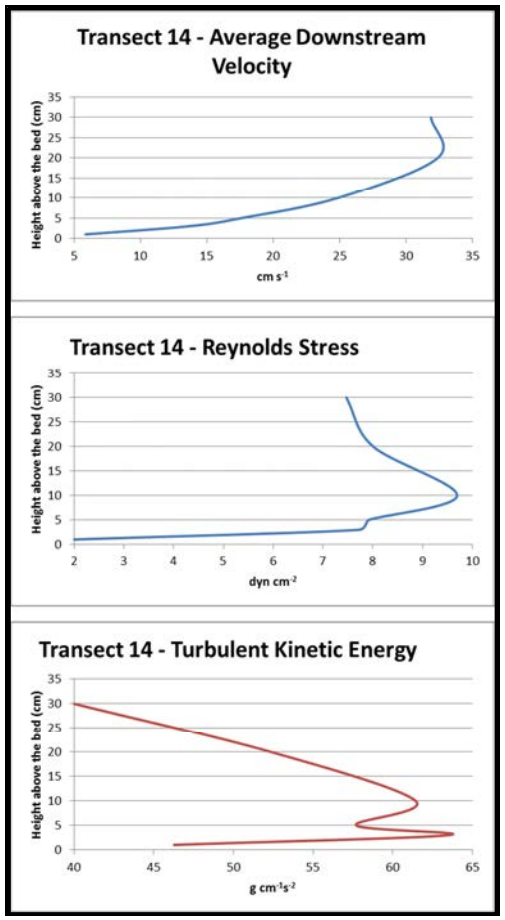

Figure 4.50: Cross channel averages of downstream velocity, Reynolds stresses and turbulent kinetic energy for zone 2, transect 14 – May, 2010.

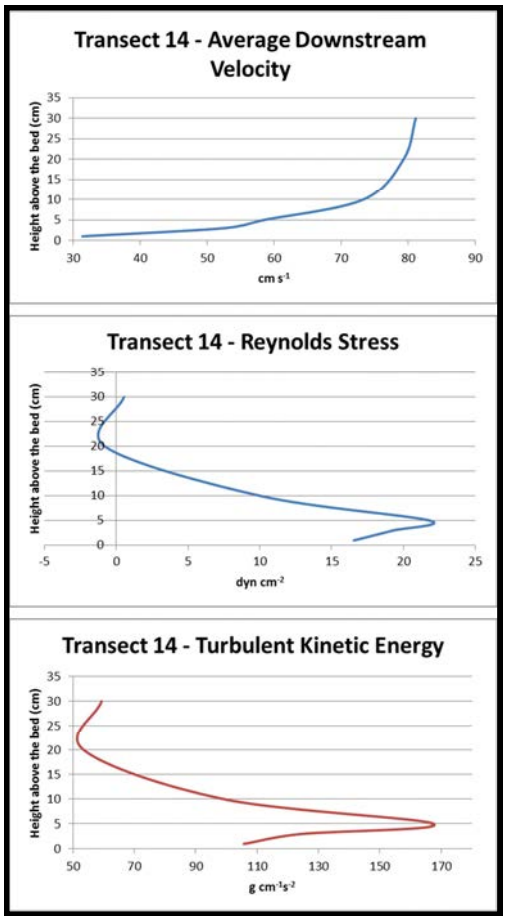

Figure 4.51: Cross channel averages of downstream velocity, Reynolds stresses and turbulent kinetic energy for zone 2, transect 14 – June, 2010.

4.3.3. Site 1 – Zone 1

The flow properties and statistics for Site 1, zones 1 - 3 are displayed in Figures 4.52 through 4.66 for low flow, moderate flow and high flow events respectfully.

Zone 1, Transect 1 represents the pool centre region for Site 1. It can be seen from the downstream velocity profiles that the maximum average downstream velocity under lower flow conditions (April 2010) near the bed was approximately 16 cm s^{-1} and approximately 20 cm s^{-1} in slightly higher discharges in May 2010. Under higher flow conditions (June 2010), the maximum velocities observed near the bed rose drastically to approximately 60 cm s^{-1}.

Reynolds stresses observed for the same time period displayed some interesting features whereby, under lower flow conditions, a drastic spike in momentum was observed near the bed with a maximum approximate value of 40 dyn cm^{-2} at 3 cm above the bed. The same drastic sudden spike pattern was not observed (in terms of magnitude) in May 2010, where smaller peaks of approximately 7 dyn cm^{-2} and 12 dyn cm^{-2} were observed at approximately 3 and 10 cm above the bed respectively. Under higher flow conditions (June 2010), the maximum momentum exchange was observed to be approximately 15 dyn cm^{-2} at 5 cm above the bed. It is clear that under all flow conditions a degree of momentum exchange is occurring near the bed. This anomaly which may have been observed in April 2010 could have likely to due to a local bed transport event that was occurring during the time of measurement or instrumentation interference.

A similar sudden spike can be observed in the turbulent statistics profile for April 2010, where a maximum value of approximately 225 g $cm^{-1}s^{-2}$ was observed 3 cm above the bed. In May 2010, the TKE values reached maximum peak values of approximately 50 g $cm^{-1}s^{-2}$ and 100 g $cm^{-1}s^{-2}$ at 3 and 10 cm above the bed, respectively. In June 2010, the maximum TKE value observed was significantly higher with an approximate value of 125 g $cm^{-1}s^{-2}$ at 5 cm above the bed. An interesting pattern seems to appear from this data, and it is that as the discharge or downstream velocity increases, the degree of momentum and TKE is concentrated to one layer above the bed rather than two. This observation may support the fact that pool centres act as a zone of sediment evacuation under higher flow conditions.

An interesting comparison can be established between the pool centre data in Site 2 and that of Zone 1 for Site 1. The pool region for Site 1 is in a portion of the channel which can be considered relatively straight and has a minimal degree of radius of curvature compared to that of Site 2 which has a much higher degree of curvature with the pool region centred within a meander bend. The noticeable absence of the potential effect that secondary flows and circulation may have on the flow profiles is observed, as the Site 2 pool region profiles deviated away from the typically observed velocity and turbulence statistic profiles, while the profiles observed over the straight reach were not influenced by surrounding flow patterns. This observation may further support the previously stated notion and observation from June 2010 for Site 2, where the profiles were drastically different than those from previous months and likely due to the fact that the flow within the channel had changed and become less meandered.

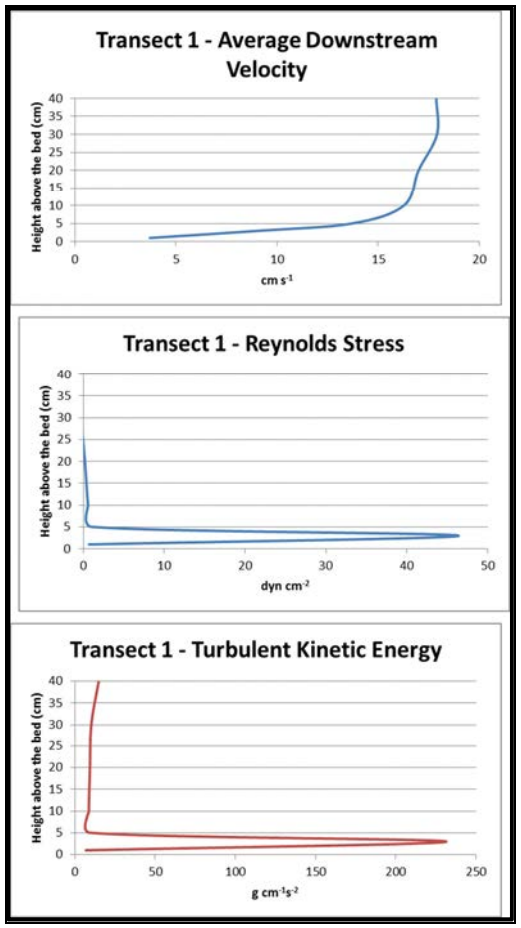

Figure 4.52: Cross channel averages of downstream velocity, Reynolds stresses and turbulent kinetic energy for zone 1, transect 1 – April, 2010.

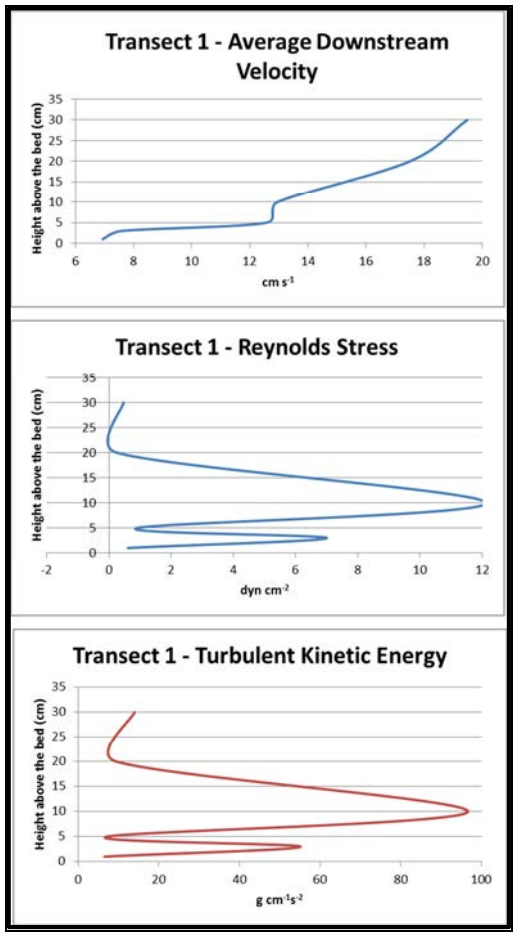

Figure 4.53: Cross channel averages of downstream velocity, Reynolds stresses and turbulent kinetic energy for zone 1, transect 1 – May, 2010.

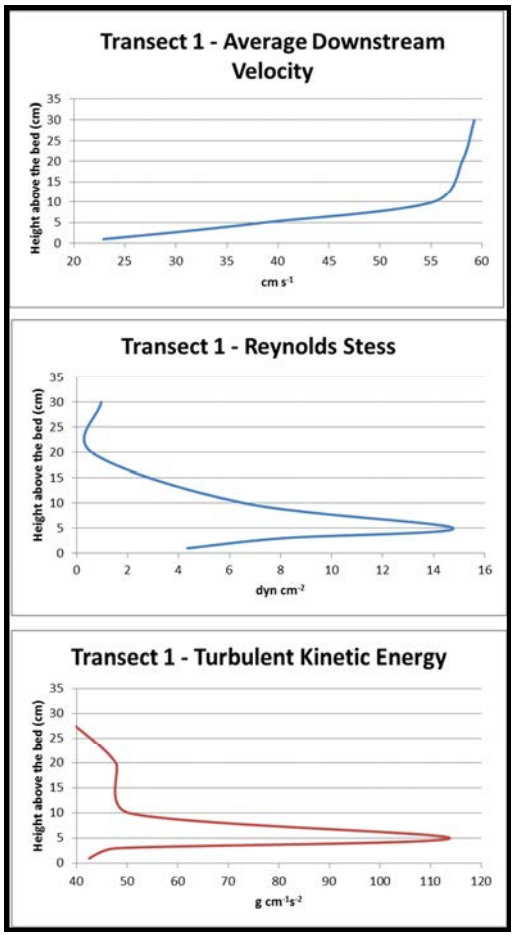

Figure 4.54: Cross channel averages of downstream velocity, Reynolds stresses and turbulent kinetic energy for zone 1, transect 1 – June, 2010.

4.3.4. Site 1 – Zone 2

Zone 2, Transect 3 of Site 1 is represented by a riffle entrance slope. The maximum average downstream velocity observed under low flow conditions (April 2010) was approximately 80 cm s^{-1}. In May 2010 and June 2010, the maximum average downstream velocity observed was approximately 40 cm s^{-1} and 90 cm s^{-1} respectively (Figures 4.55 – 4.57). The velocity profiles observed during this time period are as expected (i.e., gradual increase in velocity from the bed upwards) until just before the water surface where velocity levels off and/or decreases slightly.

The Reynolds stresses observed during April 2010 were slightly higher than those observed during May 2010. Average maximum values of approximately 26 dyn cm^{-2} occurred from 3 – 10 cm above the bed in April versus maximum values of approximately 14 dyn cm^{-2} occurred at approximately 3 cm above the bed in May. The profile observed in June 2010 differed slightly than those in April and May, with average maximum values of approximately 110 – 150 dyn cm^{-2} between 3 – 10 cm above the bed. It is clear that most of the transfer of momentum in all the profiles seems to be located within the first 10 cm of the bed surface. What is not consistent or clearly observed is the magnitude of Reynolds stresses with respect to increasing discharge. This may support the idea that local flow events or characteristics at a small scale level likely influence the near bed flow patterns in riffle regions.

The turbulent statistics observed above the bed on the riffle entrance slope reveal that TKE under varying flow conditions is highly erratic; however, it appears to be located within the first 10 cm of the bed. For example, in April 2010, the maximum TKE

values observed were approximately 220 g $cm^{-1}s^{-2}$; however, the observed values were confined to a thin layer above the bed (approximately 3 cm above the bed). In May 2010, the maximum observed TKE values observed were approximately 150 g $cm^{-1}s^{-2}$ at 3 cm above the bed and 130 g $cm^{-1}s^{-2}$ at 10 cm above the bed. In contrast, in June 2010 the observed velocity profile was very linear with TKE values increasing to approximately 4000 g $cm^{-1}s^{-2}$ near the surface.

When comparing Site 1 versus Site 2 data (Figures 4.40 – 4.51), it is clear that the profiles of velocity, Reynolds stresses and turbulent statistics are very similar. However, the magnitude of the momentum exchange and TKE in the meandering section (Site 2 – Transect 9) was observed to be nearly 2 – 3 times greater than those values observed in the straight section (Site 1 – Transect 3).

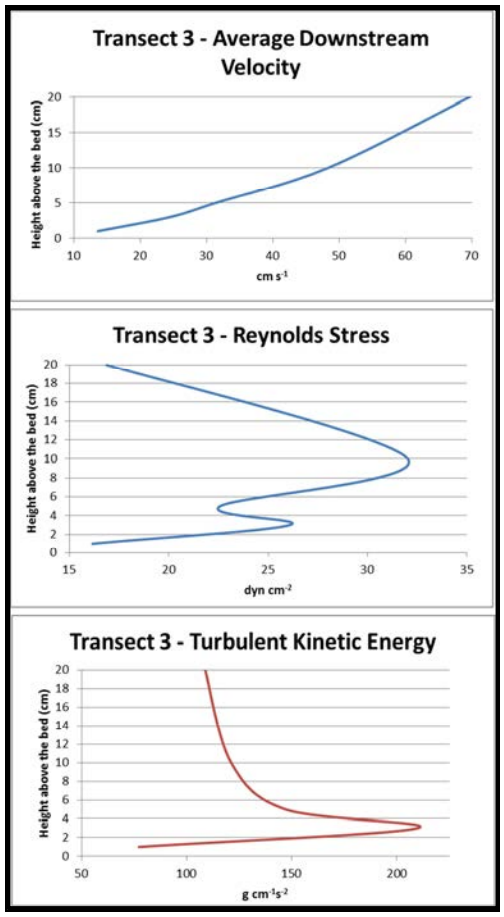

Figure 4.55: Cross channel averages of downstream velocity, Reynolds stresses and turbulent kinetic energy for zone 2, transect 3 – April, 2010.

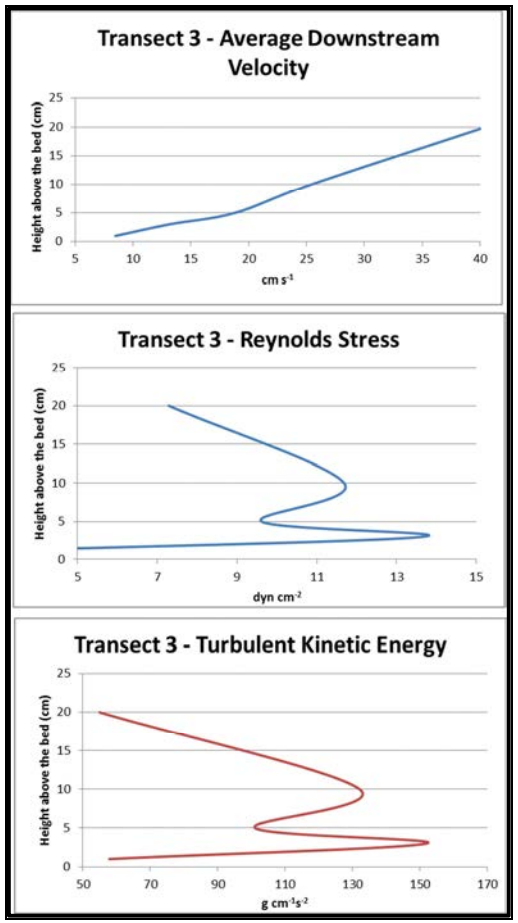

Figure 4.56: Cross channel averages of downstream velocity, Reynolds stresses and turbulent kinetic energy for zone 2, transect 3 – May, 2010.

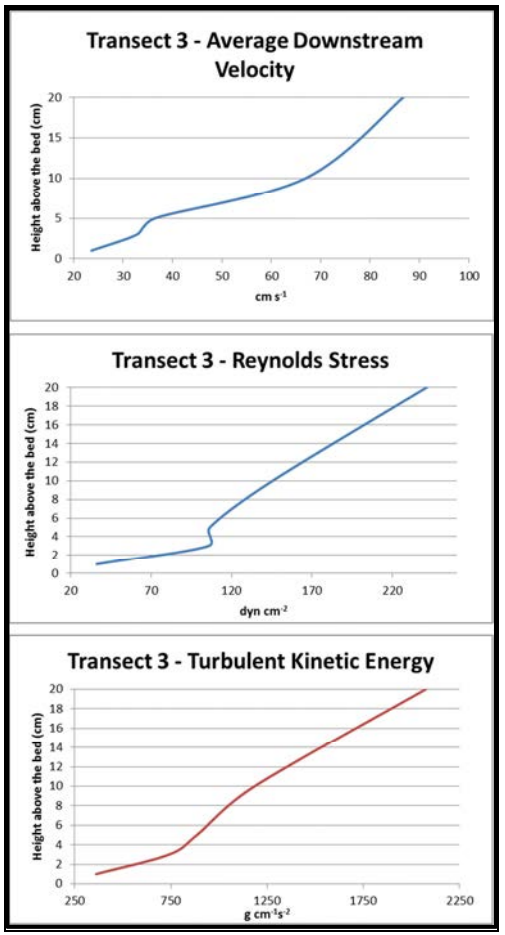

Figure 4.57: Cross channel averages of downstream velocity, Reynolds stresses and turbulent kinetic energy for zone 2, transect 3 – June, 2010.

Zone 2, Transect 4, is a riffle crest region within Site 1 of the Rouge River. The maximum average downstream velocity values under low flow conditions (April 2010) were observed to be approximately 42 cm s^{-1} (Figures 4.58 – 4.60). In May 2010 and June 2010, the maximum observed downstream velocity values were approximately 90 cm s^{-1} and 100 cm s^{-1} respectively.

The Reynolds stresses observed in April 2010 were approximately 30 dyn cm^{-2}; however these were observed over a zone from 3 – 10 cm above the bed. Interestingly, the zone of maximum momentum exchange in May 2010 shifted to 20 cm above the bed and maximum observed values were approximately 190 dyn cm^{-2}. In June 2010, the maximum observed values were concentrated at 5 cm above the bed with values of approximately 80 dyn cm^{-2}.

The maximum observed TKE values observed in April 2010 and June 2010 were very similar with values of approximately 550 g $cm^{-1}s^{-2}$ at 5 cm above the bed. In May 2010, the average maximum values observed occurred in two zones with values of approximately 700 g $cm^{-1}s^{-2}$ at 5 cm above the bed and values of approximately 1000 g $cm^{-1}s^{-2}$ at 20 cm above the bed.

Based on the distribution of the observed values of Reynolds stresses and TKE, there appears to be no relation between these values and increasing average velocity or discharge. The observed values, in terms of magnitude and relation to height above the bed, appear to be influenced by other controlling factors other than increasing average velocity and increasing discharge. The data under both low flow and high flow conditions

suggest that riffle sections are both highly turbulent no matter the stage of flow (low flow versus high flow).

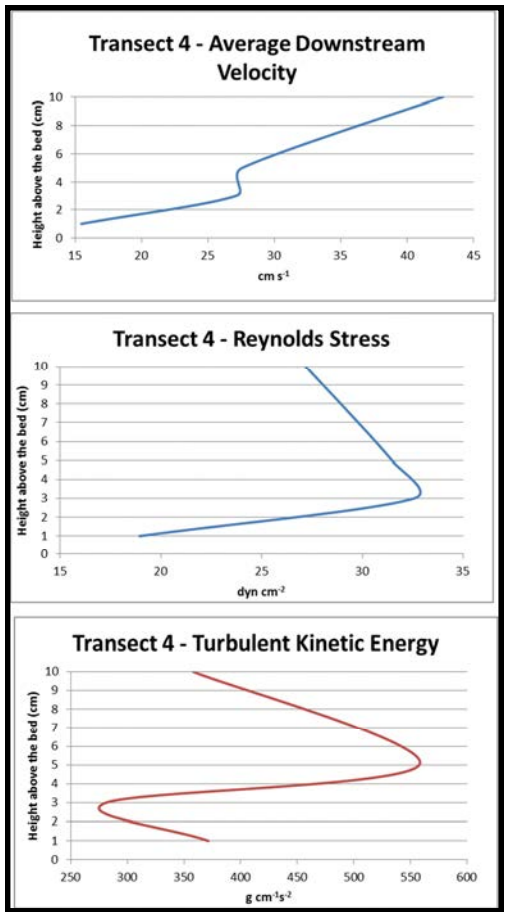

Figure 4.58: Cross channel averages of downstream velocity, Reynolds stresses and turbulent kinetic energy for zone 2, transect 4 – April, 2010.

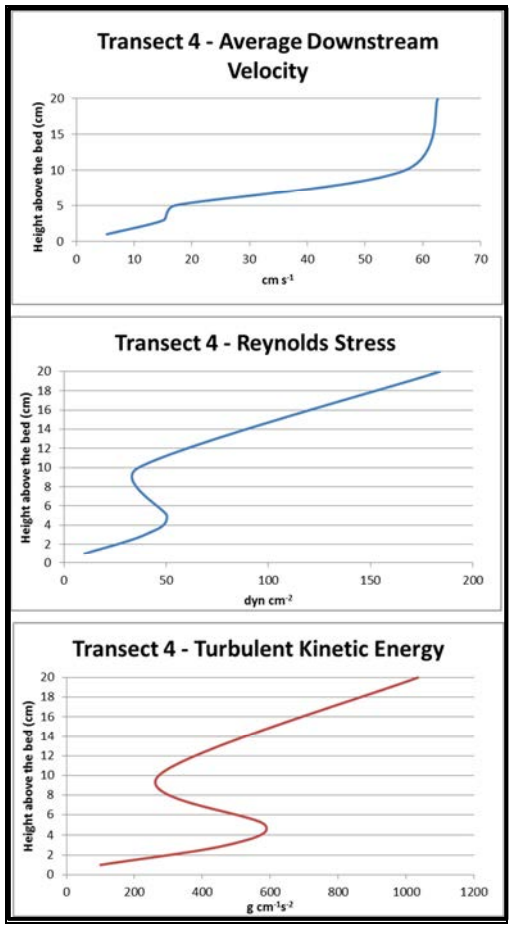

Figure 4.59: Cross channel averages of downstream velocity, Reynolds stresses and turbulent kinetic energy for zone 2, transect 4 – May, 2010.

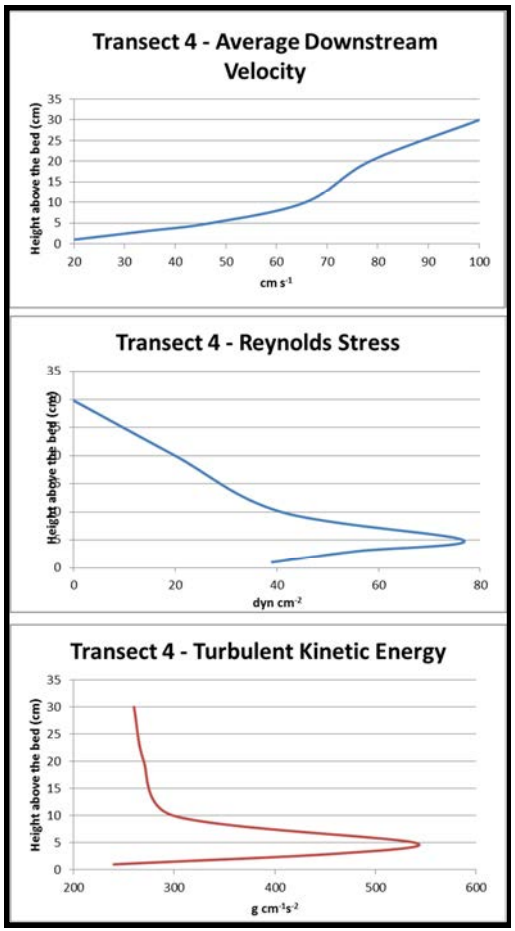

Figure 4.60: Cross channel averages of downstream velocity, Reynolds stresses and turbulent kinetic energy for zone 2, transect 4 – June, 2010.

Zone 2, Transect 5 is represented by the riffle exit slope of Site 1. The maximum average downstream velocity under low flow conditions (April 2010) was observed to be approximately 55 cm s^{-1}. The shape of the profile is not what is typically observed or expected for a velocity profile above the bed toward the water surface. Under slightly higher flow conditions (May 2010 and June 2010), it is interesting to observe that the maximum average downstream velocity was approximately 52 cm s^{-1} and 55 cm s^{-1}, respectively. The observed profiles show an interesting pattern in that the maximum average downstream velocity over the riffle exit slope did not change significantly even though the discharge increased throughout the study period.

In April 2010, the Reynolds Stresses increased linearly away from the bed until approximately 10 cm above the bed, where they drastically decreased toward zero at approximately 20 cm above the bed. Values ranged from approximately 15 dyn cm^{-2} immediately near the bed and 30 dyn cm^{-2} at 10 cm above the bed. In May 2010 and June 2010, the Reynolds stresses increased linearly from the near bed until they reached their maximum values of 30 dyn cm^{-2} and 20 dyn cm^{-2} respectively at 5 cm above the bed. Interestingly, after approximately 5 cm above the bed, the Reynolds stresses slowly decreased with height above the bed.

The TKE profiles for the riffle exit slope appear very erratic and are not consistent with the typically observed profiles observed over riffle regions. In April 2010, the maximum observed TKE values occurred at 5 cm above the bed with a value of approximately

375 g $cm^{-1}s^{-2}$. After 5 cm above the bed, values decreased slightly and then began to increase with height above the bed again at 20 cm above the bed. This sudden increase in values could be a result of air bubbles occurring around the ADV probe head due to down welling near the surface. In May 2010, the maximum TKE values showed spikes of approximately 170 g $cm^{-1}s^{-2}$ at 5 cm above the bed and 210 g $cm^{-1}s^{-2}$ at 20 cm above the bed. The occurrence of two spikes in TKE within 20 cm of the bed could play a crucial role in bed sediment transport characteristics in the riffle region of Site 1. In June 2010, the maximum average TKE values increased dramatically to approximately 1100 g $cm^{-1}s^{-2}$ at 20 cm above the bed. The observed increase in TKE with discharge in June 2010 indicates the important role that TKE plays in the near bed characteristics of the riffle region. Although an increase in average downstream velocity was not observed with increasing discharge, it is clear that the turbulent statistics in the near bed region where highly influenced by the increase in discharge.

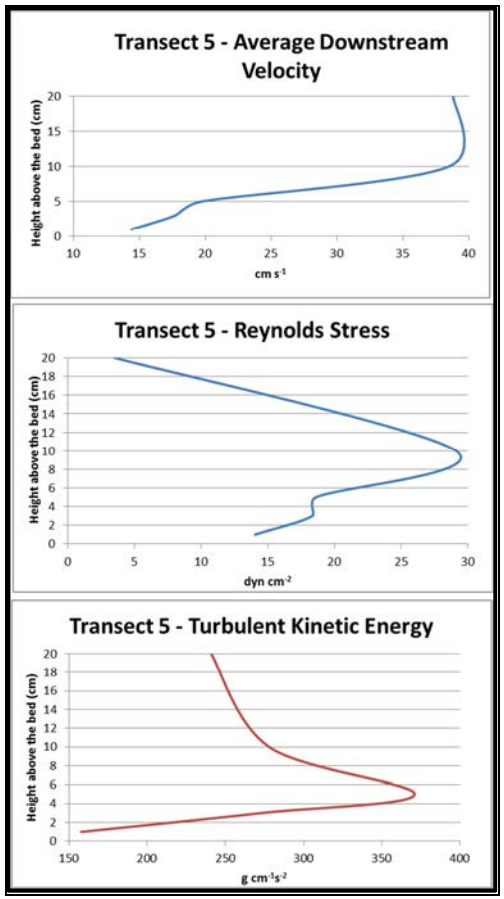

Figure 4.61: Cross channel averages of downstream velocity, Reynolds stresses and turbulent kinetic energy for zone 2, transect 5 – April, 2010.

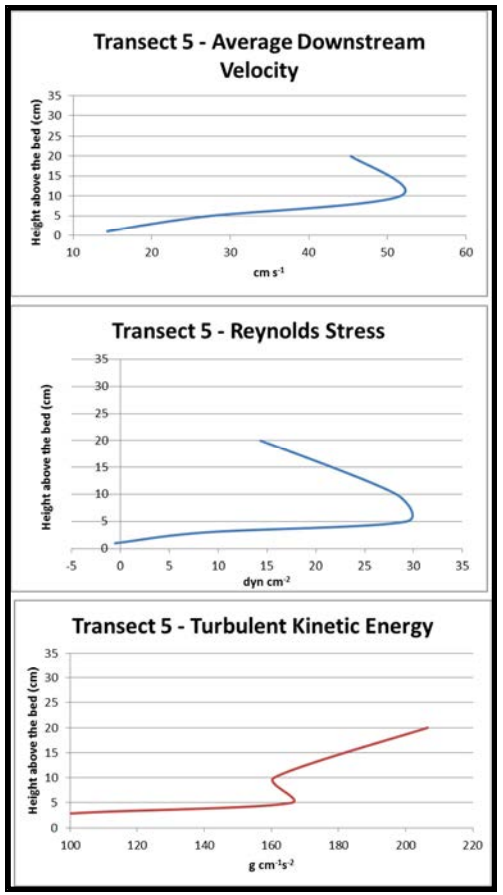

Figure 4.62: Cross channel averages of downstream velocity, Reynolds stresses and turbulent kinetic energy for zone 2, transect 5 – May, 2010.

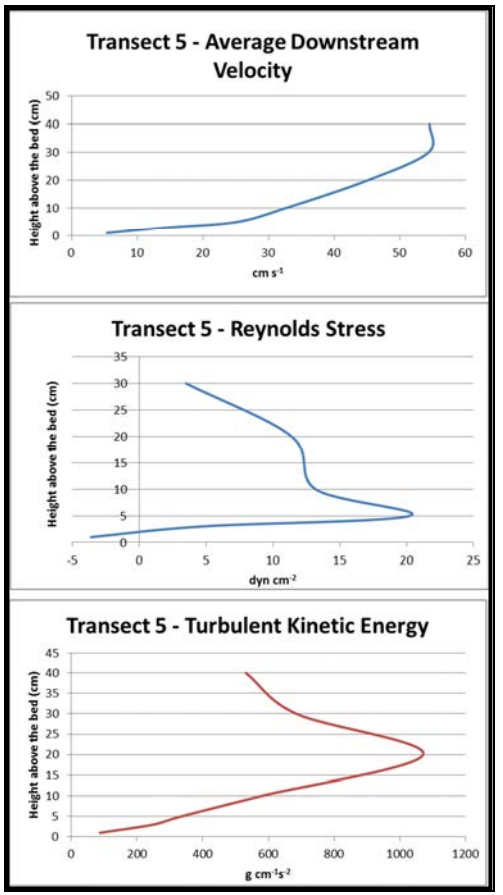

Figure 4.63: Cross channel averages of downstream velocity, Reynolds stresses and turbulent kinetic energy for zone 2, transect 5 – June, 2010.

Zone 3, Transect 6 is represented by the pool centre regions of Site 1 of the Rouge River. The average downstream velocity profiles are represented by profiles with increasing velocities with height above the bed toward the water surface. In April 2010, the maximum average downstream velocities observed were approximately 40 cm s^{-1}. Under slightly higher flow conditions (May 2010), the maximum average downstream velocities increased slightly to 42 cm s^{-1}. In June 2010, the maximum average downstream velocities increased to 50 cm s^{-1}.

The Reynolds stresses observed in April 2010, were represented by a spike of approximately 15 dyn cm^{-2} at approximately 3 cm above the bed. In May 2010, the average maximum Reynolds stress profiles was represented by two spikes in the profile with a spike of approximately 7 dyn cm^{-2} at 3 cm above the bed and approximately 17 dyn cm^{-2} at 10 cm above the bed. Similarly, in June 2010 the Reynolds stress profile exhibited two spikes that were slightly shifted up in the profile (height above the bed). At approximately 5 cm above the bed the average Reynolds stresses were approximately 20 dyn cm^{-2} and 32 dyn cm^{-2} at 20 cm above the bed. Based on the profiles observed from zone 3 (Transect 6 – pool region), it appears that the magnitude, number of Reynolds stress pikes and the shift of the spikes away from the bed are related to the increase in discharge.

Similar to the Reynolds stresses, the turbulent statistics also displayed similar profiles where an approximate value of 140 g $cm^{-1}s^{-2}$ at 3 cm above the bed in April 2010. In May 2010, a spike of TKE of 90 g $cm^{-1}s^{-2}$ was observed at 3 cm above the bed and a maximum of

225 g $cm^{-1}s^{-2}$ was observed at 10 cm above the bed. Finally, in June 2010 a maximum TKE of 200 g $cm^{-1}s^{-2}$ was observed from 10 – 20 cm above the bed.

Overall and similar to Site 2, the flow characteristics and patterns of Site 1 are highly influenced by the localized events occurring on a micro scale for riffle and pools sections. Similar to Site 2, as the discharge increased throughout the study period an increase in the magnitude of downstream velocity, momentum exchange and turbulent statistics was observed along the transects of Site 1. Also, the magnitude of turbulent kinetic energy and momentum exchange was greater for riffle sections than that of pool sections. Unlike Site 2, the pool sections of Site 1 (Transect 1 and Transect 6) did not have a similar pattern, whereby as the discharged increased the degree of momentum and turbulent kinetic energy shifted towards the bed. Rather, the pool sections of Site 1 generally had spikes of these statistics near the bed which were independent of the degree of discharge. The observations seen in the pool sections of Site 1 may prove that the shifts observed in Transect 12 of Site 2 may have been caused and influenced by the change in channel pattern (meandering to straight) rather than a change from low to high discharge.

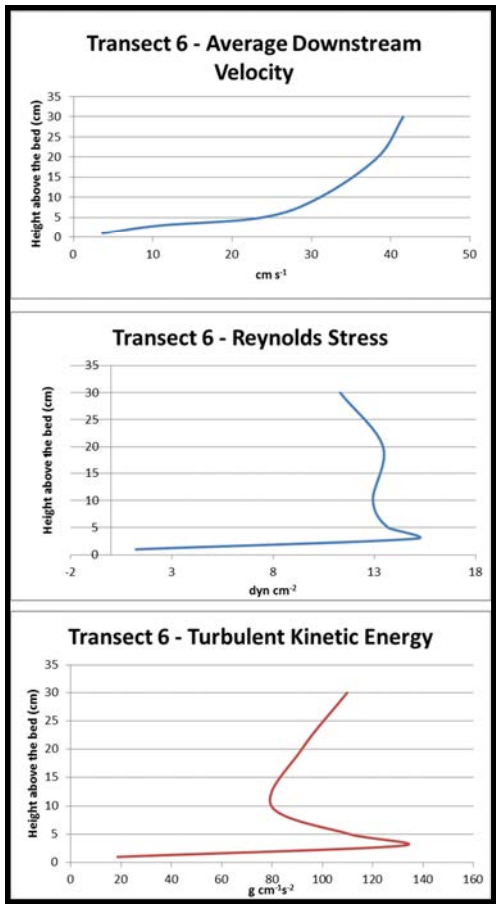

Figure 4.64: Cross channel averages of downstream velocity, Reynolds stresses and turbulent kinetic energy for zone 3, transect 6 – April, 2010.

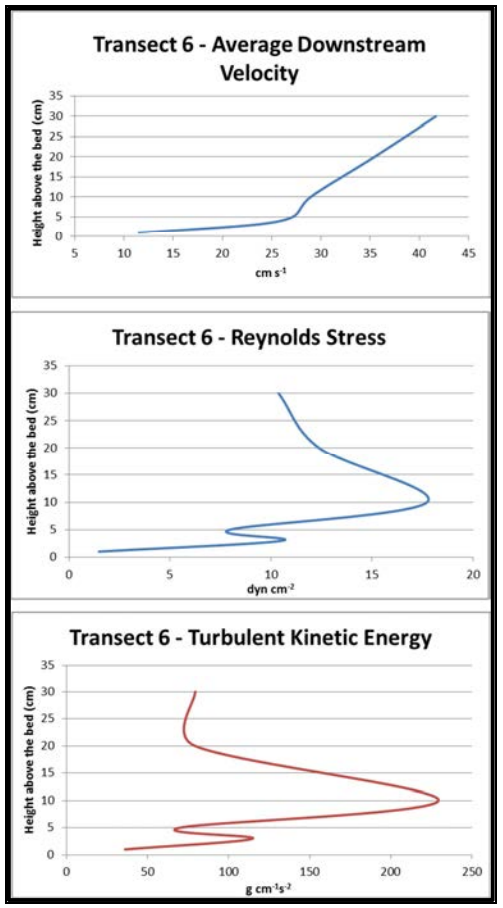

Figure 4.65: Cross channel averages of downstream velocity, Reynolds stresses and turbulent kinetic energy for zone 3, transect 6 – May, 2010.

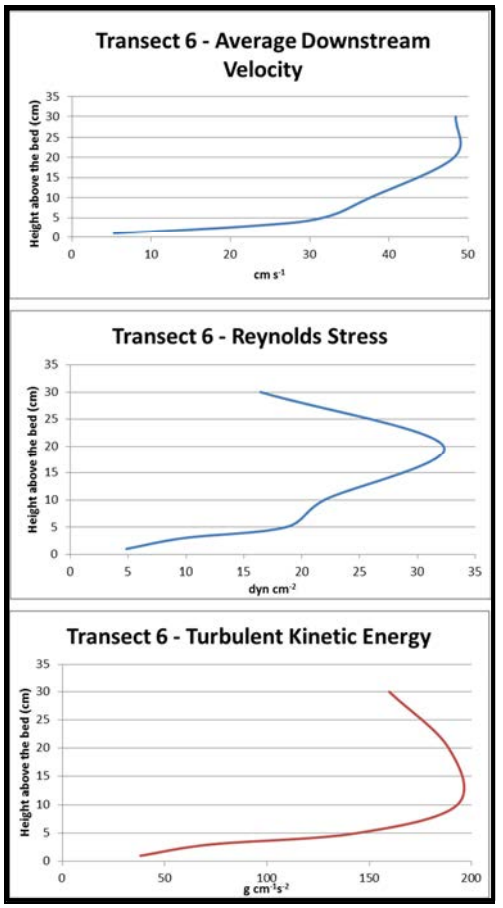

Figure 4.66: Cross channel averages of downstream velocity, Reynolds stresses and turbulent kinetic energy for zone 3, transect 6 – June, 2010.

4.4. Time Series – Velocity Fluctuations

In order to fully understand the patterns occurring in and around riffle and pool sections, we must look at the micro scale or local events that are occurring in these sections. Figures 4.67 to 4.81 are examples of time series readings that were taken at specific verticals and heights along transects of Site 1 and Site 2 during the study period. Figures 4.67 to 4.81 were obtained from a Sontek post processing program called WinADV. In order to visually access the data, a low pass filter to remove erroneous data was performed as well as the averaging out the data to 10 Hz from 20 Hz.

Transect 8 is represented by a pool exit slope of Site 2. In Figures 4.67 and 4.70, it is observed from lower flow events such as April that the flow measurements 'Y' (cross stream) and 'Z' (vertical), were fairly minimal and did not stray far from 5 cm s^{-1}. The 'Z' component is particularly important to use for comparison purposes. Strong 'Z' measurements toward the bed are likely to be representative of a transfer of momentum and turbulence characteristics in the form of a sweep. Contrasting, a spike in the 'Z' measurement toward the surface is likely representative of a transfer of momentum and turbulence characteristics in the form of an ejection.

June 2010 was a period of high flow events and it is evident from Figures 4.69 and 4.70 that the flow measurements along Transect 8 are very erratic with the cross stream and vertical measurements playing an important role in the transfer of momentum and turbulence characteristics. Interestingly, a spike in the cross stream measurement or vertical measurement is followed by a trough or decrease in the downstream velocity

component (‘X’). And a trough in cross stream and vertical measurement is followed by a spike in the downstream velocity. This is potentially important as one can visually see how the components of cross stream velocity and vertical velocity play a crucial role in the transfer of momentum and turbulence characteristics under high flow stage events. These flow events are likely important to characterize when looking at sediment transport events in riffle and pool sections.

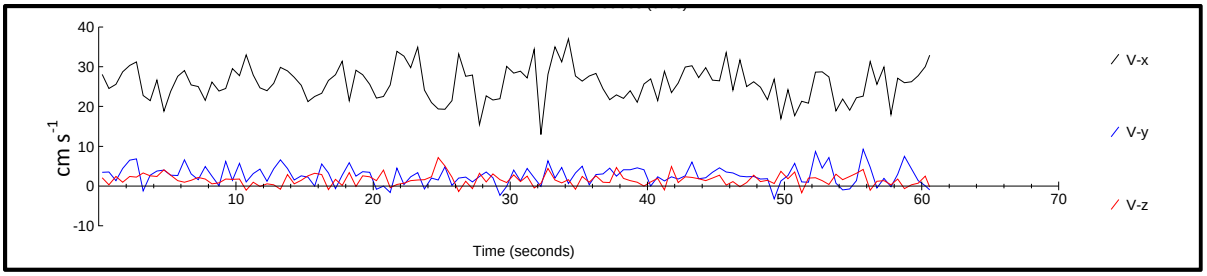

Figure 4.67: April 2010 Site 2 Transect 8, Vertical 9 – 3 cm above the bed; Time Series Data 10 Hz (Average).

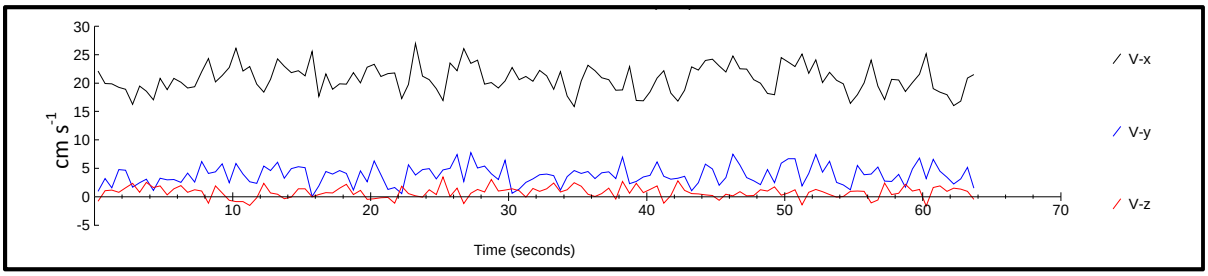

Figure 4.68: April 2010 Site 2 Transect 8, Vertical 13 – 3 cm above the bed; Time Series Data 10 Hz (Average).

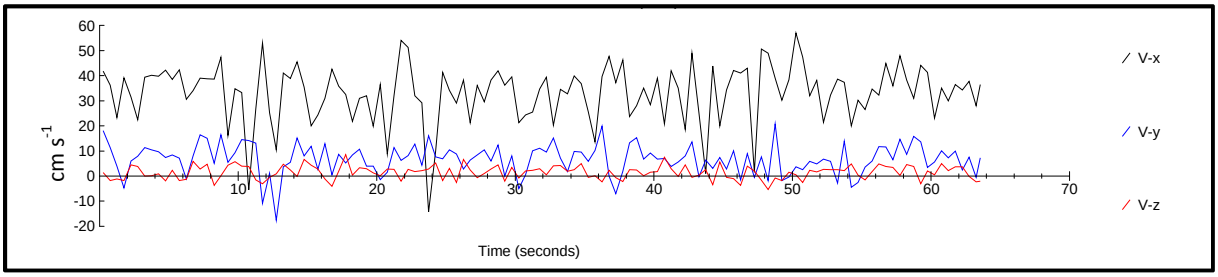

Figure 4.69: June 2010 Site 2 Transect 8, Vertical 10 – 5 cm above the bed; Time Series Data 10 Hz (Average).

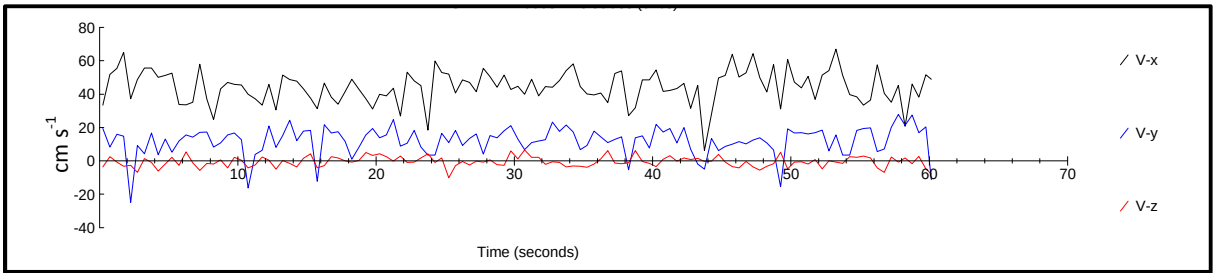

Figure 4.70: June 2010 Site 2 Transect 8, Vertical 11 – 5 cm above the bed; Time Series Data 10 Hz (Average).

Similarly, Figures 4.71 through 4.74 represent zone 2 of Site 2. More specifically, this is the pool centre of Site 2. It is apparent from Figure 4.71 and 4.72 that the cross stream component 'Y' plays a more critical role as you near the meander bend. Additionally, it is interesting to see that the vertical 'Z' component remains fairly minimal from 3 cm above the bed until 10 cm above the bed at Transect 12. However, as shown in Figure 4.72, the vertical component becomes more critical and more erratic as you move out of the pool centre and away from the meander bend. This is very important as it appears that the pool centre may act as a zone of deposition during lower flow events.

Additionally, Figures 4.71 and 4.73 display secondary circulation via the cross stream component 'Y'. In Figure 4.71 all of the 'Y' components are strongly negative, with a peak value of approximately -25 cm/s. The negative values show that secondary circulation is occurring, whereby water is downwelling at the outer meandering bend and travelling across the pool toward the point bar [as shown by the (-) values]. Similarly, Figure 4.73 is the same vertical as Figure 4.71 however 10 cm above the bed. At this position in the water column it is observed that secondary circulation still exists however the magnitude is less with values typically < -20 cm/s. Figure 4.74 displays the decreasing effect of secondary circulation as the inner bank is approached. The data for Figure 4.74 was taken from vertical 4 and it is clear that 'Y' component was fairly minimal with values typically < -10 cm/s. These time series graphs displaying secondary circulation play a very critical role in sediment transport, whereby sand and silts are

evacuated out of the pool centre and transported toward the inner bank of the meander bend. This occurrence was very evident at Site 2 by the formation of a point bar.

Under higher flow events (Figure 4.74) the downstream velocity component in the flow 'X' is increased in magnitude, while the cross stream component and vertical component remain rather negligible. This time series in the data set is very consistent with what was visually observed during the field study. During the month of June, flows were extremely high and the flow pattern within the Rouge River, specifically Site 2, changed from a meandering pattern to a straight reach (evident by the reduced role that the cross stream component played). The reduction in the magnitude of the vertical component observed during higher flows may have an influence on the number of sweep and ejection events that occur along the transect and hence a reach or a pool centre that is acting as a zone of sediment evacuation rather than deposition.

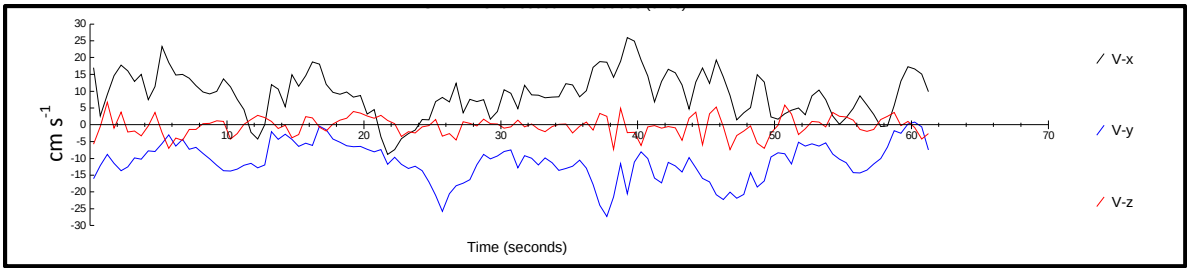

Figure 4.71: April 2010 Site 2 Transect 12, Vertical 18 – 3 cm above the bed; Time Series Data 10 Hz (Average).

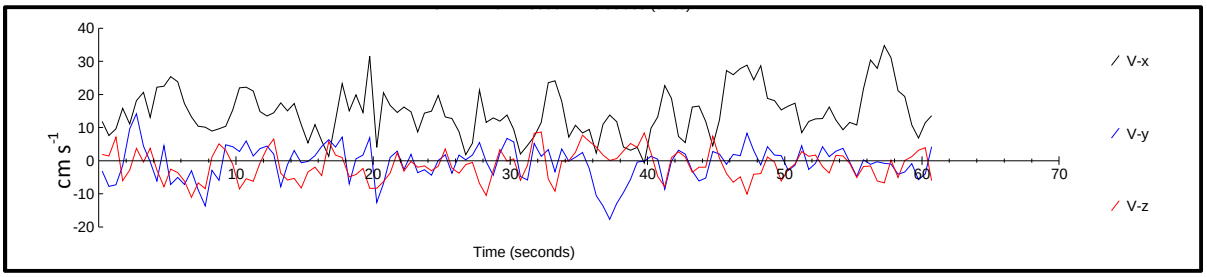

Figure 4.72: April 2010 Site 2 Transect 12, Vertical 13 – 5 cm above the bed; Time Series Data 10 Hz (Average).

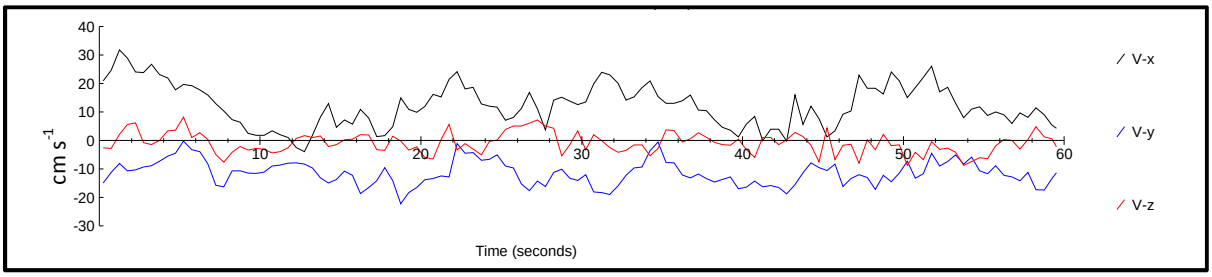

Figure 4.73: April 2010 Site 2 Transect 12, Vertical 18 – 10 cm above the bed; Time Series Data 10 Hz (Average).

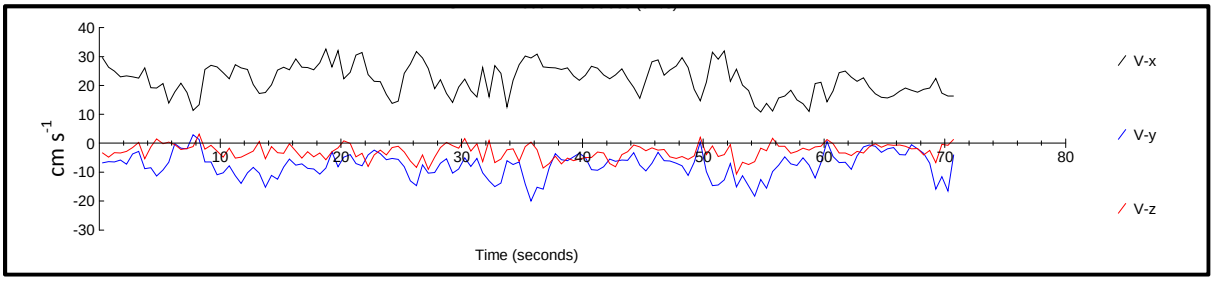

Figure 4.74: June 2010 Site 2 Transect 12, Vertical 4 – 10 cm above the bed; Time Series Data 10 Hz (Average).

Zone 2, Transect 4 is represented by the riffle crest section of Site 1. It is apparent from Figure 4.75 and 4.76 that the flow components during lower flow events (April 2010) are highly dominated by the downstream velocity component. It is also clear from Figure 4.75, which represents data taken from 5 cm above the bed, that more fluctuations and variability exist in the cross stream and vertical components than measurements taken at 3 cm above the bed in Figure 4.76.

Figures 4.77 and 4.78 represent time series data that was taken during higher flow events in June 2010. From Figure 4.77, one might conclude that the cross stream and vertical components play a more crucial role during high flow events. However, in comparison to Figure 4.77, Figure 4.78 is quite the opposite with the vertical and cross stream components being very minimal with not much variation. Even though both Figure 4.77 and 4.78 represent data taken from 5 cm above the bed but only two meters away from each other on the transect, the variation in the flow components with respect to scale is highly location specific on a micro scale. It is clear that the bed formations and bed arrangement is highly location specific, thus certain areas along a transect have varying flow dynamics and variability when observed on a micro scale. This data may be important to refute the notion that certain zones within the riffle-pool sequence act as zones of deposition or evacuation at varying flow stages. This data may suggest that areas of deposition versus entrainment are highly location specific on a micro scale within the river bed.

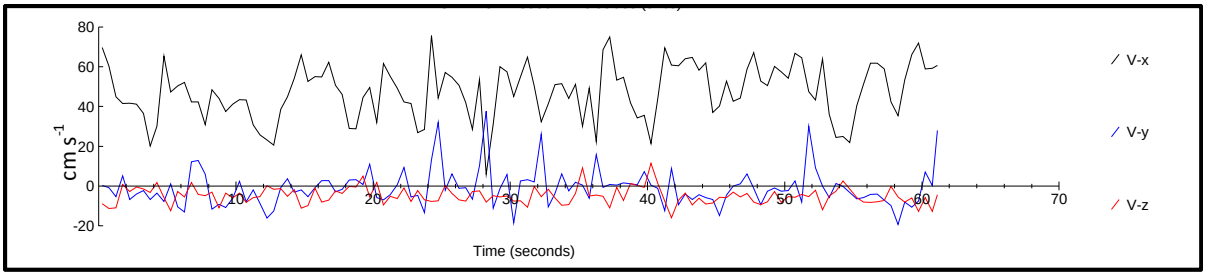

Figure 4.75: April 2010 Site 1 Transect 4, Vertical 3 – 5 cm above the bed; Time Series Data 10 Hz (Average).

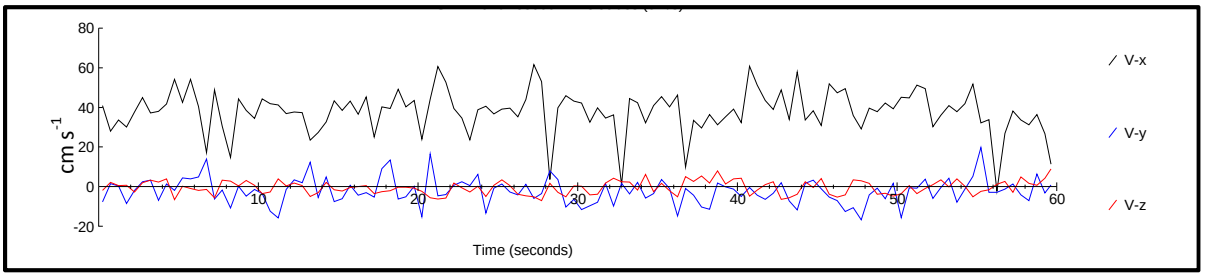

Figure 4.76: April 2010 Site 1 Transect 4, Vertical 6 – 3 cm above the bed; Time Series Data 10 Hz (Average).

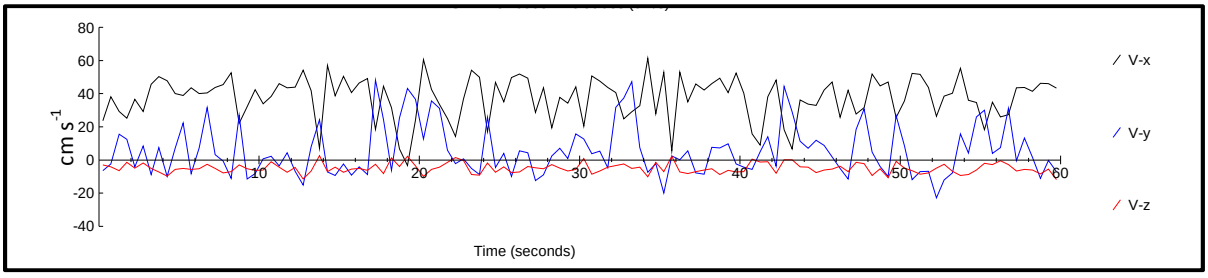

Figure 4.77: June 2010 Site 1 Transect 4, Vertical 5 – 5 cm above the bed; Time Series Data 10 Hz (Average).

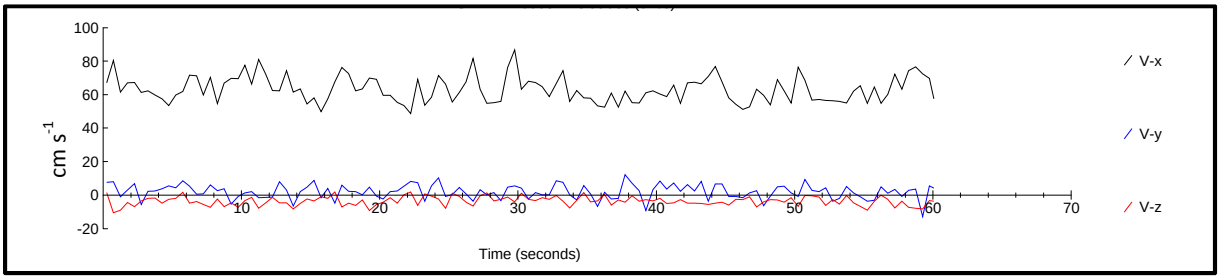

Figure 4.78: June 2010 Site 1 Transect 4, Vertical 7 – 5 cm above the bed; Time Series Data 10 Hz (Average).

Zone 3, Transect 6 is represented by the pool centre region of Site 1. Interestingly, during low flow events in April 2010 (Figure 4.79), Transect 6 in the near bed region (3 cm above the bed) had highly erratic flow components with cross stream and downstream flow components being equally dominant. Additionally, fluid movements away from the bed and toward the bed were observed. In contrast, during higher flow events (June 2010), the vertical and cross stream components were not as variable and dominant as the downstream component. However, for the same transect but 10 cm above the bed, an increase cross stream component was observed. Figure 4.79 through 4.81 further support the notion that variability along the bed is high, not only specific to location at the micro-scale but also specific for the position with respect to distance away from the bed in the water column. It must also be kept in mind that changes in the bed arrangement due to sediment transport likely occurred from April through to June (study period), thus the observed changes could be due to changes in the bed arrangement itself. Figure 4.34 and 4.35 support this idea as bed height changed from April to June 2010.

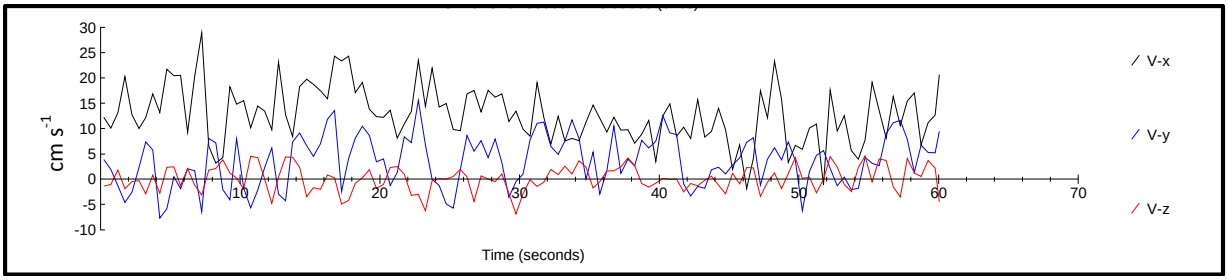

Figure 4.79: April 2010 Site 1 Transect 6, Vertical 8 – 3 cm above the bed; Time Series Data 10 Hz (Average).

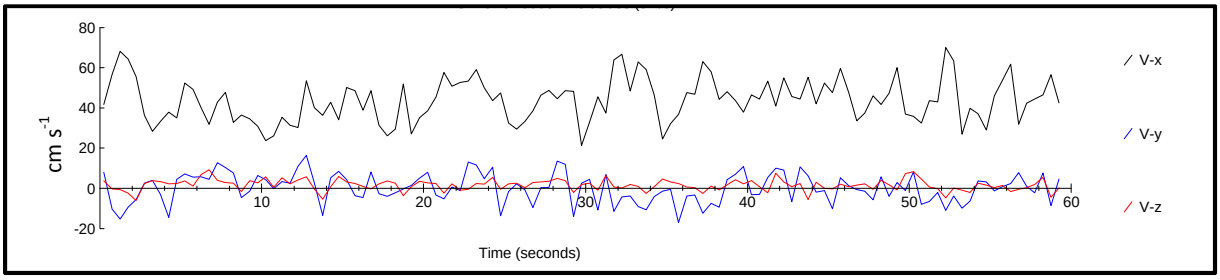

Figure 4.80: June 2010 Site 1 Transect 6, Vertical 8 – 5 cm above the bed; Time Series Data 10 Hz (Average).

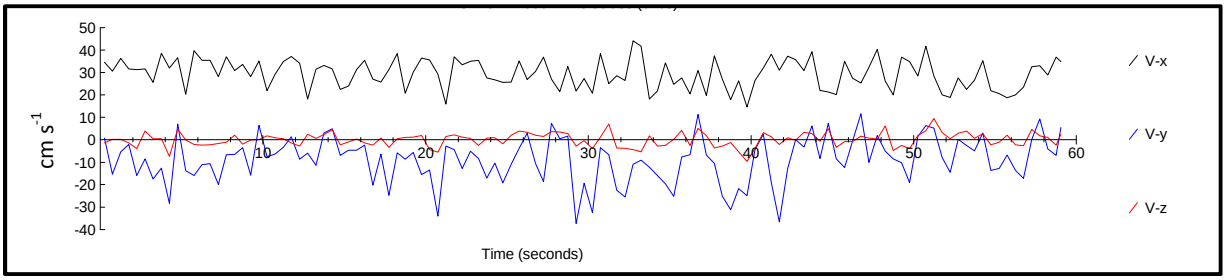

Figure 4.81: June 2010 Site 1 Transect 6, Vertical 10 – 10 cm above the bed; Time Series Data 10 Hz (Average).

Figures 4.82 through 4.86 display the variation in the flow parameters with respect to height above the bed, both during a low flow event and a high flow event. From Figure 4.82 it is observed that the downstream component ‘X’ and the cross stream component ‘Y” dominate the flow regime. The vertical component ‘Z’ does not play much of a crucial role in the near bed region. From Figure 4.82 which is 1 cm above the bed toward Figure 4.86 which is 20 cm above the bed, it is apparent that the velocity

increases as expected toward the water surface. Additionally, it appears as if the 'X' and 'Y" components become less erratic as the water surface is approached and that the 'Z' vertical component increases in magnitude (vales nearing 10 cm s^{-1}).

An interesting observation from Figures 4.82 – 4.86 is the strongly positive 'Y' component toward the inner bank (Figure 4.34 – inner bank defined on right side of diagram). With the exception of Figure 4.83 the 'Y' component is strongly positive toward the inner bank with values increasing with height above the bed (peak values range from 4 – 40 cm s^{-1}). The strongly positive 'Y' component is caused by a slight meander bend near Transect 3 forcing water toward the inner bank and causing secondary circulation. These observations refer to Site 1 with a gravel and sand point bar running along the east side of the river reach. Under sediment transport events water downwells at the outter bank and travels toward the inner bank via secondary circulation toward the inner bank.

It is interesting to note that the vertical 'Z' component under low flow conditions remains relatively insignificant with the majority of the values <10 cm s^{-1}. This may support the notion that minimal sediment transport occurs under low flow conditions and that riffle zones act as a zone of deposition rather than evacuation.

In contrast to April 2010 (Figures 4.82 – 4.86) which was a low flow event, Figures 4.87 – 4.91 display the variation in the flow components under a high flow event.

Similar to April 2010 (low flow event) the 'X' and 'Y" components are very erratic and dominate the flow near the boundary. However, it is interesting to observe that the downstream 'X' component tends to dominate the flow >10cm away from the bend.

Additionally, unlike the low flow events in April 2010 the 'Z' vertical component is a lot stronger in magnitude near the boundary till approximately 5 cm away from the bed. This data likely supports the belief that sediment transport is related to the sweep and ejections events that dominate the flow under higher flow conditions. From this data it is likely that sediment transport was occurring during this data accumulation. To further support this point, at 20 cm above the bed the 'Z' component is minimal in magnitude as the 'X' downstream component dominates the flow.

When comparing high versus low flow events in relation to sediment transport it seems clear that site specific micro scale events play a large role, however the dominating contributing factor seems to be linked to the magnitude of the "Z' (vertical) component.

4.4.1 April Events:

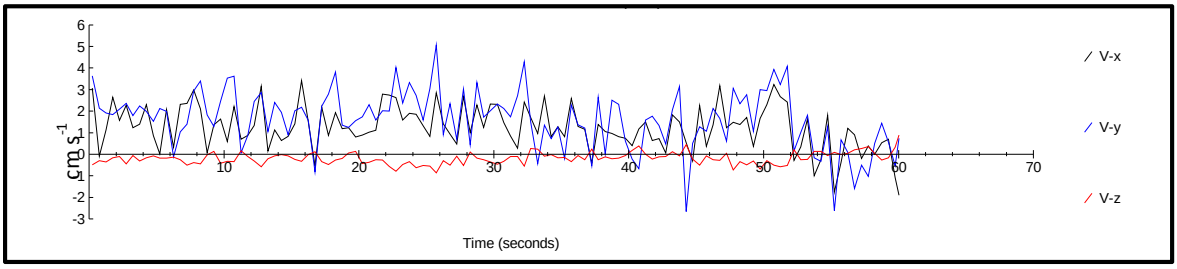

Figure 4.82: April 2010 Site 1 Transect 3, Vertical 4 – 1 cm above the bed; Time Series Data 10 Hz (Average).

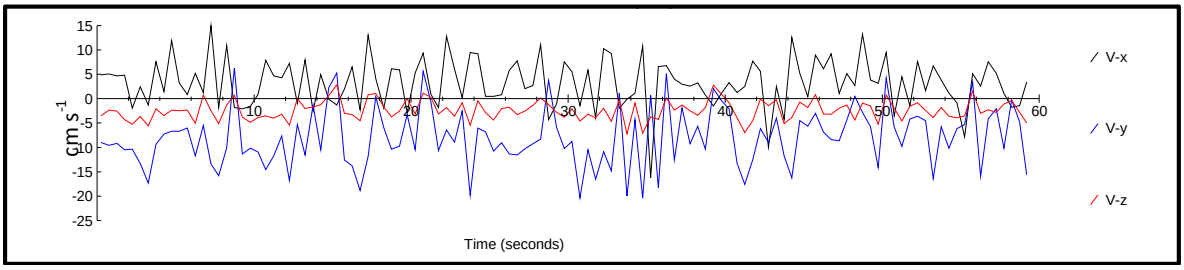

Figure 4.83: April 2010 Site 1 Transect 3, Vertical 4 – 3 cm above the bed; Time Series Data 10 Hz (Average).

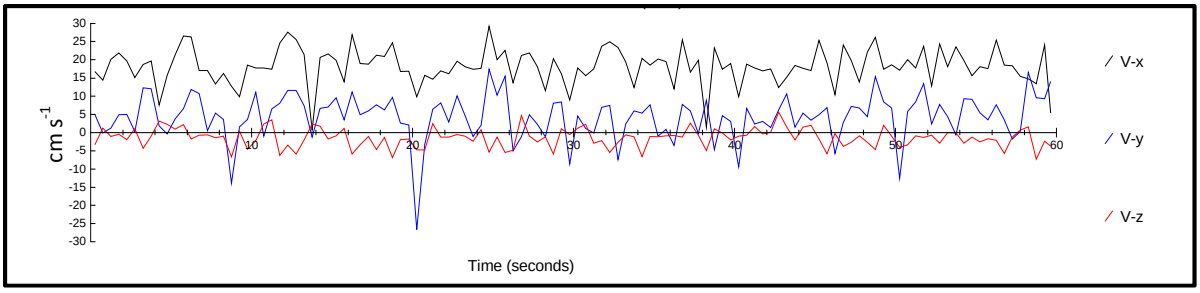

Figure 4.84: April 2010 Site 1 Transect 3, Vertical 4 – 5 cm above the bed; Time Series Data 10 Hz (Average).

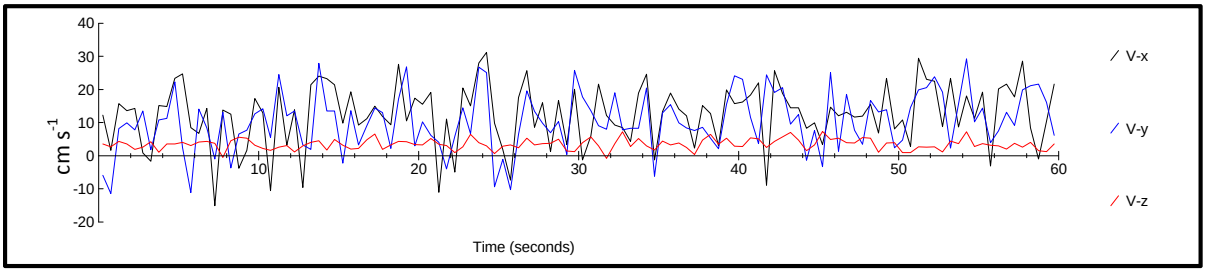

Figure 4.85: April 2010 Site 1 Transect 3, Vertical 4 – 10 cm above the bed; Time Series Data 10 Hz (Average).

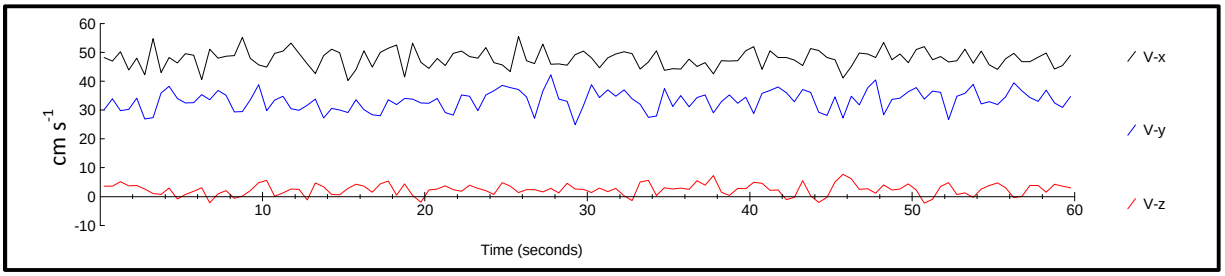

Figure 4.86: April 2010 Site 1 Transect 3, Vertical 4 – 20 cm above the bed; Time Series Data 10 Hz (Average).

4.4.2 June Events:

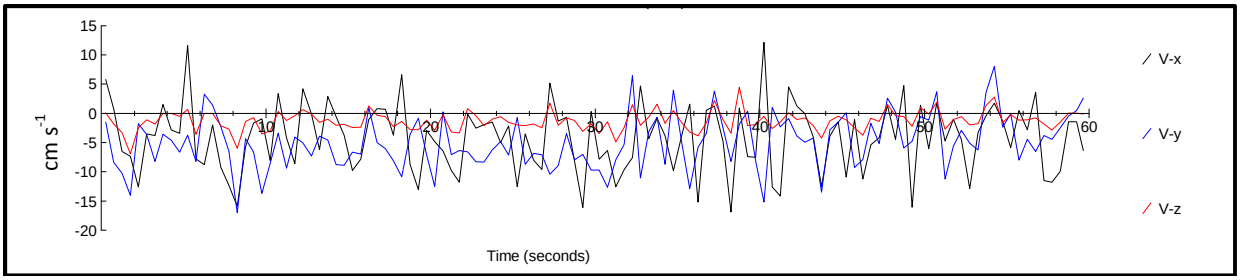

Figure 4.87: June 2010 Site 1 Transect 3, Vertical 4 – 1 cm above the bed; Time Series Data 10 Hz (Average).

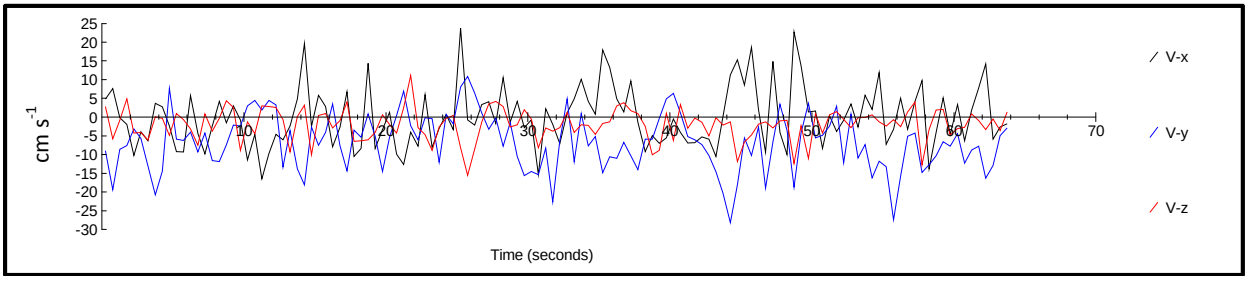

Figure 4.88: June 2010 Site 1 Transect 3, Vertical 4 – 3 cm above the bed; Time Series Data 10 Hz (Average).

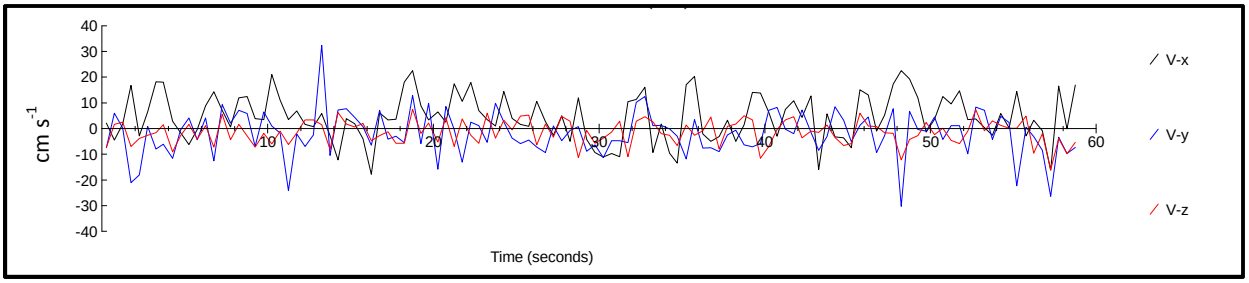

Figure 4.89: June 2010 Site 1 Transect 3, Vertical 4 – 5 cm above the bed; Time Series Data 10 Hz (Average).

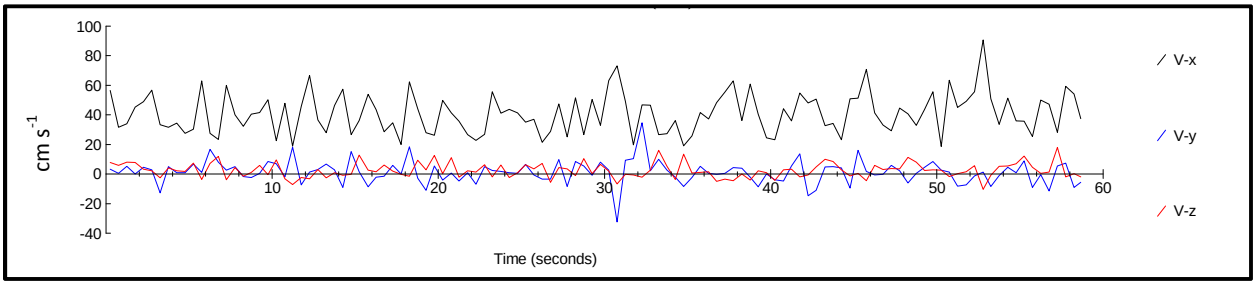

Figure 4.90: June 2010 Site 1 Transect 3, Vertical 4 – 10 cm above the bed; Time Series Data 10 Hz (Average).

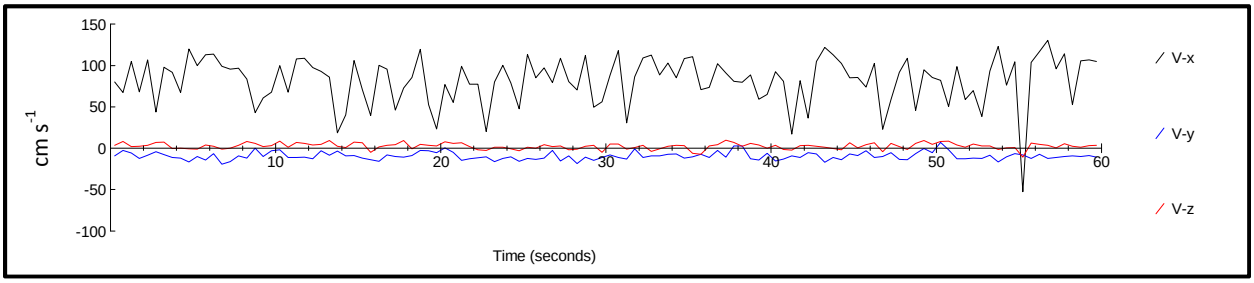

Figure 4.91: June 2010 Site 1 Transect 3, Vertical 4 – 20 cm above the bed; Time Series Data 10 Hz (Average).

SECTION FIVE: DISCUSSION

The primary objective of this study was to assess the turbulence structure and potential scour in riffle-pool sequences in both straight and meandering channel sections of the Rouge River. This study attempted to assess the complex turbulent flow structure in riffle-pool sequences at study sites 1 and 2. Additionally, the project considered the role of turbulence structure above riffles and pools in relation to the depth of scour in pools and deposition height on riffles (at varying flow stages). Finally, the study assessed how the controlling factors influencing riffle height and scour depth differ in straight versus meandering reaches by characterizing bed and sediment transport (at each site).

As previously discussed, a lot of past research suggested that downstream velocities, Reynolds stresses and TKE are higher in pools under high flow events, which leads to scour and deposition on riffles (e.g., Keller, 1971; Milan et al. 2001). Additionally, research suggested that the turbulent structure is responsible for scour in pools and therefore pool maintenance and formation (Clifford, 1993). This study looked at patterns of downstream velocity, Reynolds stresses and TKE along various transects of Site 1 and 2 during the study period. By using an ADV, this study allowed for a better understanding and comparison of the forces responsible for riffle-pool formation, maintenance and sediment transport regimes. The study enabled the comparison of visual observations of the turbulent structure and allowed the mapping of the locations of sediment deposition and evacuation.

Figures 4.40 - 4.66 show interesting observations whereby transfer of momentum exchange (Reynolds Stresses) and the degree of TKE is concentrated near the boundary,

typically 5 – 10 cm above the bed. In some instances a second spike of momentum exchange or TKE was observed. These spikes were observed at both riffle and pool locations, with the degree of magnitude being greater on riffles then pools. In contrast to past research, under higher flow events, pool locations did not exhibit higher degrees of momentum exchange or TKE. This could be due to the fact that measurements were taken after the peak discharge events and on the declining side of the hydrograph. Also, Site 2 was observed to change channel pattern during the storm events in June 2010. During the noted storm events the inner bank of Site 2 was breached and the channel pattern was observed to be straight. With increasing discharge during the study period (Figure 4.33), as expected the downstream velocity increased. Similar to Reynolds Stresses and TKE, downstream velocity was observed to be higher in riffle sections under low flow and high flow events in comparison to pool sections. As previously noted measurements in the pool section could not be completed at heights greater than 40 cm due to equipment limitations. It could be very plausible that riffle sections actually experienced high downstream velocity measurements under peak flow events.

Observed Reynolds Stresses and TKE likely played an important role in depth of scour in pools and deposition height on riffles. Figures 4.36 – 4.39 indicated that both Site 1 and Site 2 displayed scour in pools and riffle height increase from April – June 2010. Additionally, as observed the pool sections appeared to elongate further downstream during the study period. Measurements of TKE and Reynolds stresses as well as map comparisons indicated that the pool-exit slope scoured during high flow events and filled during low flow events. From figures 4.40 - 4.66 it can be observed that

TKE formation and momentum exchange is highly scale dependent with individual measurements being highly affected by the individual clasts and bed formations around the measurement position. The observed change in pool depth and position could support Yang (1971 and 1987) theory that rivers generally adjust their morphology to minimize the rate of energy dissipation. These observations were enabled by collecting TKE and momentum exchange data at low, moderate and high flow events. Doing this allowed a comparison of location with the greatest sediment transport potential.

Sediment sampling techniques showed that Site 2 experienced sediment transport events during the study period. Observations from figures 4.17 – 4.30 showed that Site 2 was highly mobile during peak flow events. Under base flow conditions bedload trap data indicated that riffle sections acted as evacuation sites of gravel material while pool sections acted as a deposition site for finer materials such as sand, silt and clays. Under high flow events pool sections were observed to act as sites of evacuation. Bedload traps set up along the point bar of the meander bend in Site 2 indicated that secondary circulation was apparent by moving finer bed material towards the inner bank (establishment of a point bar). Finally, tracer pebbles of varying shape and size were observed to be immobile during lower flow events and highly mobile during peak discharge events. Continuous storm events in June 2010 revealed that all the tracer pebbles had been moved out of the study site, leading to a recovery of 0%.

As previously mentioned, it was observed that rates of momentum exchange (Reynolds Stresses) and TKE were highly micro scale specific with data suggesting that local influences were the main controlling factors affecting the magnitude and occurrence

of these events. Figures 4.67 – 4.91 display the time series data taken at Site 1 and Site 2. From these graphs it is evident that measurements are high erratic during the 60 second measurement period. Figures 4.71 – 4.74 and figures 4.82 – 4.86 to some degree illustrate the controlling factors influencing depth of scour in pools in straight versus meandering sections. The magnitude of the 'Y' component (cross-stream) indicates the importance of secondary circulation as one of the key controlling factors of the depth of scour in straight versus meandering reaches. In meandering sections, the cross stream component plays a critical role in moving the fine sediment out of the pool centre and toward the inner bank. This notion is evident by the formation of a point bar located near the inner bank and a deeper scour hole on the pool centre (Figure 4.38 - 4.39). The degree of curvature of Site 2 leads to a high magnitude in the cross stream component. Thompson et al. (1998) indicted that upwelling is a crucial component in the adjustment of the water-surface slope on the outer bank, that helps drive the recirculation of the eddy and hence downweling. In comparison to Site 2, Site 1 (Figures 4.82 – 4.86) degree of curvature is less influential. Secondary circulation is evident as indicated from the point bar located on the east side of the site (Figure 4.36 – 4.37). Although the magnitude of the cross stream component is similar to that of Site 2 (approximately 20 cm s^{-1}) the bed structure likely leads the more erratic nature of the 'Y' component signal. Site 1, Transect 3 is characterized as a pool exit/riffle entrance slope. The bed structure consisted of interlocked gravels, whereas the pool centre of Site 2 (Transect 12) was characterized by fine sands, silt and clay. However, the near-bed TKE was higher for that of Site 1 (Transect 3) than that of Site 2 (Transect 12). Typically areas of highest TKE occur in

zones where individual clasts and boulders are present in the bed structure (Thompson and Wohl, 2009). Overall, it is evident that the degree of curvature is a controlling factor for sediment transport regimes within riffle and pool sections. The cause of secondary circulation moves finer bed materials toward the inner bank where they are deposited and form point bars.

SECTION SIX: SUMMARY

Riffle-pool sequences are commonly observed in coarse grained river channels and are important for meander development and channel evolution (Gregory et al. 1994). The mechanisms by which riffles and pools are formed and maintained are fundamental aspects of channel form and process. Past research has focused largely on the maintenance of riffle-pool sequences, specifically in the context of stage dependant VRH. Numerous mechanisms have been proposed to explain riffle and pool formation and maintenance. However, little research has been completed on the three dimensional flow structures of these sequences and how this affects the depth of scour in pools and deposition height in riffles.

The primary objective of this study was to assess the turbulence structure and potential scour in riffle-pool sequences in both straight and meandering channel sections of the Rouge River, Toronto, Ontario, Canada. This study showed that TKE and Reynolds stresses were typically maximized at 5 – 10 cm above the bed. The magnitude for TKE and Reynolds stresses is highly scale dependent with local micro-scale influences in bed structure likely leading the high variability in terms of magnitude and location along riffle and pool sections.

Additionally, bathymetric maps displayed that the pool centre shifted downstream during the study period. At Site 1, the pool centre was observed to be linked wholly to an increase in discharge. The pool centre not only shifted downstream as the higher flow events were approached at the end of the study season, but it also shifted laterally across the river, suggesting that channel curvature likely plays a large role in pool position. At

both Site 1 and Site 2, the pool region was noticeably shallower at the end of the study (after high flow discharge events). Riffle regions at both sites were also observed to be higher near the end of the study. These observations are interesting as the data suggests that zones of accumulation and deposition are very dependent on the stage of discharge.

Sediment transport was observed during the study period and data suggested that Site 2 was highly mobile during peak discharge events in June 2010. Time series data indicated that the degree of curvature influences secondary circulation and hence sediment transport and channel form. It is clear then that riffle height and depth of scour in pools is strongly linked to channel morphologies as well as the aforementioned micro scale variables.

Finally, it is recommended that further research be completed on the instantaneous velocities around riffle-pool sequences to better understand the controlling factors affection pool depth and deposition height on riffles. A study with a higher measurement density is likely needed to better understand the controlling factors surrounding channel form and process for riffle-pool sequences.

LIST OF REFERENCES

Allen, J. (1994). Fundamental properties of fluids and their relation to sediment transport processes. In K. Pye, *Sediment transport and depositional processes* (pp. 51-60). Oxford: Blackwell Scientific Publications.

Ashmore, P., Conly, F., DeBoer, D., Martin, Y., Petticrew, E., & Roy, A. (2000). Recent (1995–1998) Canadian research on contemporary processes of river erosion and sedimentation, and river mechanics. *Hydrological Processes*, (14) 1687-1706.

Ashworth, P., & Ferguson, R. (1989). Size-selective entrainment of bed load in gravel bed streams. *Water Resources Research* , (25) 627-634.

Bagnold, R. (1977). Bed load transport by natural rivers. *Water Resources Research* , (13) 303-312.

Bagnold, R. (1980). An empirical correlation of bedload transport rates in flumes and natural rivers. *Proceedings of the Royal Society of London*, (372) 453-473.

Bagnold, R. (1986). Transport of solids by natural water flow: evidence for a world-wide correlation. *Proceedings of the Royal Society of London*, (405) 369-374.

Beschta, R., & Platts, W. (1986). Morphological features of small streams: significance and function. *Water Resources Bulletin*, (3) 369–379.

Biron, P., Robson, C., Lapointe, M., & Gaskin, S. (2004). Comparing different methods of bed shear stress estimates in simple and complex flow fields. *Earth Surface Processes and Landforms*, (29) 1403–1415.

Bisson, P., Bilby, R., Bryant, M., Dolloff, C., Grette, G., House, R., et al. (1987). Large woody debris in forested streams in the Pacific Northwest: past, present and future. In E. Salo, & T. Tundy, *Streamside Management; Forestry and Fishery Interactions* (pp. 143-190). Seattle, WA: University of Washington Institute of Forest Resources.

Booker, D., Sear, D., & Payne, A. (2001). Modelling three-dimensional flow structures and patterns of boundary shear stress in a natural pool-riffle sequence. *Earth Surface Processes and Landforms*, (26) 553-576.

Bradshaw, A. (1985). Bed microtopography and entrainment thresholds in gravel bed rivers. *Geological Society of America Bulletin*, (96) 218-223.

Buffin-Bélanger, T., & Roy, A. (2005). 1 min in the life of a river: selecting the optimal record length for the measurement of turbulence in fluvial boundary layers. *Geomorphology*, (68) 77-94.

Buffin-Belanger, T., Roy, A., & Kirkbride, A. (2000). On large-scale flow structures in a gravel-bed river. *Geomorphology*, (32) 417-435.

Bunte, K., Asce, S., Potyondy, J., & Ryan, S. (2004). Measurement of coarse gravel and cobble transport using portable bedload traps. *Journal of Hydraulic Engineering*, 879-893.

Carey, W., & Hubbell, D. (1986). Probability distributions for bedload transport. *Proc. 4th. Fed. Inter-Agency Sediment. Conf*, (4) 131-4.140.

Carling, P. (1991). An appraisel of the velocity-reversal hypothesis for stable pool-riffle sequences in the River Severn, England. *Earth Surface Processes and Landforms*, (16) 19-31.

Carling, P., & Orr, G. (2000). Morphology of riffle-pool sequences in the River Severn, England. *Earth Surface Processes and Landforms*, (25) 369-384.

Chanson, H. (1999). *The hydraulics of open channel flow. An introduction.* London: Arnold.

Church, M., & Hassan, M. (2002). Mobility of bed material in Harris Creek. *Water Resources Research*, (38) 1 - 12.

Clifford, N. (1993). Differential bed sedimentology and the maintenance of riffle-pool sequences. *Catena*, (20) 447-468.

Clifford, N. (1993). Formation of riffle-pool sequences: field evidence for an autogenic process. *Sedimentary Geology*, (85) 39-51.

Clifford, N., & Richards, K. (1992). The reversal hypothesis and the maintenance of riffle-pool sequences. In P. Carling, & P. G, *Lowland rivers: geomorphological perspectives* (pp. 43-70). Chichester: Wiley.

Clifford, N., McClatchey, J., & French, J. (1991). Discussion of 'Measurements of turbulence in the benthic boundary layer over a gravel bed' and 'Comparison between acoustic measurements and predictions of the bedload transport of marine gravels'. *Sedimentology*, (38) 161-171.

Clifford, N., Richards, K., & Robert, A. (1992). The influence of microform bed roughness elements on flow and sediment transport in gravels bed rivers. *Earth Surface Processes and Landforms* , 529-534.

Clifford, N., Robert, A., & Richards, K. (1992). Estimation of flow resistence in gravel-bedded rivers: a physical explanation of the mulitplier of roughness length. *Earth Surface Processes and Landforms*, 111-126.

Dietrich, W. (1987). Mechanics of flow and sediment transport in river bends. In *River channels: environment and process* (pp. 179-227). Oxford: Basil Blackwell.

Dietrich, W., & Whiting, P. (1989). Boundary shear stress and sediment transport in river meanders of sand and gravel. *American Geophysical Union*, 1-50.

Dollar, E. (2002). Fluvial Geomorphology . *Progress in Physical Geography*, (26) 123-143.

Drake, T., Shreve, R., Dietrich, W., Whiting, P., & Leopold, L. (1988). Bedload transport of fine gravel observed by motion-picture photography. *Journal of Fluid Mechanics*, (192) 193-217.

First Base Solutions Inc. "Orthophotos of the City of Toronto" [electronic resource: raster]. Markham, Ontario: First Base Solutions Inc., 2007

Gilbert, G. (1914). The transportation of debris by running water. *U.S. Geological Survey Professional Paper*, (86) 263.

Grant, G., Swanson, S., & Wolman, M. (1990). Pattern and origin of stepped-bed morphology in high-gradient stream, western Cascades, Oregon. *Geologic Society of America Bulletin*, (102) 340-352.

Gregory, K., Gurnell, A., Hill, C., & Tooth, S. (1994). Stability of the pool-riffle sequences in changong river channels. *Regulated Rivers: Research and Management*, (9) 35-43.

Habersack, H. (2001). Radio-tracking gravel particles in a larger braided river in New Zealand: a field test of the stochastic theory of bed load transport proposed by Einstein. *Hydrological Processes*, (15) 377-391.

Harrison, L., & Keller, E. (2007). Modeling forced pool–riffle hydraulics in a boulder-bed stream, southern California. *Geomorphology*, (83) 232-248.

Hassan, M., & Church, M. (2001). Sensitivity of bed load transport in Harris Creek: Seasonal and spatial variation over a cobble-gravel bar. *Water Resources Research*, (37) 813-825.

Hassan, M., & Ergenzinger, P. (2003). Use of tracers in fluvial geomorphology. In G. Kondolf, & H. Piegay, *Tools in Fluvial Geomorphology* (pp. 397-424). West Sussex: Wiley.

Heritage, G., & Milan, D. (2004). A conceptual model of the role of excess energy in the maintenance of a riffle-pool sequence. *Catena* , (58) 235-257.

Hicks, D., & Gomez, B. (2003). Sediment transport. In G. Kondolf, & H. Piegay, *Tools in Fluvial Geomorphology* (pp. 425-462). West Sussex: Wiley.

Jackson, W., & Beschta, R. (1982). A model of two-phase bedload transport in an Oregon coast range stream. *Earth Surface Processes and Landforms*, (7) 517-528.

Keller, E. (1971). Areal sorting of bes load material - the hypothesis of velocity reversal. *Geological Society of America Bulletin*, (82) 753-756.

Keller, E., & Melhorn, N. (1978). Rhythmic spacing and origin of pools and riffles. *Geological Society America Bulletin*, (89) 753-756.

Keller, E., & Melhorn, W. (1973). Bedforms and Fluvial Processes in Alluvial Stream Channels: Selected Observations. In M. Morisawa, *Fluvial Geomorphology* (pp. 253-283). New York: Binghamton.

Knighton, A. (1998). *Fluvial forms and processes. A new perspective.* London: Arnold.

Lane, S., Biron, P., & Bradbrook, K. (1998). Three-dimensional measurement of river channel flow processes using acoustic Doppler velocimetry. *Earth Surface Processes and Landforms*, (23) 1247-1267.

Lapointe, M. (1992). Burst-like sediment suspension events in a sand bed river. *Earth Surface Processes and Landforms*, (17) 253-270.

Laronne, J., & Carson, M. (1976). Interrelationship between bed morphology and bed material transport for a small gravel bed channel. *Sedimentology*, (23) 67-85.

Lawless, M., & Robert, A. (2001). Three-dimensional flow structure around small-scale bedforms in a simulated gravel-bed environment. *Earth Surface Processes*, (26) 221-238.

Leopold, L., & Wolman, M. (1957). River Channel Patterns: Braided, meandering and straight. *US Geological Survey*, 39-85.

Leopold, L., Wolman, G., & Miller, J. (1964). *Fluvial processes in geomorphology.* San Fransisco: W.H. Freeman and Company.

Levi, E. (1991). Vortices in hydraulics. *Journal of Hydraulic Engineering*, (117) 399-413.

Lisle, T. (1979). A sorting mechanism for a riffle-pool sequence . *Geological Society of America Bulletin*, (90) 1142-1157.

Lu, S., & Willmarth, W. (1973). Measurements of the structure of the Reynolds stress in a turbulent boundary layer. *Journal of Fluid Mechanics*, (60) 481-511.

MacVicar, B., & Roy, A. (2011). Sediment mobility in a forced riffle-pool. *Geomorphology*, (125) 445-456.

Meters, S. D. (1997, November). Frequently Asked ADV Questions. San Diego, USA: Sontek.

Milan, D., Heritage, G., Large, A., & Charlton, M. (2001). Stage dependent variability in tractive force distribution through a riffle-pool sequence. *Catena*, (44) 85-109.

Milne, J. (1982). Bed-material size and the riffle-pool sequence. *Sedimentology*, (29) 267-278.

Montgomery, D., & Buffington, J. (1997). Channel reach morphology in mountain drainage basins. *Geological Society of America Bulletin*, (109) 596-611.

Mosley, P., & Tindale, D. (1985). Sediment variability and bed material sampling in gravel-bed rivers. *Earth Surface Processes and Landforms*, (10) 465–482.

Nelson, J., Shreve, R., McLean, S., & Drake, T. (1995). Role of nearbed turbulence structure in bed transport and bed form mechanics. *Water Resources Research*, (31) 2071–2086.

Powell, D. (1998). Patterns and processes of sediment sorting in gravel-bed rivers. *Progress in Physical Geography* , (22) 1-32.

Rayburg, S. C., & Neave, M. (2008). Assessing Morphologic Complexity and Diversity in River Systems using Three-dimensional asymmetry indices for bed elements, bedforms and bar units. *River Research and Applications* , 1343-1361.

Rhoads, B., & Welford, M. (1991). Initiation of river meandering. *Progress in Physical Geography*, (15) 127-156.

Robert, A. (1993). Bed configuration and microscale processes in alluvial channels. *Progress in Physical Geography*, (17) 123-136.

Robert, A. (1997). Characteristics of velocity profiles along riffle-pool sequences and estimates of bed shear stress. *Geomorphology*, (19) 89-98.

Robert, A. (2003). *River Processes: An Introduction to Fluvial Dynamics.* London: Hodder Arnold.

Robert, A., Roy, A., & De Serres, B. (1993). Space-time correlations of velocity measurements at a roughness transition in a gravel-bed river. In N. Clifford, J. French, & J. Hardisty, *Turbulence: perspectives on flow and sediment transport* (pp. 165-183). Chichester: Wiley.

Roy, A., Biron, P., Buffin-Belanger, T., & Levasseur, M. (1999). Combined visual and quantitive techniques in the study of natural turbulent flows. *Water Resources Research*, (35) 871-877.

Sawyer, A., Pasternack, G., Moir, H., & Fulton, A. (2010). Riffle-pool maintenance and flow convergence routing observed on a large gravel-bed river. *Geomorphology*, (114) 143-160.

Sear, D. (1996). Sediment transport processes in riffle-pool sequences. *Earth Surface Processes and Landforms*, (21) 241-262.

Sear, D., Damon, W., Booker, D., & Anderson, D. (2000). A load cell based continuous recording bedload trap . *Earth Surface Processes and Landforms*, (25) 659-672.

Tennekes, H., & Lumley, J. (1994). A First Course in Turbulence. *The MIT Press*. Cambridge MA.

Thompson, D. (2007). Turbulence characteristics in a shear zone downstream of a channel constriction in a coarse-grained pool. *Geomorphology*, (83) 199-214.

Thompson, D., & Wohl, E. (2009). The linkage between velocity patterns and sediment entrainment in a forced-pool and riffle unit. *Earth Surface Processes and Landforms*, (34) 177-192.

Thompson, D., & Wohl, E. J. (1999). Pool sediment sorting processes and the velocity-reversal hypothesis. *Geomorphology*, (17) 142-156.

TRCA. (2007). *Rouge River: State of the Watershed Report.* Toronto: Toronto: Toronto Regional Conservation Authority.

Whitting, P. (1996). Sediment sorting over bed topography. In P. Carling, & M. Dawson, *Advances in Fluvial Dynamics and Stratigraphy* (pp. 204-228). Chichester: Wiley.

Wilcock, P., & DeTemple, B. (2005). Persistence of armor layers in gravel-bed streams. *Geophysical Research Letters*, 32.

Wohl, E., & Thompson, D. (2000). Velocity flucuations along a small step-pool channel. *Earth Surface Processes and Landforms*, (25) 353-367.

Yang, C. (1971). Potential Energy and Stream Morphology. *Water Resources Research*, (7) 311-322.

Yang, C. (1987). *Sediment Transport in Gravel-Bed River - Energy dissipation rate approach in river mechanics.* New York: 735-766.